HYDRODENITROGENATION OF A COAL

DERIVED LIQUID

By

DON P. SATCHELL

Bachelor of Science
Michigan State University
East Lansing, Michigan
1969

Master of Science
Oklahoma State University
Stillwater, Oklahoma
1972

Submitted to the Faculty of the Graduate College
of the Oklahoma State University
in partial fulfullment of the requirements
for the Degree of
DOCTOR OF PHILOSOPHY
May, 1974

HYDRODENITROGENATION OF A COAL

DERIVED LIQUID

Thesis Approved:

Billy L Crynes
Thesis Adviser

Robert H Robinson, Jr.

John H Erbar

Jerald W Parker

N N Durham
Dean of the Graduate College

PREFACE

Experimental equipment was constructed for hydrodenitrogenation of anthracene oil, an aromatic hydrocarbon liquid obtained from coal, over a cobalt-molybdenum on alumina catalyst. The total nitrogen concentration of the reactor product oil was measured as a function of: (1) reactor temperature in the range of 600 to 800°F, (2) pressures of 500, 1000, and 1500 psig, (3) average catalyst particle sizes of 44 and 9 mesh (particle diameters of about .013 and .078 inches, respectively), (4) hydrogen gas rates of about 1500 and 20,000 standard cubic feet per barrel of oil fed, (5) liquid hourly space times of 0.375, 0.75, and 1.5 hours. Three catalysts with identical metals content and most frequent pore diameters of 50, 50, and 66 angstroms were used to test for the effect of pore size on the rate of hydro-denitrogenation.

TABLE OF CONTENTS

LIST OF TABLES

LIST OF FIGURES

NOMENCLATURE

a	arbitrary constant
A	frequency factor
b	arbitrary constant
C	carbon atom
E	activation energy
H	hydrogen atom
k_i	rate constant for cut i
$k_{i.i}$	rate constant introduced in Equation i.i
n	reaction order
N	nitrogen atom
N_f	weight percent nitrogen in the reactor feed
Np	weight percent nitrogen in the reactor oil product
N_{fi}	weight percent nitrogen in the reactor feed in cut i
N_{pi}	weight percent nitrogen in the reactor oil product in cut i
P	reactor operating pressure
r_i	activity ratio (k_i/k_8) for boiling range i
R	universal gas constant
T	reactor operating temperature
V_{HCL}	volume, milliliter, of .01 Normal hydrochloric acid solution titrated with sample less the volume titrated without sample

w_i	mass fraction of oil in cut i
w, x, y, z	arbitrary constants
Θ_v	volume hourly space time
Θ_w	weight hourly space time

Abreviations

bbl	petroleum barrel
BTU	British thermal unit
cc	cubic centimeter
$^\circ F$	degree Fahrenheit
gr	gram
hr	hour
lb.	pound
SCF	standard cubic feet

CHAPTER I

INTRODUCTION

This work is part of an effort by the Office of Coal Research to
develop a solvent process to convert coal to a low sulfur and ash oil.
The process consists of the following steps:

1. Coal is crushed in hammer mills.

2. The pulverized coal is mixed with a solvent which is
   recycled dissolver effluent (See Figure 1.).

3. The oil-coal slurry is mixed with hydrogen at about 1000
   psig, heated, and fed to the dissolver.

4. The dissolver effluent is filtered to remove the ash
   (mostly mineral matter in the coal feed).

5. The deashed dissolver effluent can either be separated into
   an oil and deashed coal by vacuum distillation or hydro-
   treated to produce an oil with low nitrogen and sulfur
   content.

A block flow diagram of the process is presented on Figure 1. Details
of the process are given in a progress report (1) from the Pittsburg
and Midway Coal Mining Company to the Office of Coal Research.

The deashed coal and oil products will find immediate use as
substitutes for coal and residual fuel oil in electric power generation.
If the coal feed is high in sulfur content, the deashed dissolver

1
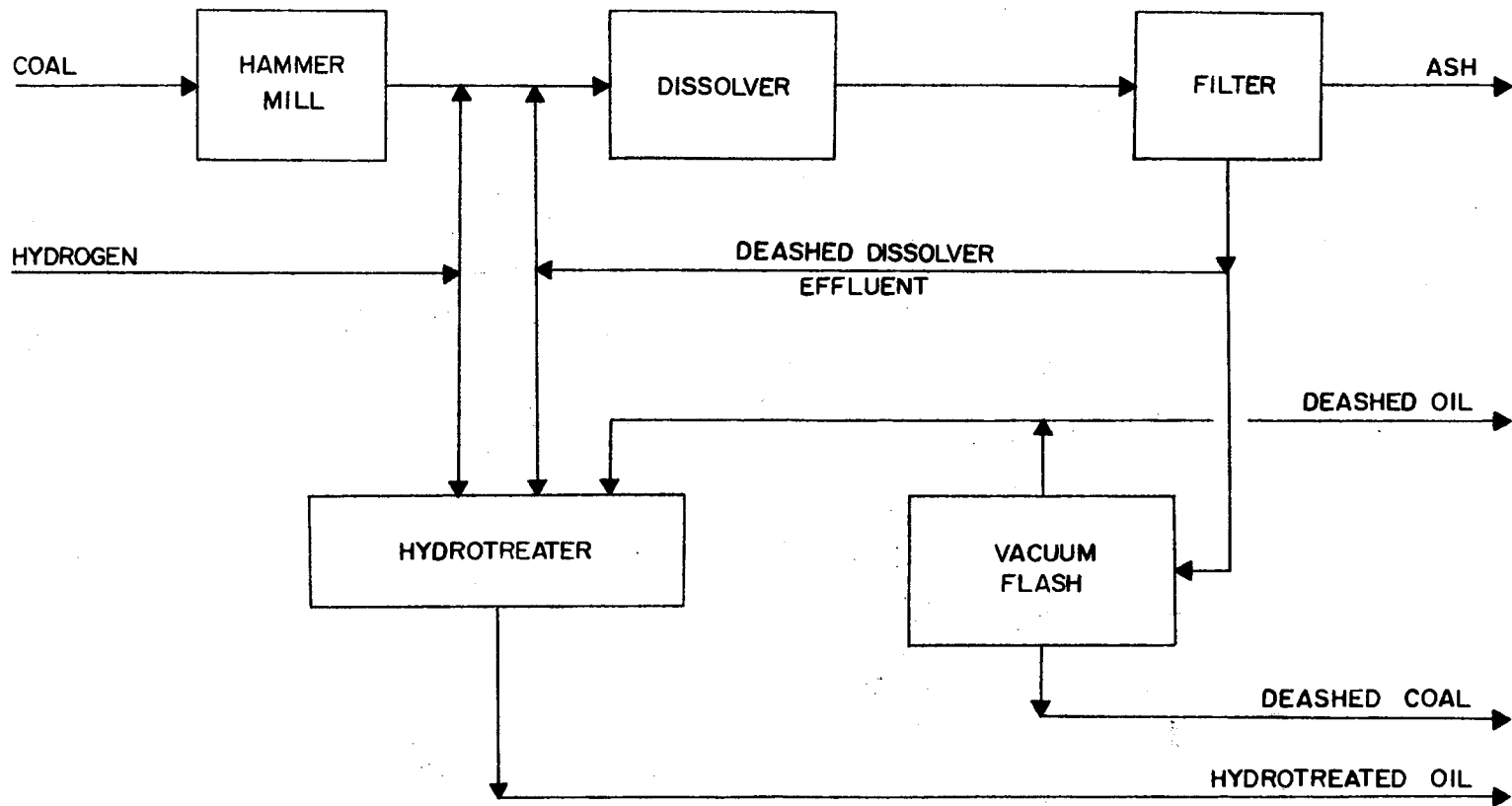
Figure 1. Block Flow Diagram of Solvent Liquefaction Process

effluent can be hydrotreated to decrease the sulfur content to an acceptable level. In the future, the hydrotreated oil could be used as an alternative feedstock for petroleum refineries. The presence of organonitrogen compounds reduces the activity of catalytic cracking (2), reforming (3), and isomerization (4) catalysts. The susceptibility of these refining catalysts to poisoning by organonitrogen species makes the degree of nitrogen removal in the hydrotreating step an important factor affecting the desirability of the hydrotreated oil as a refinery feedstock.

Hydrodenitrogenation in a hydrotreater reactor is accomplished by hydrogenolysis of organonitrogen compounds to ammonia and the corresponding hydrocarbon. The reaction can be represented by Equation (1.1).

$$C_w H_x N_y + \frac{z+3y-x}{2} H_2 \longrightarrow y\ NH_3 + C_w H_z$$

<div align="right">(1.1)</div>
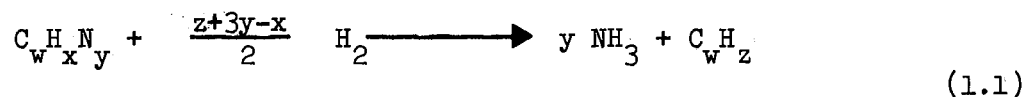
Organonitrogen Specie   Hydrogen   Ammonia   Hydrocarbon

Where, C, H, and N represent carbon, hydrogen, and nitrogen atoms, respectively; w, x, y, and z are unspecified integers. Since hydrogenation usually accompanies denitrogenation, z is typically greater than x.

Hydrotreating of petroleum oils is typically carried out in the temperature range of 600 to 800°F, with pressures of 300 to 4000 psig, and hydrogen flows rates from 300 to 15,000 standard cubic feet per barrel. The hydrogen and oil are usually contacted in a fixed catalyst bed in a down flow reactor. The typical catalyst consists

of cobalt and molybdenum oxides supported on alumina. Figure 2 is a diagram of a typical hydrotreater unit.

The specific goals of this work are the following:

1. Construct and test a laboratory reactor for catalyst studies of hydrotreating coal derived and petroleum liquids.

2. Determine the effect of reactant mass flux on the rate of denitrogenation.

3. Determining the rate controlling step for hydrodenitrogenation.

4. Determine the effect of alternative operating conditions on the rate of denitrogenation.

5. Determine the effect of mean pore diameter on the rate of hydrodenitrogenation.

Pertinent literature will be reviewed, in the next chapter, to serve as a basis for this work.

HYDROGEN

FEED OIL

LIGHT ENDS

PRODUCT OIL

FURNACE   REACTOR   HIGH PRESSURE   STRIPPER
                                  FLASH DRUM   COLUMN
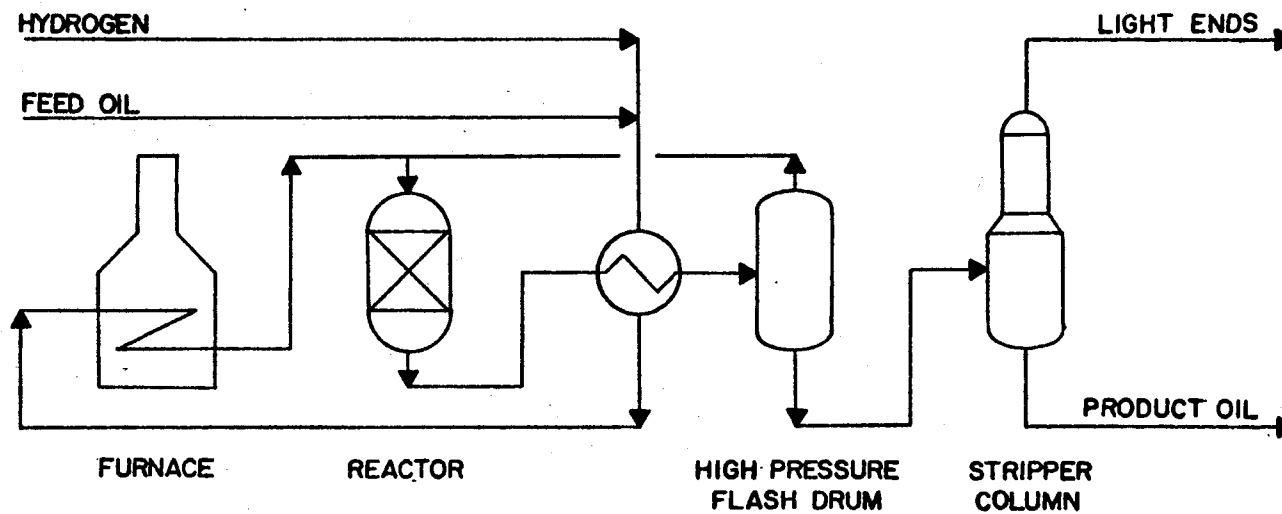
Figure 2. Typical Hydrotreater Unit

CHAPTER II

LITERATURE REVIEW

The hydrotreating literature is both vast and plagued by many
apparent contradictions. One reason for so many anomalies is that
both the feed and the catalyst are often defined only in the most
general terms. Obscure properties of the catalyst and feed, such as
the heavy metals content of the feed, can have a significant effect
on the rate of reaction. Therefore, the emphasis will be placed on
trends exhibited by the data in the literature rather than on absolute
rates of reaction.

The areas of interest fall under two general categories. The
first deals with hydrotreater reactor design. This information is
useful in the design of experimental apparatus and interpreting the
data. The second area of interest consists of studies that share
one or more objectives with this study.

Reactor Engineering

There are three basic reactor types for commercial hydrotreating
of high boiling hydrocarbons:

1. trickle flow reactor

2. up flow reactor

3. ebullient bed reactor

In the trickle flow reactor, the hydrogen and oil are fed at the top of the reactor and allowed to pass through a fixed catalyst bed. This is by far the most common contacting scheme in commercial plants. Universal Oil Products (5), Gulf Research Co. (6), and Institut Francais de Petrole (7) have processes using trickle flow reactors.

By comparison, in the up flow reactor, the hydrogen and oil are fed to the bottom of the reactor and pass up through a fixed catalyst bed. The up flow reactor also differs from the trickle flow reactor in the manner in which the reactants pass through the void volume of the catalyst bed. In the up flow reactor, hydrogen bubbles through an oil pool. In the trickle flow reactor, oil drips through hydrogen. Thus, one would expect greater contact between the catalyst and oil in an up flow reactor than in a trickle flow reactor. The liquid is thought (8) to wash polymer precursors and ash from the catalyst. Therefore, one might expect that the up flow reactor would have less tendency to plug (due to coke formation or deposition of ash) than a trickle flow reactor. However, a study (9), using a coal derived liquid feedstock, found that the trickle flow and up flow reactor types showed roughly equal tendency to plug.

In ebullient bed reactor, like the up flow, the reactants are fed from the bottom. However, unlike the up flow reactor, the feed is introduced at a sufficient rate to cause an expansion of the catalyst bed. The licenser (10) claims the following advantages for the ebullient bed reactor:

1. Less susceptible to plugging.

2. Operation is much closer to isothermal.

3. Smaller catalyst particles can be used without excessive
    pressure drop across the catalyst bed.

The trickle flow reactor was selected for this study primarily
because it has been widely used in the petroleum industry in similar
services. In addition, the trickle flow reactor is probably easier to
operate than either the up flow or the ebullient bed reactor.

Factors affecting the performance of a trickle flow reactor can
be divided into the following categories:

1. liquid hydrodynamics
2. diffusion resistances
3. denitrogenation kinetics

Each of these topics will be considered in detail in the following
discussion.

Liquid Hydrodynamics

Maldistribution of the liquid portion of the oil over the catalyst
bed can adversely affect the performance of a trickle flow reactor
(11). Concurrent down flow of the hydrogen and oil has been shown
(12) to improve the liquid distribution. Liquid fluxes in the range
of 150-500 gallons per hour per square foot and vapor velocities of
.1 to .15 feet per second are recommended (13) to insure good liquid
distribution of the reactants. Occasionally, a disproportionate
amount of liquid will flow near the reactor wall. If the ratio of
the diameter of the reactor to the diameter of the catalyst particle
is greater than 25 to 1 (14), then this effect is probably negligible.
Mears (15) offers a method for predicting the adverse effects of
axial dispersion (backmixing) on a trickle flow reactor's performance.

However, one study (16) suggests that the above criteria are not sufficient to insure that the liquid is well distributed over the catalyst. Identical feed, catalyst, and operating conditions were run in a pilot plant and a commercial reactor. Tracer studies indicated that the dispersion was more severe in the pilot plant reactor than the commercial reactor. Thus, based on backmixing effects, one would predict that the performance of the commercial reactor should be superior to the pilot unit. The reactor to pellet diameter ratio was 12 to 1 for the pilot reactor and 42 to 1 for the commercial reactor. Therefore, bypassing of reactants around the catalyst bed should be more severe in the pilot unit than in the commercial reactor. This effect should adversely affect the performance of the pilot unit relative to the commercial reactor. Oil fluxes were 44 and 210 gallons per foot squared per hour for the pilot unit and the commercial reactor, respectively. The oil flux in the pilot unit was below the previously cited recommended minimum to insure good liquid distribution. In contrast, the oil flux in the commercial reactor is in the proper range. Since the catalyst and operating conditions were identical in both reactors, pore diffusion resistances and the intrinsic kinetics should have been identical. Based on this data and all of the above criteria for liquid distribution, one would predict that the commercial reactor should achieve a higher conversion than the pilot unit at a fixed set of operating conditions. However, the observed conversion in the pilot unit was much greater than the commercial reactor. A possible explanation for the anomaly is that the commerical reactor is thought to be more sensitive to an initial maldistribution of the liquid than a narrow pilot unit (17). The

study did not specify a liquid distributor for either reactor. There-
fore, the literature indicates that the effect of liquid maldistribu-
tion on the performance of a trickle flow reactor can be substantial
and unpredictable.

Diffusion Resistances

Diffusion resistances to reaction in a trickle flow reactor can
be divided into two areas:

1. resistances encountered in the liquid film surrounding the
   catalyst pellet

2. pore diffusion resistances

Satterfield (18) showed that the liquid film around catalyst particles
has an average thickness in the range of .01 to .1 millimeter under
typical hydrotreating conditions. This is much less than the radius
of typical catalyst particles used in trickle flow reactors. Since
the catalyst pores are liquid filled under normal hydrotreating con-
ditions (19), the diffusivity of a specie in the catalyst pore should
be roughly equal to that specie's diffusivity in the liquid film
around the catalyst particle. Therefore, diffusion resistances
encountered in the film around the catalyst particle are typically
much less than pore diffusion resistances in a typical trickle flow
reactor.

Pore diffusion resistances cause a decrease in reactant concen-
tration from the catalyst particle outer boundary to the center,
which results in a decrease in the rate of reaction. Since the
relative magnitude of pore diffusion resistances to the total resis-
tance to reaction is of primary importance, the role of pore diffusion

will be discussed in terms of an effectiveness factor. The effective-
ness factor is usually defined (2) as the ratio fo the actual reaction
rate to that which would occur if all of the surface throughout the
inside of the catalyst were exposed to the catalyst outer boundary
reactant concentration and temperature. The catalyst activity
(the rate of heterogeneous reaction at a specified set of operating
conditions) without pore diffusion resistances can be determined
experimentally by extrapolating a plot of catalyst activity as a
function of catalyst particle diameter to zero diameter. Then the
effectiveness factor is the ratio of the catalyst activity at any
diameter of interest to the extrapolated activity. This method is
limited in trickle flow reactors by the large pressure drop across
the catalyst bed encountered when very small catalyst particles are
used. However, the effectiveness factor can be estimated using the
catalyst activity at a given set of operating conditions and two
catalyst particle diameters (21).

Van Zoonen and Douwes (22) hydrotreated a straight-run gas oil
at about 500 psig and 707°F over a cobalt-molybdenum on alumina
catalyst with dimensions of 3 x 3 millimeters and 25-50 mesh (range
of particle diameters from about .707 to .297 millimeters). The
greater than four fold reduction in the catalyst particle size did
not result in an increase in the conversion of organonitrogen species.
This indicates that the effectiveness factor was near one (pore
diffusion resistances were negligible) for the system studied. Since
film diffusion resistances are typically much less than pore diffusion
resistances in a trickle flow reactor (18), an effectiveness factor

of one implies that resistances to reaction encountered at the catalyst surface control the rate of denitrogenation.

In a hydrotreating study (23) of a coal derived liquid at 770°F and 3000 psig over a nickel-cobalt-molybdenum on alumina catalyst, a three fold reduction in the catalyst particle diameter resulted in almost a four fold reduction in the percent of organonitrogen species remaining in the product. Thus, the rate of reaction was roughly proportional to the catalyst outer surface area, which implies that film diffusion controlled the rate of denitrogenation of the coal derived liquid and the effectiveness factor was near zero.

Denitrogenation Kinetics

McIlvried (24) studied the denitrogenation of piperidine and pyridine over a nickel-cobalt on alumina catalyst at 600°F. The author offered the following scheme for denitrogenation of pyridine:

Pyridine   Piperidine   N-Pentylamine N-Pentane Ammonia
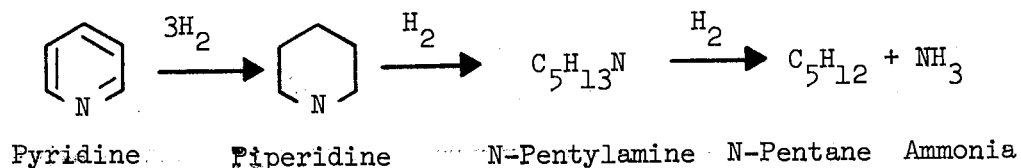
The author concluded that the rupture of the piperidine ring was the rate controlling step in the denitrogenation of pyridine at these conditions. The Langmuir-Hinshelwood form (25) adequately accounted for the decrease in the first order rate constant with increasing feed nitrogen content.

Doelman (25) studied the denitrogenation of quinoline using a cobalt-molybdenum on alumina catalyst. The following scheme for denitrogenation of quinoline was presented:

| Quinoline | 1,2,3,4, Tetra-hydroquinoline | Propyl-aniline | Propyl-benezene | Ammonia |

In the first step, the hydrogen containing ring is saturated. Then the ring is opened to form anilines or amines, which undergo hydrogenolysis to form ammonia and hydrocarbon. Doelman found that the rate of both aromatic ring saturation and saturated ring opening steps have a significant effect on the rate of denitrogenation of quinoline.

Various pure component studies (24, 26, 27) have established that denitrogenation is first order with respect to the concentration of nitrogen species. The rate of denitrogenation of quinoline was found to be practically proportional to the hydrogen partial pressure (25).

A discussion of the kinetics of denitrogenation becomes much more complicated when one considers industrially important feeds like petroleum stocks, shale oil, and coal derived liquids. These feedstocks typically contain a large number of unspecified organonitrogen species. Flinn et al (27) showed that even species in the same boiling range can have radically different kinetics of denitrogenation. The same study found that the ease of denitrogenation tends to decrease with increasing boiling point of a petroleum feed. To handle a system such as this with any degree of rigor is a very formidable task. Rather than try to cope with the complexity of the intrinsic kinetics of the system, a qualitative discussion of the effect of reactor

operating conditions on the rate of denitrogenation of coal derived
liquids will follow.

Effect of Reactor Operating Conditions

A hydrotreating study (23) by ARCO (Atlantic Richfield Company)
on a coal derived liquid from the COED Process (1) is the only study,
in the open literature, using a coal-derived oil feed. A hydrotreat-
ing study (28) by Wan, using the same feedstock as this work, is
also of interest. These two works will serve as a basis for the
following discussion of the effect of space time, temperature, pressure,
and hydrogen rate on the rate of denitrogenation.

Space Time

ARCO (23) tested for the effect of space time on denitrogenation
of COED oil derived from Illinois 6 Seam (Crown) Coal at 3,000 psig
and 725°F over a nickel-cobalt-molybdenum on alumina catalyst.
Figure 3 is a plot of the logarithm of the percent of the organonitro-
gen species fed to the reactor that remained in the product as a
function of 1.0/WHSV (reciprocal of the weight hourly space velocity).
WHSV was defined as the mass of oil charged per hour per mass of
catalyst bed. For any given feed and catalyst, 1.0/WHSV is proportional
to the space time. If the rate of denitrogenation could be described
by a first order rate expression with respect to organonitrogen con-
tent, then a plot of the logarithm of the percent total nitrogen
remaining as a function of 1.0/WHSV, or space time, should yield a
straight line. Thus, the data in Figure 3 show that a first order
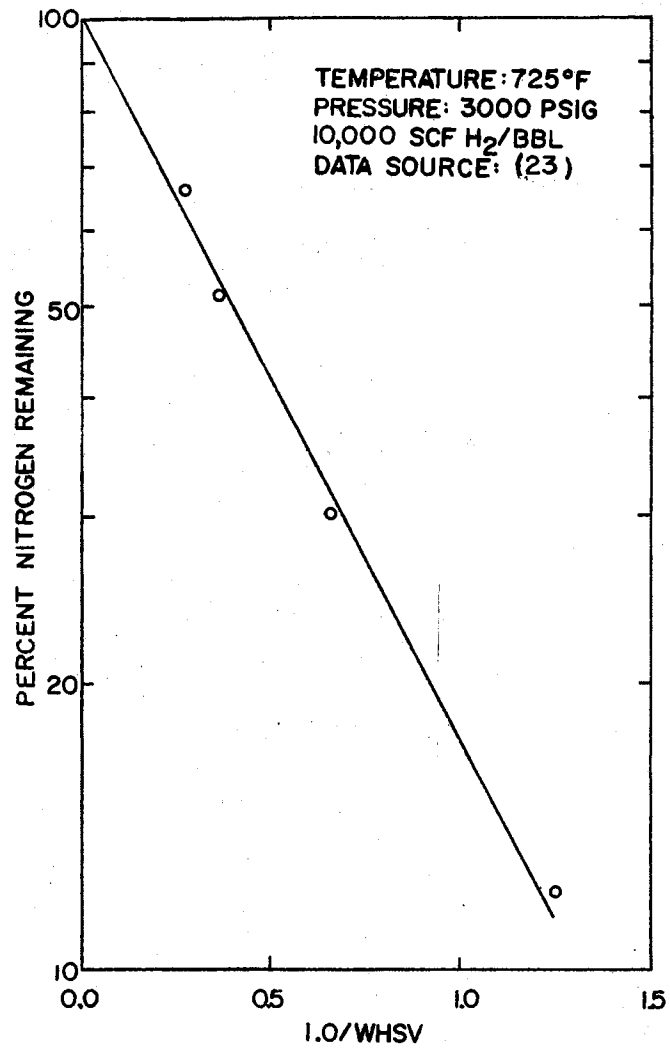
Figure 3. Effect of Weight Hourly Space
Time on Denitrogenation of
COED Oil.

rate expression is not an unreasonable representation of the kinetics of denitrogenation of the COED oil over the range of operating conditions studied.

Figure 4 is a plot of the logarithm of the percent of organo-nitrogen in the feed reamining in the product as a function of space time with parameters of pressure at $800^\circ F$, the most complete isotherm, from the study by Wan (28). The plot indicates that the percent nitrogen remaining is a very weak function of space time beyond 0.4 hours for the system under study.

Temperature

ARCO (23) found that the activation energy for denitrogenation, assuming first order kinetics with respect to organonitrogen species' content, was 48,500 BTU/lb. mole below $752^\circ F$ and 16,400 BTU/lb. mole above $752^\circ F$. The authors rationalized the result by noting that Flinn, Larson, and Beuther (27) have postulated that saturation of resonance-stabilized structures is the rate controlling step for hydrodenitro-genation. In addition, another study (29) of hydrogenation equilibria of aromatic species shows a shift toward dehydrogenation between 750 and $800^\circ F$. Thus, the reduction in activation for hydrodenitro-genation could be the result to competing dehydrogenation reactions.

Pressure

In the original work (23), the effect of pressure on the rate of denitrogenation of a COED coal derived liquid was represented by a plot of the percent nitrogen removed as a function of the reactor
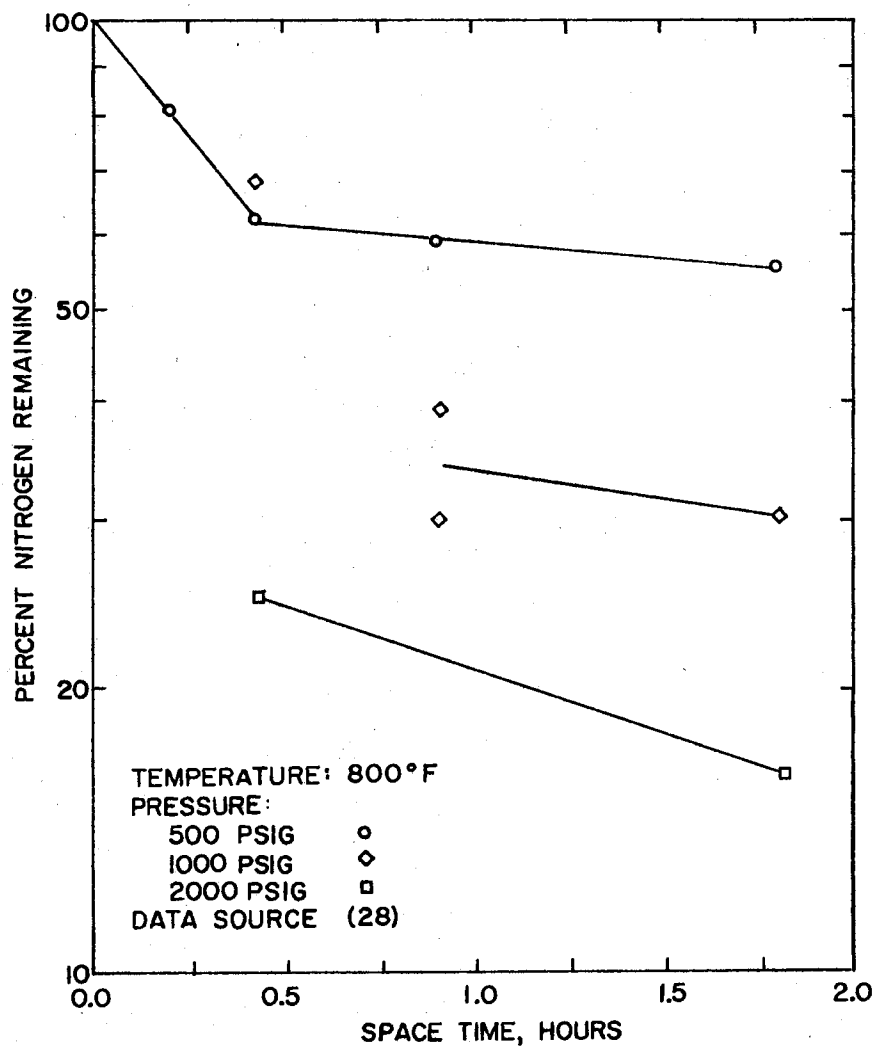
Figure 4. Effect of Space Time on Denitrogenation of Anthracene Oil

pressure. The following derivation will be used to obtain a slightly more mechanistic representation of the same data. Figure 3 suggests that a first order rate expression (Equation 2.1) with respect to organonitrogen content is reasonable for a COED oil.

$$\frac{d\ N}{d\ \Theta_w} = k_{2.1}\ N \qquad (2.1)$$

Where, N is the mass percent atomic nitrogen in the oil and Θ_w is the weight hourly space time (gm catalyst per gm of oil per hour); $k_{2.1}$ is the rate constant. The subscript on the rate constant specifies the equation number that the constant was first introduced. The effect of the reactor total pressure on the hydrodenitrogenation rate constant, $k_{2.1}$, will be represented by Equation 2.2.

$$k_{2.1} = k_{2.2}\ P^a \qquad (2.2)$$

Where, P is the absolute reactor pressure, psia, and a is a constant to be determined by least square analysis. Substitution of Equation 2.2 into 2.1 yields Equation 2.3.

$$\frac{dN}{d\Theta_w} = -k_{2.2}\ P^a\ N \qquad (2.3)$$

Integrating Equation 2.3 yields Equation 2.4.

$$\ln\ (N_f/N_p) = k_{2.2}\ P^a\ \Theta_w \qquad (2.4)$$

Where, N_f and N_p are the mass percent atomic nitrogen in the reactor feed and product, respectively. Rearranging Equation 2.4 and taking

the logarithm of the result gives Equation 2.5.

$$\ln\left(\ln(N_f/N_p) \,/\, \Theta_w\right) = \ln k_{2.2} + a \ln P \qquad (2.5)$$

Figure 5 is a log-log plot of $\ln(N_f/N_p)/\Theta_w$ as a function of reactor total pressure. The slope of such a plot should be equal to the value of a. A least squares regression (30) of the data in Figure 5 yielded a value of 1.1 for a. Several pure component studies (24) found that the rate of hydrodenitrogenation was proportional to the hydrogen partial pressure. The large hydrogen rates (18,200 SCF H_2 / bbl) used in the COED hydrotreating study made the hydrogen partial pressure nearly proportional to the total pressure. Therefore, hydrodenitrogenation of this COED coal derived liquid appears to be first order with respect to hydrogen partial pressure under normal reactor operating conditions.

Effect of Hydrogen Rate

Wan (28) found that increasing the hydrogen rate from 3980 to 39,800 SCF/bbl resulted in an increase of the percent conversion of total nitrogen from 61.2 to only 69.7%. Several pure component studies (25, 26) also found that the rate of denitrogenation was a weak function of the hydrogen circulation rate.

Effect of Pore Diameter

Van Zoonen and Douwes (22) studied the effect of volume average pore diameter in the range of 66 to 464 angstroms with a cobalt-molybdenum on alumina catalyst on the rate of denitrogenation of a
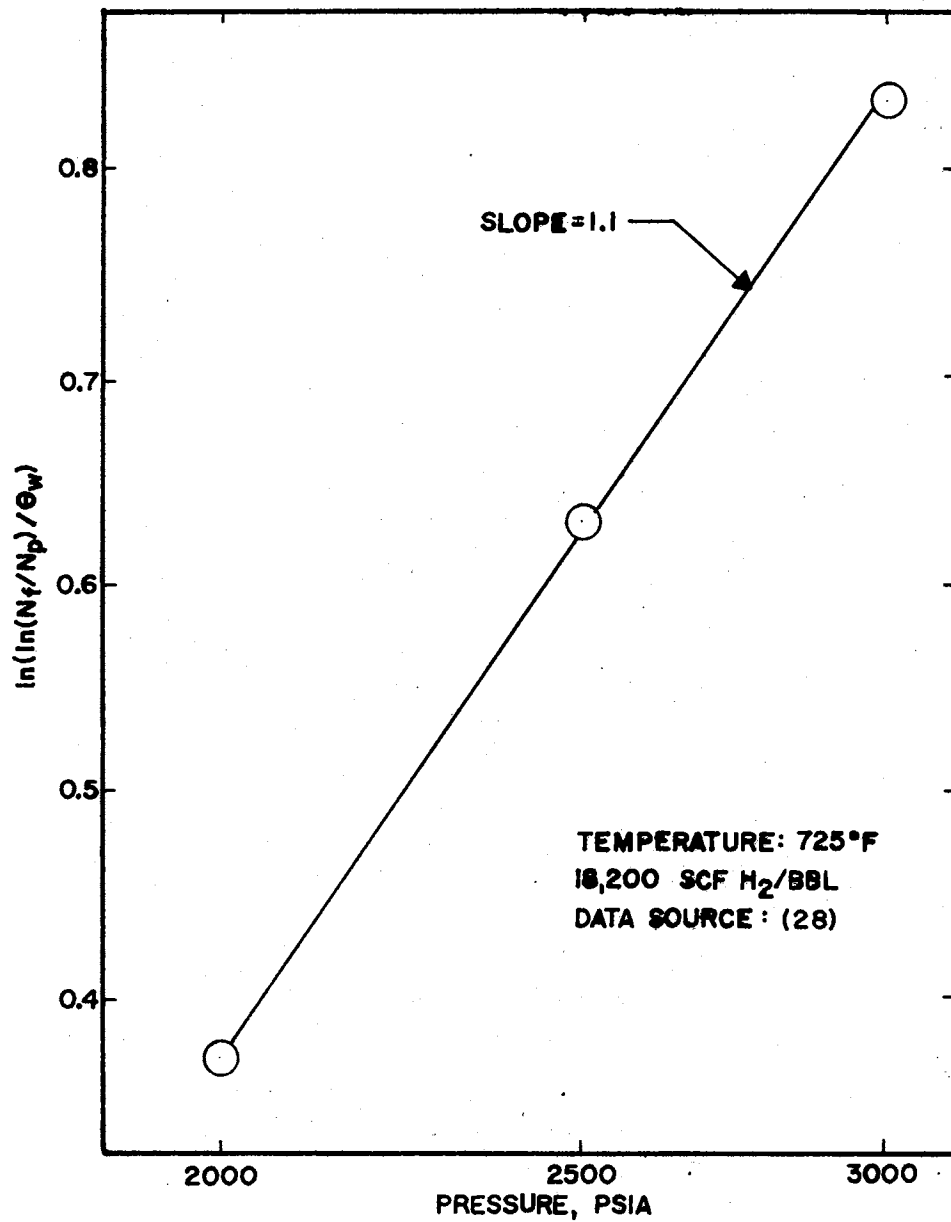
Figure 5. Effect of Pressure on Denitrogenation
of COED Oil

Middle East gas oil at 707^OF and about 500 psig. The study indicated that the volume average pore diameter had a negligible effect on the rate of denitrogenation over the entire range studied.

Summary

The following generalities can be made based on the preceding discussion. Maldistribution of the liquid portion of the oil feed over the catalyst bed can have a large and rather unpredictable effect on the rate of denitrogenation. The rate of denitrogenation has been usually found to be first order with respect to the organonitrogen level. However, side reactions can apparently have a significant effect on the kinetics. The rate of hydrodenitrogenation is probably controlled by the rate of surface reaction. The rate of denitrogenation appears to be proportional to the total pressure at normal commercial reactor operating conditions.

CHAPTER III

EXPERIMENTAL APPARATUS

A trickle flow reactor system was designed and constructed to fulfill the following requirements:

1. The reactor should be capable of nearly isothermal operation with operating temperatures up to 800°F.

2. The maximum operating pressure was set at 1500 psig.

3. Continuous operation must be possible.

4. A change of catalyst bed height at constant operating conditions must be possible.

5. The flow rates of oil and hydrogen must be measured and controlled accurately.

6. The reactor operating pressure must be controlled and a method of estimating the pressure drop across the catalyst bed must be provided.

Figure 6 is a diagram of the system used in this study. Hydrogen and oil entered the reactor at the top and flowed concurrently through the catalyst bed. The liquid and vapor portions of the reactor product were separated in the sample bombs. The unit pressure was controlled by a pressure controller on the hydrogen feed to the reactor. The hydrogen rate was controlled using a microvalve on the sample bomb off gas. The oil rate to the reactor
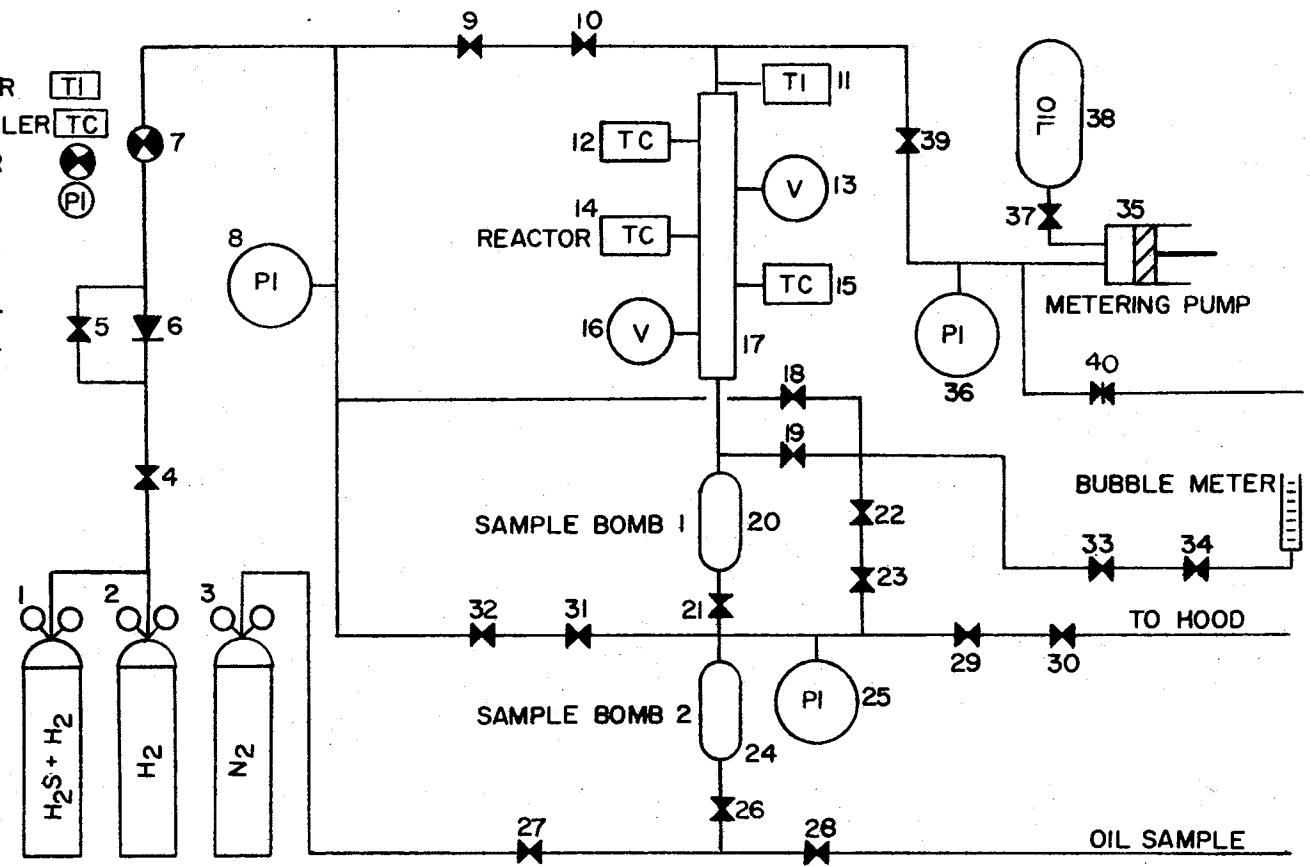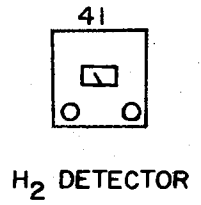
Figure 6. Experimental Apparatus

was controlled by a positive displacement pump. A detailed description of each section of the equipment follows.

Reactor

The reactor was constructed from a 33 inch long, 1/2 inch O.D. stainless steel tube. Figure 7 is a drawing of the reactor. The connections at the top and bottom were 1/2 inch swagelock cross and straight union, respectively. As can be seen from Figure 7, a 1/8 inch stainless steel tube was used as a thermowell down the center of the reactor. The thermowell was welded shut on the bottom and secured at the top of the reactor by another swagelock fitting. The 1/4 to 1/8 inch reducer through which the thermowell passed was drilled out to allow the thermowell to pass. A 36 inch thermocouple was moved along the length of the well to take temperature profiles along the length of the reactor. Fifty mesh stainless steel screens were used to hold the catalyst bed in the reactor.

Reactor Heaters

Aluminum blocks wrapped with electrical resistance heaters provided heat to the reactor. Figure 8 gives the dimensions of the aluminum heating blocks. The blocks were split in the middle and hinged on one side to facilitate mounting and removal. Control of the heaters was maintained using a Hewlett-Packard Model 240 temperature controller or a variac. Control thermocouples were placed in small holes drilled into the aluminum heating blocks adjacent to the resistance heaters. Control with the variacs was maintained by balancing heat input with the heat loss by trial and error. The
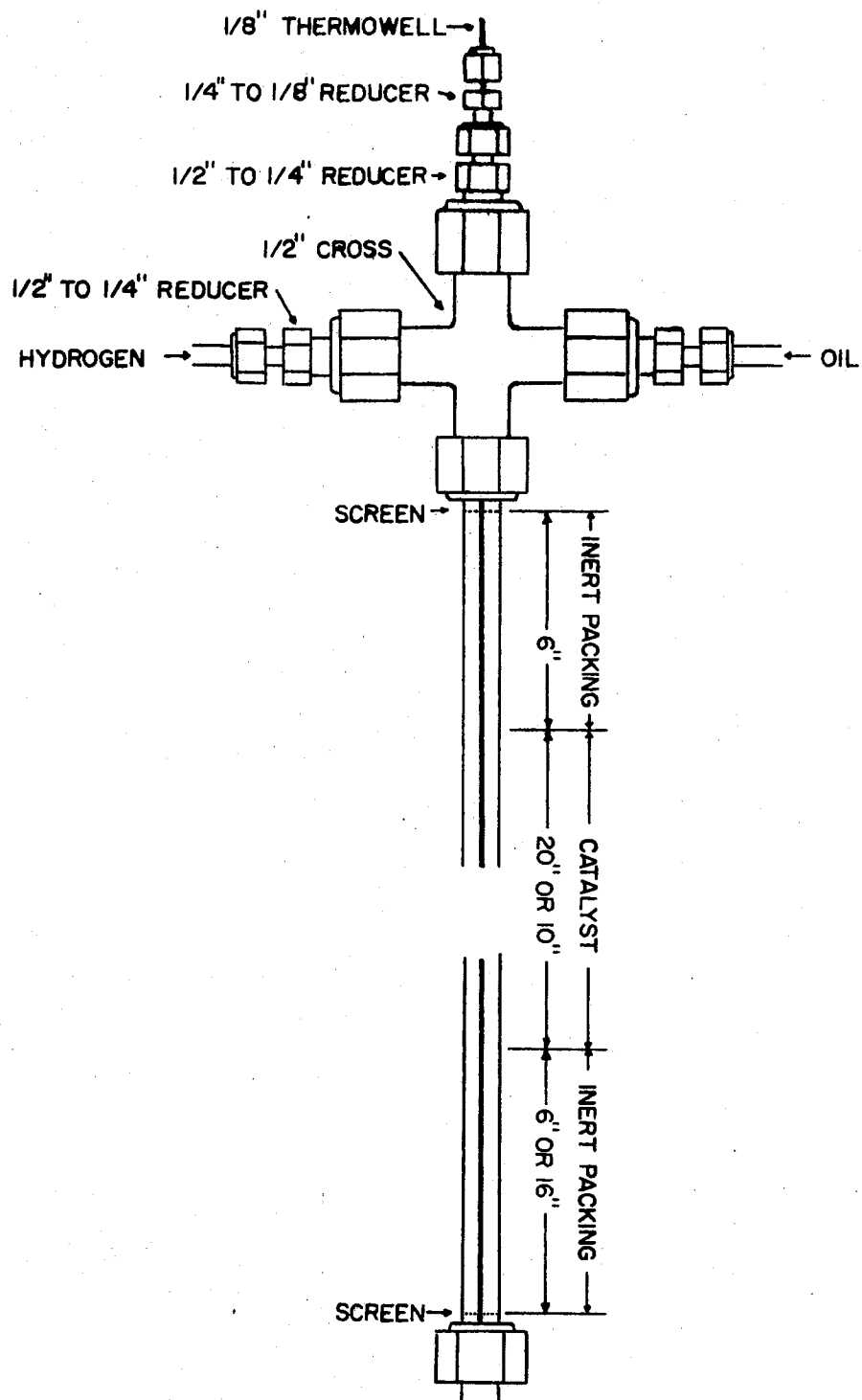
Figure 7. Reactor Design
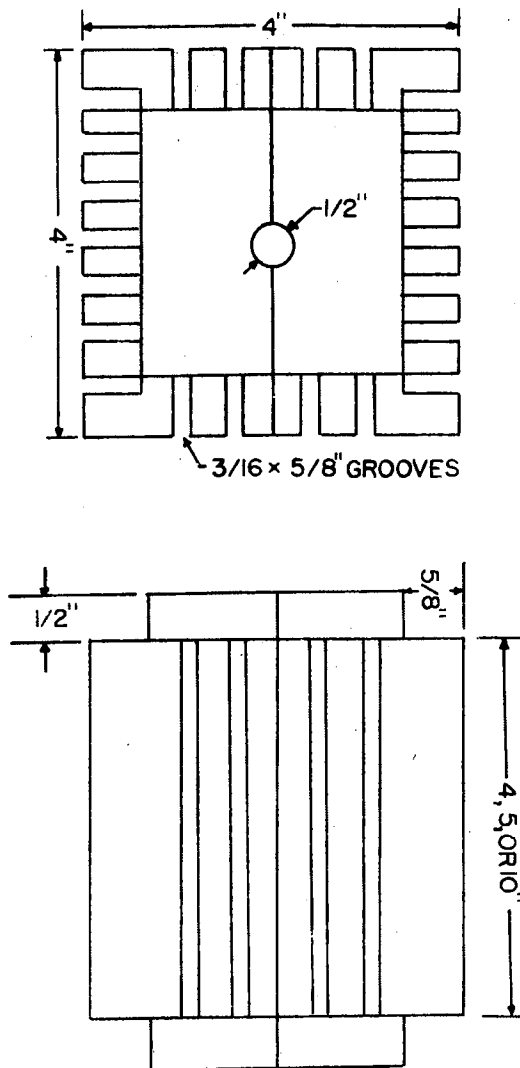
Figure 8. Reactor Heater Block Design

final placement of the controllers, variacs, and aluminum blocks
from the inlet of the reactor are summarized in Table I.

TABLE I

REACTOR HEATER CONFIGURATION

Block Number from Reactor Inlet	Aluminum Block Height, Inches	Control Type	Maximum Heater Wattage
1	4	Hewlett-Packard	244
2	5	Variac	305
3	10	Hewlett-Packard	611
4	5	Hewlett-Packard	305
5	4	Variac	244

Reactor Insulation

The aluminum blocks were first wrapped with a one inch layer of
felt insulation. Next, a two inch layer of fiberglass insulation was
wrapped around the reactor. The insulation was held in place using
asbestos tape.

Sampling System

The sampling system was designed to provide continuous operation
of the reactor. The bottom of the reactor was attached to Sample

Bomb 1 using a 1/2 inch stainless steel tube. The sample bomb was
constructed from a one liter stainless steel bomb rated at 1800 psig
at ambient temperature. Figure 9 is a drawing of the sample bomb
design. The 1/4 inch stainless steel tube passes through a reamed
1/2 to 1/4 inch swagelock reducer. The seal on the tube was made by
a swagelock fitting on the 1/4 inch tube. Vapor and liquid dis-
engagement was affected in the sample bomb and the liquid was allowed
to collect at the bottom of the bomb before removal. The liquid flow
scheme and sampling techniques will be described in the experimental
procedure section.

<div align="center">Pressure and Flow Control</div>

The inlet pressure to the reactor was controlled using a Mitey-
Mite pressure controller. An internally loaded Mitey-Mite pressure
regulator was used in this study. However, a Mitey-Mite with an
externally loaded dome is recommended for future work. Pressure up
stream from the Mitey-Mite pressure controller was maintained with
Matheson Model 8 regulators. The system pressure was monitored using
a 0-5000 psig Heise guage. A Whitey needle valve was used to control
the off gas rate from the sample bombs. The off gas flow rate was
measured with either a 25 ml. bubble meter or a Precision Scientific
wet test meter.

<div align="center">Oil and Hydrogen Feed System</div>

The oil feed system consisted of a Ruska Model 2236 metering
pump and a 2250 ml stainless steel storage tank. One disadvantage of
this system was that the oil feed to the reactor had to be momentarily
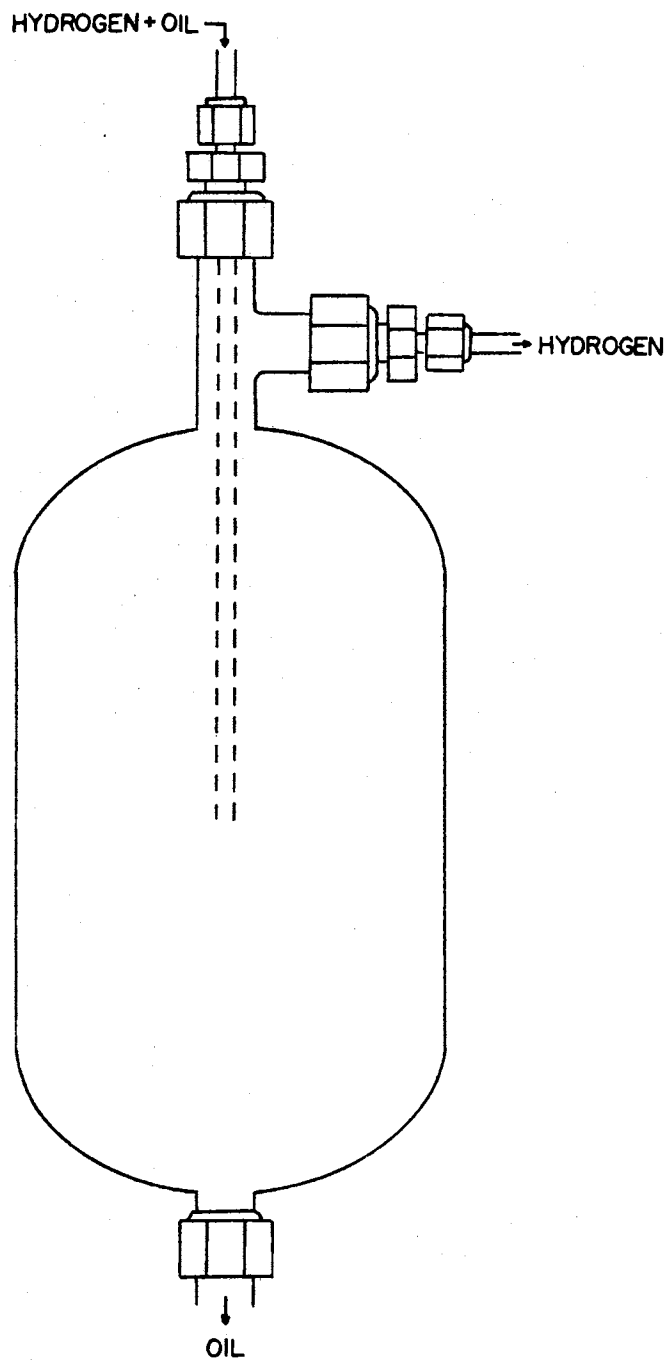
Figure 9. Sample Bomb Design

stopped to refill the pump syringe. This problem could be alleviated by using s Ruska pump equipped with two syringes. This arrangement would allow one syringe to be filled while the other fed oil to the reactor.

The hydrogen was fed directly to the reactor from storage bottles. A manifold was constructed to allow switching hydrogen bottles without disrupting the operation of the reactor. The only other special provision in the hydrogen feed system was an excess flow valve which would stop the hydrogen feed if a sudden pressure drop in the system occurred.

Temperature Measurement

The reactor temperature was monitored as a function of position in the reactor by moving a Conax J-SS4-G-T3 iron-constantan thermocouple along the reactor thermowell. The thermocouple voltage was converted to a digital temperature reading using a Leeds and Northrup 900 Series numatron. The digital readout was linearized according to the procedure given in Leeds and Northrup booklet 177626 Issue 2. The thermocouples were calibrated using a platinum resistance thermometer or platinum-platinum+10%rhodium thermocouple secondary standard.

Materials

The identification numbers on Figure 6 correspond to the equipment numbers given in Table II. Table II is a list of equipment used to construct the experimental apparatus.

TABLE II

LIST OF EXPERIMENTAL EQUIPMENT

Tubing: 1/4 inch O.D. stainless steel

1. Gas regulator - Air Products number E11-7-C485F

2. Gas regulator - Matheson number 26263-10

3. Gas regulator - Air Products E11-F-N1156

4. Valve - 1/4 inch brass Whitey bar stock ball valve

5. Vee tip valve - Autoclave number 10V-4071

6. Check valve - Autoclave number 10-6904-316-CW

7. Pressure reducing regulator - Grove Mitey-Mite model 94

8. Pressure guage - Heise bourdon tube gauge, 3000 psig maximum
    pressure

9. Vee tip valve - Autoclave number 10V-4071

10. Valve - Whitey 3TS4

11. Temperature Display - Leeds and Northrup 900 Series numatron with
    a Conax J-SS4-G-T3 thermocouple

12. Hewlett-Packard Model 240 Temperature Programmer with Marsh
    resistance heater

13. Powerstat - Curtin type 316 with Marsh resistance heater

14. Hewlett Packard Model 240 Temperature Programmer with Marsh
    resistance heater

15. Hewlett Packard Model 240 Temperature Programmer with Marsh
    resistance heater

16. Powerstat - Curtin type 316 with Marsh resistance heater

17. Reactor - 1/2 inch 316 stainless steel tube (see Figure 7)
    with aluminum block heaters (see Figure 8 insulated with McMaster

TABLE II (Continued)

Carr fiberglas insulation

18. Valve - Whitey 1VS4

19. Valve - Autoclave 10V-4071

20. Sample bomb - Hoke DOT3A18000

21. Valve - Autoclave 10V-4071

22. Valve - Autoclave 10V-4071

23. Valve - Whitey 3TS4

24. Sample bomb - Hoke DOT3A1800

25. Pressure guage - 0-3000 psig, Autoclave number P-480

26. Valve - Whitey 1VS4

27. Valve - Whitey 1VS4

28. Valve - Whitey 1VS4

29. Valve - Whitey 21RS4

30. Valve - Autoclave 10V-4071

31. Valve - Autoclave 10V-4071

32. Valve - Whitey 1VS4

33. Valve - Autoclave 10V-4071

34. Valve - Whitey 21RS4

35. Metering pump - Ruska 2236 metering pump

36. Pressure guage - Autoclave P-480

37. Valve - Autoclave 10V-4071

38. Oil Storage - Hoke 8HD2250

39. Valve - Autoclave 10V-4071

40. Rupture disk - 3000 psig, Autoclave

41. MSA Hydrogen Detector Model I-501

TABLE III

LIST OF CHEMICALS USED

Hydrogen - prepurified, 99.95%, 3500 psig - Matheson Company

Nitrogen - purity 99.997%, 2200 psig.- Matheson Company

10% Hydrogen Sulfide in Hydrogen - Matheson Company

Inert Reactor Packing - Maurice A semiporcelain berl saddles

Concentrated Sulfuric Acid - Baker reagent grade

Sodium Hydroxide - Baker reagent grade

Boric Acid - Baker reagent grade

Bromocresol Green - Allied Chemical

Methy Red - Allied Chemical

Hydrochloric Acid - Fisher Certified

Catalyst Preparation and Loading

The catalyst was crushed from 1/8 inch extrudates, as received

from Nalco Chemical Company, to 8-10 mesh particles. The catalyst

particle size was reduced to discourage bypassing of the reactants

around the catalyst bed. A catalyst bed depth of 20 inches was chosen

to allow volume hourly space times of 1.5, 0.75, and 0.375 hours

for oil flow rates of 25, 50, and 100 cc/hr. respectively. The

twenty inch catalyst bed was placed in the middle of the reactor to

minimize end effects. The following procedure was used to pack the

catalyst into the reactor:

1. Pour six inches of inert packing, 8-10 mesh, tapping the reactor to pack the inerts.

2. Pour twenty inches of catalyst, 8-10 mesh.

3. Pour six inches of inert packing, 8-10 mesh.

4. Place a small fifty mesh screen on the bottom of inerts.

5. Put a straight union on the reactor tube and screen.

The packed reactor was then secured in the system by the two feed lines at the top and the product line at the bottom. Immediately after connecting the reactor to the rest of the system, the system was pressure tested at room temperature using 2000 psig nitrogen. Then each fitting in the entire system was checked for leaks using a soap solution. Once the system was found to be free of leaks, the heating blocks were put in position and the insulation was installed. Next, the temperature controllers were connected to the heating blocks and the thermocouple was placed in the thermowell.

The catalyst was then heated to $450^{\circ}F$ for 12 hours with a low flow rate of prepurified nitrogen passing over the catalyst bed. The heating in the nitrogen atmosphere was done to remove water from the catalyst.

The last step in the catalyst preparation was sulfiding. Before sulfiding, the Mitey-Mite regulator and Heise guage were isolated from the system. Then, a five mole percent H_2S in hydrogen gas mixture was allowed to flow over the catalyst bed at a rate of a half cc/sec for 1.5 hours. The catalyst bed temperature was maintained at $450^{\circ}F$ throughout the sulfiding operation. The pressure was essentially atmospheric. Gases from the sulfiding step were

scrubbed with a caustic solution. After the sulfiding operation, the system was flushed with nitrogen before reconnecting the Mitey-Mite and Heise guage.

Normal Operation

First, the system pressure was raised to the planned operating pressure. Next, the temperature controllers were set at the proposed reactor operating temperature and the system was allowed to reach steady state. Temperature profiles were recorded every 15 minutes. The system was initially run for 48 hours on oil to obtain a stable catalyst activity. Table IV gives the valve positions for "normal operation." The identification numbers in Table IV correspond to the equipment identification numbers on Figure 6.

TABLE IV

VALVE POSITION SUMMARY FOR "NORMAL OPERATION"

Valve		Valve		Valve	
4	open	22	open	31	closed
5	closed	23	open	32	open
9	open	26	closed	33	open
10	open	27	closed	34	open
18	closed	28	closed	37	closed
19	closed	29	open	39	open
21	open	30	closed		

Sampling Procedure

Liquid samples were taken about an hour after the reactor had stabilized at the desired operating conditions. Fifty milliliter oil samples were taken. The following procedure was used to obtain a sample of the liquid portion of the reactor product starting from "normal operation."

1. Simultaneously open Valve 19 and close Valves 21 and 22.

2. Open Valve 30.

3. Open Valves 26 and 27 and allow nitrogen to bubble through Sample Bomb 2.

4. Close Valves 27 and 30.

5. Open Valve 28 to remove oil.

6. Close Valve 28 when all the oil has been removed.

7. Close Valves 9 and 19 to isolate the reactor.

8. Open Valve 31 to repressurize Sample Bomb 2.

9. Close Valve 31 when Sample Bomb 2 has reached the reactor operating pressure.

10. Open Valves 9, 21, and 22 to return to normal operation.

Reactor Shutdown Procedure

The shutdown procedure was initiated from the "normal operation" by closing Valve 4. Then, the temperature controllers and pump were turned off. The pressure was allowed to bleed down to 200 psig. When the reactor temperature reached ambient, the system pressure was further reduced to atmospheric pressure.

Temperature Measurement

The reactor temperature was measured using a thermocouple in a thermowell running the length of the reactor (see Figure 7). The temperature was taken at one inch intervals along the length of the catalyst bed. Figure 10 is a typical plot of reactor temperature as a function of distance from the top of the catalyst bed. The position the heater blocks are also shown.

The radial temperature gradient in the catalyst bed was estimated by measuring the temperature of the outside of the reactor wall and the temperature in the thermowell at the same location in the reactor using the same thermowell. These tests indicate that the temperature in the thermowell was typically about $3^{o}F$ higher than the temperature of the outside of the reactor wall at the same distance from the top of the catalyst bed.

In this chapter, the design and operation of the experimental apparatus was described. In the next chapter, methods used to analyze the reactor feed and product and characterize the catalyst will be described.
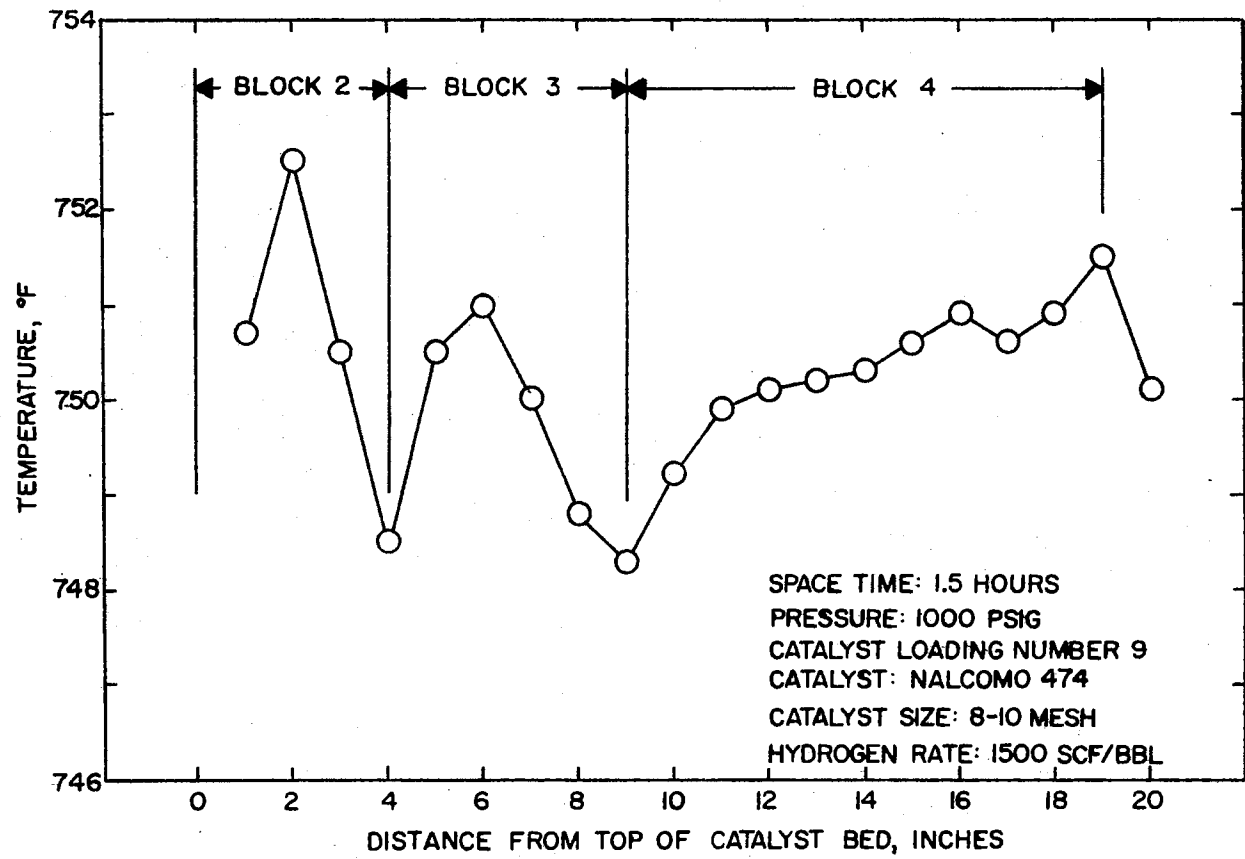
Figure 10. Typical Temperature Profile

CHAPTER IV

FEEDSTOCK AND CATALYST CHARACTERIZATION

In the previous chapter, the design and operating procedure for the hydrotreating reactor was described. This chapter will consider the techniques used to characterize the reactor feedstock and product oil and the hydrotreating catalyst. An estimate of both the precision and accuracy of the analysis will be given.

Nitrogen Analysis

The total organonitrogen concentration in the reactor feed and product was used to evaluate the reactor performance. The nitrogen analysis procedure used in this work was developed by Kjeldahl (31). The method consists of four steps: digestion, neutralization, distillation, and titration.

Digestion

The following procedure was used in the digestion step of the analysis:

1. Thirty milliliters of concentrated sulfuric acid (Baker reagent grade) was poured into a standard two hundred milliliter Kjeldahl flask.

2. A known mass, about one gram, of the oil was then mixed with the sulfuric acid.

3. Next, ten Hegar selenium crystals were added to the oil-sulfuric acid mixture.

4. The oil-sulfuric acid mixture was heated using a heating mantle (Glas-Col, Series 0, 100 watts) with a powerstat (Curtin Number 232-801) set at 75 volts in a hood.

5. After 12 hours of heating at 75 volts, the voltage was increased to 100 volts.

6. The oil-sulfuric acid mixture was cooled after 36 hours of digestion at 100 volts. This completed the digestion phase of the nitrogen analysis.

Neutralization

7. After the oil-sulfuric acid mixture had cooled to essentially room temperature, one hundred milliliters of distilled water was added to the mixture.

8. Then, sixty milliliters of a solution of fifty percent sodium hydroxide (Baker Reagent Grade) and distilled water was poured into the Kjeldahl flask.

Distillation

9. The indicator solution was prepared according to the following procedure:
   a. Heat 340 grams of boric acid (Baker Reagent Grade) in three liters of distilled water.
   b. Mix 65 milliliters of ethanol, .0625 grams of bromocresol green (Allied Chemical), and .0625 grams of methyl red (Allied Chemical).

c. Mix the above solution with 8160 milliliters of distilled
water.

10. The arrangement of the distillation apparatus is presented
in Figure 11.

11. After the sample solution started to boil, 40 milliliters
of a fifty percent sodium hydroxide solution were slowly
added to the boiling mixture.

12. The sample was boiled until one hundred milliliters were
distilled into the indicator solution.

<u>Tritration</u>

13. The indicator solution was titrated using .01 normal hydro-
chloric acid (Fisher Certified). The titration was considered
complete when any pink color was observed.

14. The weight percent nitrogen was calculated using Equation 4.1.

$$\text{Weight Percent Nitrogen} = \frac{1.4 \, V_{HCl}}{\text{Oil Mass}} \tag{4.1}$$

Where, V_{HCl} is the volume, milliliters, of .01 normal hydro-
cloric acid solution titrated with the sample under analysis
less the volume titrated when the above procedure was per-
formed without an oil sample. The oil mass is the mass,
grams, of oil sample used in Step 2.

Distillation

Since the ease of denitrogenation has been shown (6) to be a
function of boiling point, the boiling range of the hydrocarbon
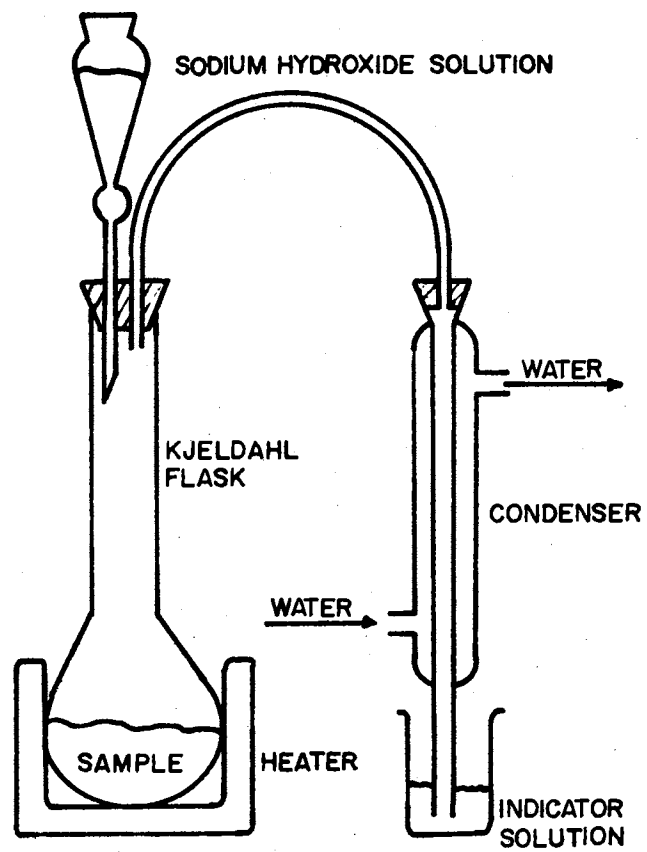
Figure 11.   Distillation Apparatus for
                Kjeldahl Nitrogen Analysis

feedstock is an important characterization parameter. The boiling

point range of the feedstock used in this work was estimated using the

ASTM D1160 procedure (32). This is a standard procedure and will not be

discussed in detail here. The reactor feed and product were fractionated

into boiling ranges by stopping the ASTM D1160 distillation at prede-

termined temperatures, repressurizing the system to atmospheric pressure,

removing the distillate, evacuating the still, and continuing the dis-

tillation. These samples were analyzed to obtain the total nitrogen

content as a function of boiling range in the reactor feed and product.

Accuracy and Precision of Nitrogen Analysis

The first step in establishing the accuracy and precision of the

organonitrogen analysis is to consider the analysis of known mixtures.

Since the reactor feedstock used in this work was highly aromatic,

pyridine (Baker Analyzed), aniline (Fisher Certified), indole (Fisher

Certified), and quinoline (Fisher reagent) were selected as model com-

pounds. Toluene (Fisher reagent) and cyclohexane (Baker Analyzed)

were used as solvents. All known samples were mixed to have a nitrogen

content of about one percent total nitrogen, the organonitrogen content

of the feedstock used in this study.

Figure 12 is a plot of the logarithm of the weight percent nitro-

gen remaining unanalyzed in the known solutions of model compounds in

cyclohexane as a function of total digestion time. One can conclude

from Figure 2 that (1) a first order rate expression is a reasonable

description of the kinetics of the digestion step of the nitrogen

analysis, (2) the amine group in analine is much easier to analyze

than nitrogen in an aromatic ring as in the case of pyridine, quinoline,
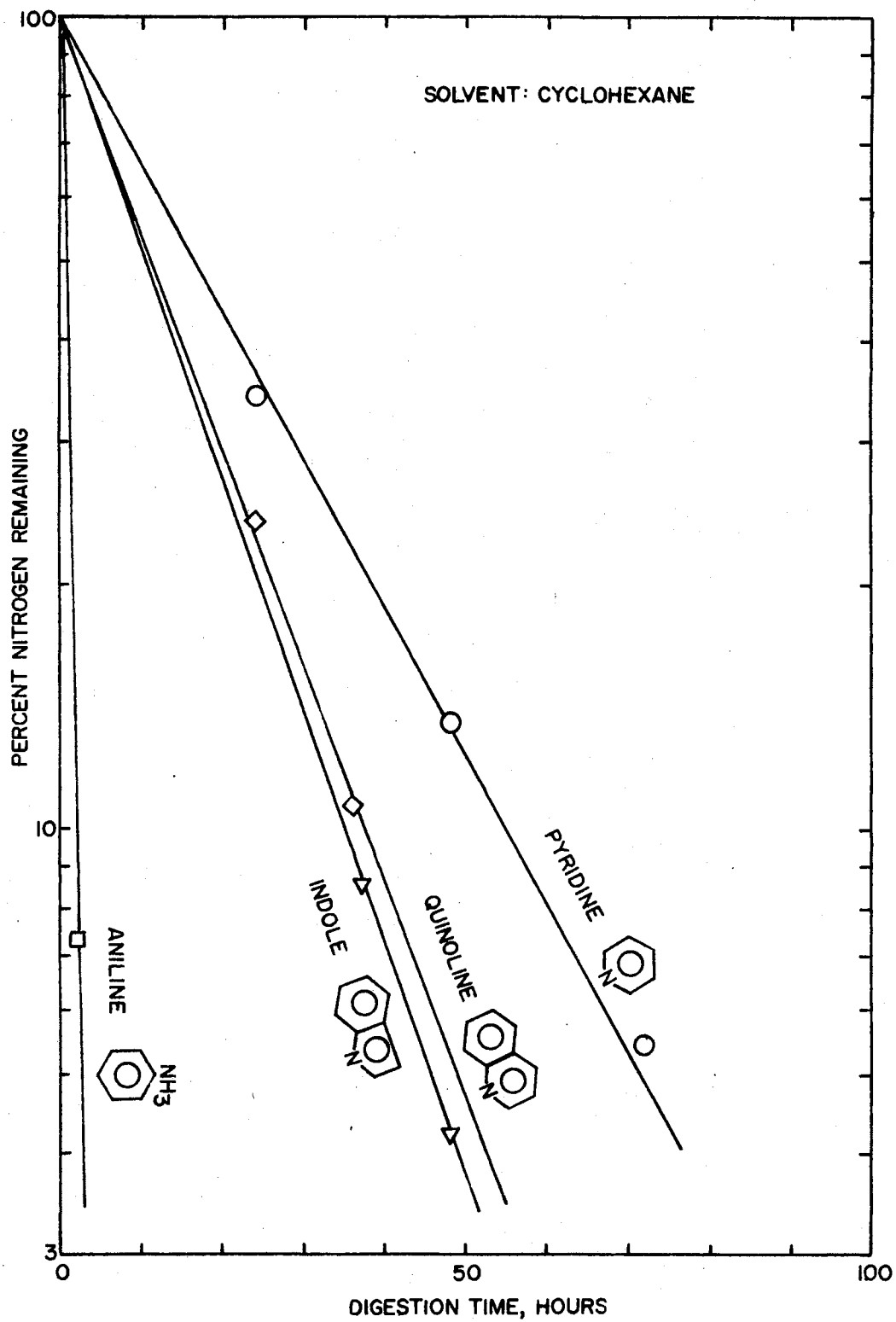
Figure 12. Kinetics of Digestion of Model Organonitrogen Species

and indole, (3) the two aromatic ring structures, indole and quinoline, with the nitrogen in the aromatic ring are easier to digest than the single ring structure, pyridine. These data also indicate that nitrogen analysis with the nitrogen atom in the aromatic ring requires a very long digestion time.

Table V is a comparison of the known and measured nitrogen levels. The data in Table V indicate that the nitrogen analysis method used in this work is capable of analyzing the model compounds. However, the ability to analyze the organonitrogen level in the reactor feed and product is of primary interest in this study.

TABLE V

DENITROGENATION OF MODEL COMPOUNDS

Compound	Digestion Time Required for 99% Conversion, Hours	99% of Known Organonitrogen Level, Wt.% Nitrogen	Nitrogen Level Analyzed, Wt.% Nitrogen
Pyridine	109	.88	.87
Quinoline	75	.94	.94
Indole	4	1.06	1.04

The first step in establishing the ability to analyze the reactor feedstock and product oil will be to consider the ease of digestion as

a function of boiling point of the oil. Figure 13 is a plot of the
percent nitrogen remaining as a function of digestion time with para-
meters of boiling point range of the feed material. T_{50} is the boil-
ing point of the material at fifty millimeter mercury total pressure.
The results for the model compounds (previously presented in Figure
12) are given for comparison. Although, eight boiling ranges were
studied, the kinetic data tended to group into three boiling ranges
(<429°F, 429-506°F, and >506°F at fifty millimeters mercury total
pressure). These boiling ranges roughly correspond to species con-
taining two conjugated aromatic rings, three conjugated aromatic
rings, and greater than three conjugated aromatic rings, respectively.
Apparently, the larger the organonitrogen specie, the easier it is to
digest. The results of the model compounds tend to support this con-
clusion. Figure 13 also shows that the analysis of the model organo-
nitrogen species was much more difficult than the analysis of any of
the boiling ranges of the feedstock used in this work. Therfore, it
seems reasonable to assume that if one could analyze the model com-
pounds, then that person could also analyze the feedstock used in this
work.

The next step will be to determine the digestion time required
to analyze the feed material. Since the reactor feedstock is highly
aromatic and the reactor product is an aromatic-naphthenic oil, one
would like to know if this difference in oil solvent type affects the
ease of digestion. In order to test for this effect, pyridine was
analyzed using cyclohexane and toluene as solvents. Figure 14 is a
plot of the weight percent nitrogen remaining as a function of the
digestion time for pyridine with parameters of solvent type. These
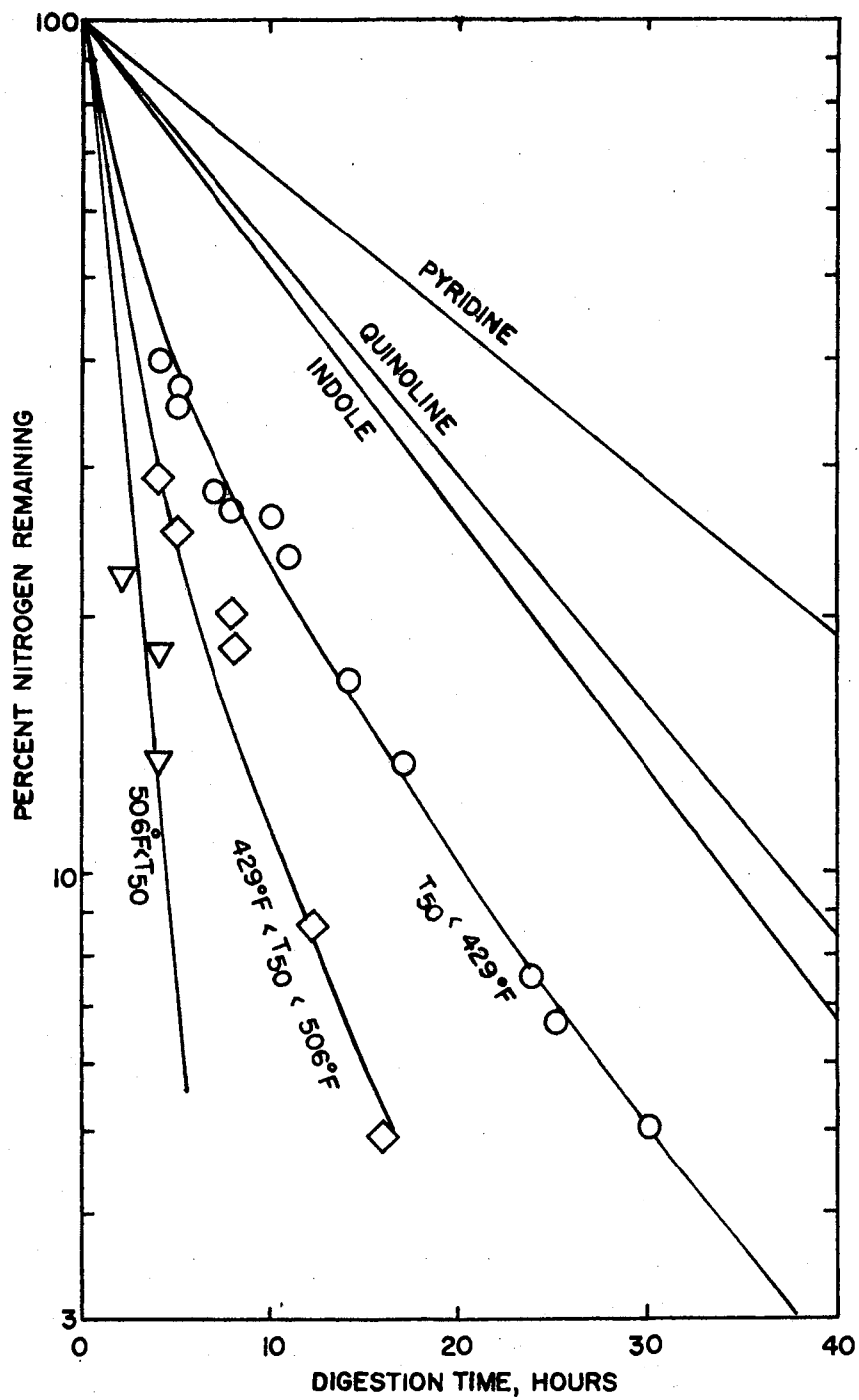
Figure 13. Kinetics of Digestion of Anthracene
Oil
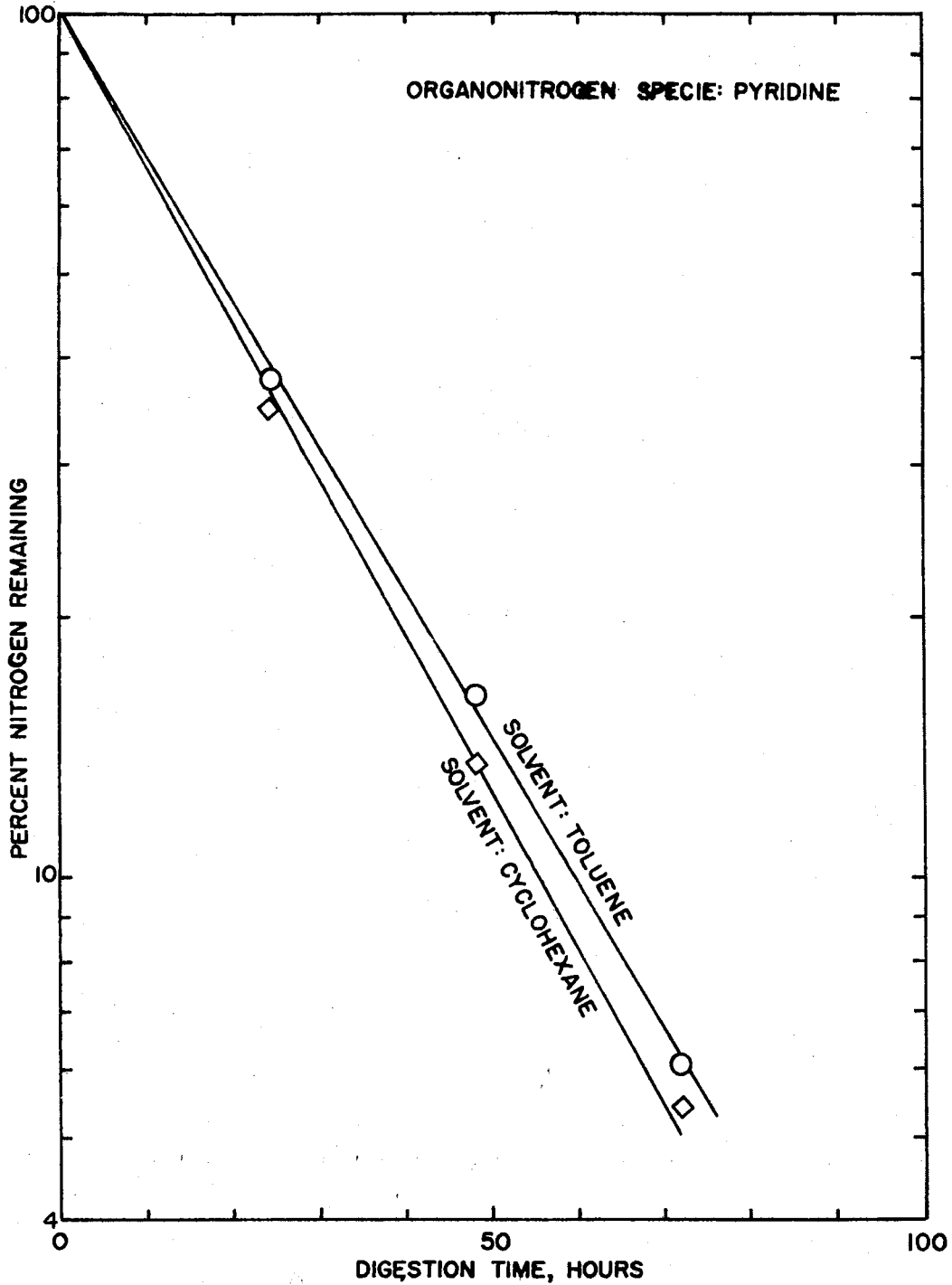
Figure 14. Solvent Effect on the Kinetics of Digestion

results indicate that the solvent effect is small. Therefore, a single digestion time can be established for both the reactor feed and product. All that remains to be done is to determine the digestion time required to analyze the feedstock used in this work.

Figure 15 is a plot of the weight percent nitrogen analyzed as a function of digestion time. The plot shows that for digestion times of 48 hours or more, the organonitrogen level measured is approximately constant. The digestion time for the oil used in this work was set at 48 hours. The next step of the analysis will be to estimate the accuracy and precision of the nitrogen analysis.

Nitrogen Analysis Precision

Six samples of the reactor feedstock were analyzed to determine the organonitrogen content of the oil and estimate the precision of the analysis. The average value of the organonitrogen level analyzed was .984 weight percent nitrogen. A standard deviation of .00345 weight percent nitrogen was calculated from these data. Since most of the imprecision in the analysis is thought to be in obtaining reproducible end point, the imprecision of the analysis should be approximately independent of the organonitrogen level.

Accuracy of Nitrogen Analysis

The accuracy of the nitrogen analysis is primarily a function of the digestion time and the accuracy of the hydrochloric acid solution used in the titration. The inaccuracy introduced by not having an infinite digestion time can be estimated from Figure 13 and the analysis of the feedstock as a function of boiling point. These calculations
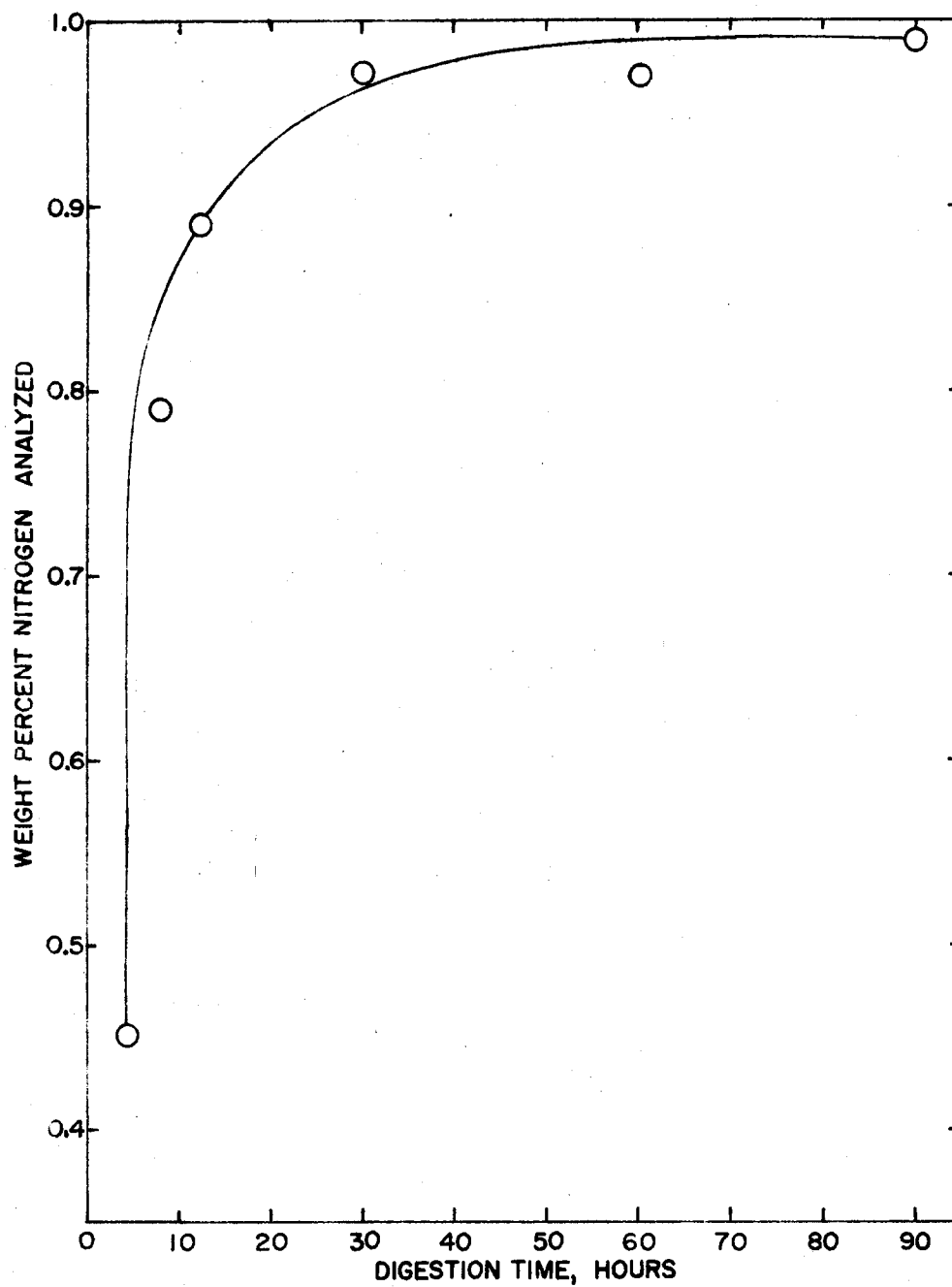
Figure 15.   Weight Percent Nitrogen Analyzed in the
Reactor Feedstock as a Function of
Digestion Time

indicate that the analysis of the feed should be about .005 weight percent nitrogen (about .5 percent error) low. In addition, some nitrogen is probably lost to the atmosphere in the digestion step of the analysis. This effect would also have the effect of making the analyzed nitrogen level less than the actual content. The error introduced by the standarization of the hydrochloric acid solution is thought to be small compared to the above sources of error. Therefore, the analysis of the organonitrogen level is probably between .5 and 1 percent low.

Feedstock Characterization

Table VI is a summary of the characteristics of the feedstock used in this work.

TABLE VI (28)

FEEDSTOCK PROPERTIES

Carbon, wt%	90.65
Hydrogen, wt%	5.76
Sulfur, wt%	.486
Nitrogen, wt%	.984
Ash	Nil
API at 60°F	-7

TABLE VI (28) (Continued)

True Boiling Cruve*	380°F
10 vol%	450
30	450
50	650
70	700
90	815

*Estimated from an ASTM D 1160 at 50 mm Hg.

However, this study is primarily interested in the organonitrogen level and distribution in the feedstock. Table VII gives the organonitrogen level as a function of boiling point at 50 mm Hg. The boiling ranges were set such that approximately equal volumes of material were in each boiling range. The maximum still temperature was set at 550°F to prevent excessive cracking.

TABLE VII

ORGANONITROGEN CONTENT DISTRIBUTION

Weight Percent Nitrogen	Boiling Range Endpoing, °F at 50 mm Hg.	Percent of Feed Mass in Boiling Range
.60	328	10.5
1.07	394	10.6

TABLE VII (Continued)

Weight Percent Nitrogen	Boiling Range Endpoint, $^{\circ}F$ at 50 mm Hg.	Percent of Feed Mass in Boiling Range
.93	429	11.0
.81	472	11.2
.96	485	11.0
.99	507	12.7
1.03	548	12.7
1.21	–	21.0

Catalyst Characterization

The catalysts used in this work were obtained from the Nalco Chemical Company. The details of the catalyst preparation are not available. However, Nalco attempted to vary the pore size distribution while leaving the intrinsic activity unchanged. Tabel VIII is a summary of the properties of the catalysts used in this work.

In the preceding two chapters, the design and operating procedure for the reactor and product analysis equipment were presented. In the next chapter, the results of all the experimental runs will be presented.

TABLE VIII

CATALYST PROPERTIES

Chemical Analysis Wt%, Dry Basis:	Nalcomo 474	Nalco 72-4710A	Nalco 72-4710B
% MoO_3	12.5	12.5	12.5
% CoO	3.5	3.5	3.5
%Na_2O	0.08	0.08	0.08
% Fe	0.03	0.03	0.03
% SiO_2	1.5	1.5	1.5
% Al_2O_3	82.39	82.39	82.39
Physical	Nalcomo 474	Nalco 72-4710A	Nalco 72-4710B
Pore Volume, cc/gm	.463	.441	.556
Surface Area, m^2/gm	240.	298.	303.
Apparent Bulk Density, gm/cc	.73	.79	.73
Particle Size, Mesh	8-10	8-10	8-10

CHAPTER V

RESULTS

After several preliminary runs, to establish the operability
of the experimental apparatus, 328 experimental runs were made to
determine the total nitrogen concentration of the reactor product oil
as a function of: (1) reactor temperature in the range of 600 to
800°F, (2) pressures of 500, 1000, and 1500 psig, (3) catalyst particle
sizes of 44 and 9 mesh (particle diameters of about .013 and .078
inches), (4) hydrogen gas rates of about 1500 and 20,000 standard
cubic feet per barrel of oil fed, (5) liquid volume hourly space times
of 0.375, 0.75, and 1.5 hours, (6) catalyst bed depths of 10 and 20
inches. Most of the runs were made using Nalcomo 474 catalyst. Proper-
ties of this catalyst are given on Table VIII. Two other catalysts
obtained from the Nalco Chemical Company with identical metals content
to Nalcomo 474 but with slightly different pore size distributions were
studied to determine the effect of catalyst pore size distribution.
The data from all the runs are tabulated in Appendix A.

Inert Runs

Runs 1-27 were made with the reactor loaded with crushed ceramic
beryl saddles to estimate the conversion of organonitrogen species
due to noncatalyzed reactions. All runs were made with a total
reactor pressure of 1000 psig and a hydrogen rate of 1500 standard

cubic feet per petroleum barrel. Volume hourly space times of 0.375,
0.75, and 1.5 hours and reactor temperatures of 700, 750, and 800°F
were studied. Figure 16 is a plot of the weight percent atomic
nitrogen present in the reactor product as a function of volume hourly
space time.

The conversion at a space time of 0.375 hours was nearly inde-
pendent of the reactor operating temperature in the range of 700 to
800°F. A possible explanation for this observation is that the feed
contained some organonitrogen species that were very easily hydro-
denitrogenated at 700°F even without catalyst. This hypothesis sug-
gests that the oil could contain organonitrogen species with a wide
range of reactivities with respect to hydrodenitrogenation.

The reactivity of organonitrogen species with respect to
denitrogenation as a function of boiling point was then estimated by
analyzing the total nitrogen content of oil in fixed boiling ranges
from an ASTM D1160 (32) of the reactor feedstock and product. Figure
17 is a plot of the logarithm of the weight percent elemental nitrogen
content as a function of the arithmetic mean of the boiling point of
each cut at a pressure of 50 mm Hg. of the feedstock and reactor
product from Run 3.

<center>Reference Runs</center>

A set of reference runs was taken to establish a basis for the
balance of the study. Specifically, Runs 27-70 were made to determine:

1. Number of hours of continuous operating required to obtain
   reasonably stable catalyst activity.
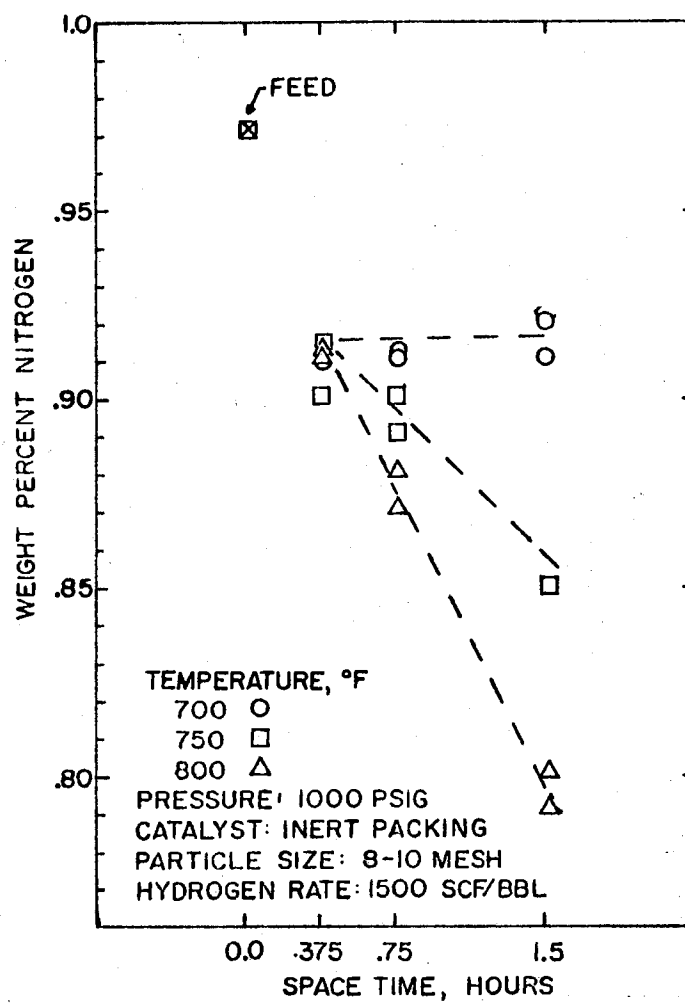
Figure 16. Denitrogenation with Ceramic
Packing
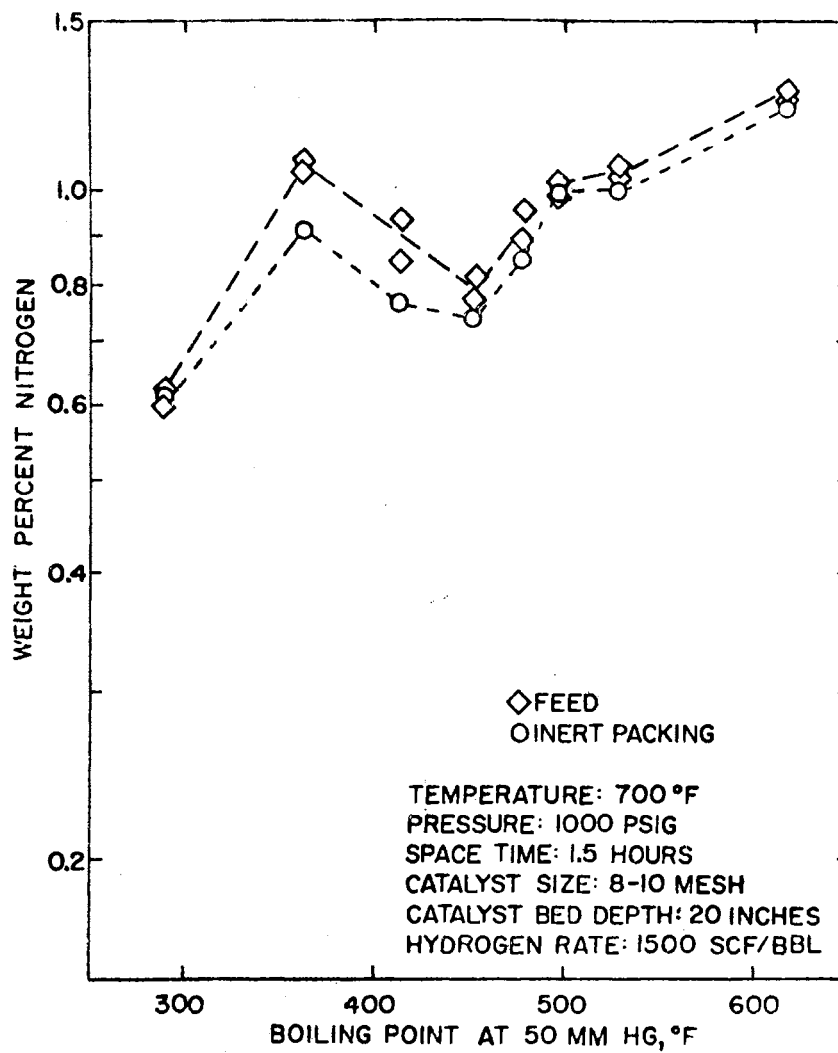
Figure 17. Denitrogenation with Ceramic
Packing as a Function of
Boiling Point at 50 mm Hg

2. Practical reactor operating temperature range for the
    remainder of this study.

3. The effect of increasing the hydrogen flow rate from 1500
    to 20,000 standard cubic feet per petroleum barrel.

The reactor was operated for 42 hours at $700^{\circ}F$, 1000 psig,
hydrogen rate of 1500 standard cubic feet per barrel, a space time of
1.5 hours, and using Nalcomo 474 catalyst. Figure 18 is a plot
of the weight percent nitrogen in the reactor effluent as a function
of the number of hours of continuous operation at the specified con-
ditions. Figure 18 indicates that after 35 hours of continuous
operation, the measured product nitrogen level remained within .01
weight percent of .39 weight percent total nitrogen.

The stability of the catalyst at any temperature was estimated
by comparing the 1.5 hour space time results at the beginning and the
end of a series of isothermal and isobaric runs. Typically, the
catalyst deactivation was measured over about a 20-hour interval.
Figure 19 is a plot of the difference between the weight percent
nitrogen obtained at the beginning and the end of the series of iso-
thermal and isobaric runs as a function of reactor operating tempera-
ture. Thus, a negative value indicates catalyst deactivation; a
negligible difference indicates stable catalyst activity. At tempera-
tures less than $800^{\circ}F$, no catalyst deactivation was detected. The
data indicate that catalyst deactivation may become significant at
$800^{\circ}F$.

During the series of runs, the reactor product organosulfur
content for a companion desulfurization study (33) was too low to

CATALYST LOADING NUMBER 2
TEMPERATURE 700°F
SPACE TIME: 1.5 HOURS
PRESSURE: 1000 PSIG
CATALYST: NALCOMO 474
CATALYST BED DEPTH: 20 INCHES
CATALYST SIZE: 8-10 MESH
HYDROGEN RATE: 1500 SCF/BBL
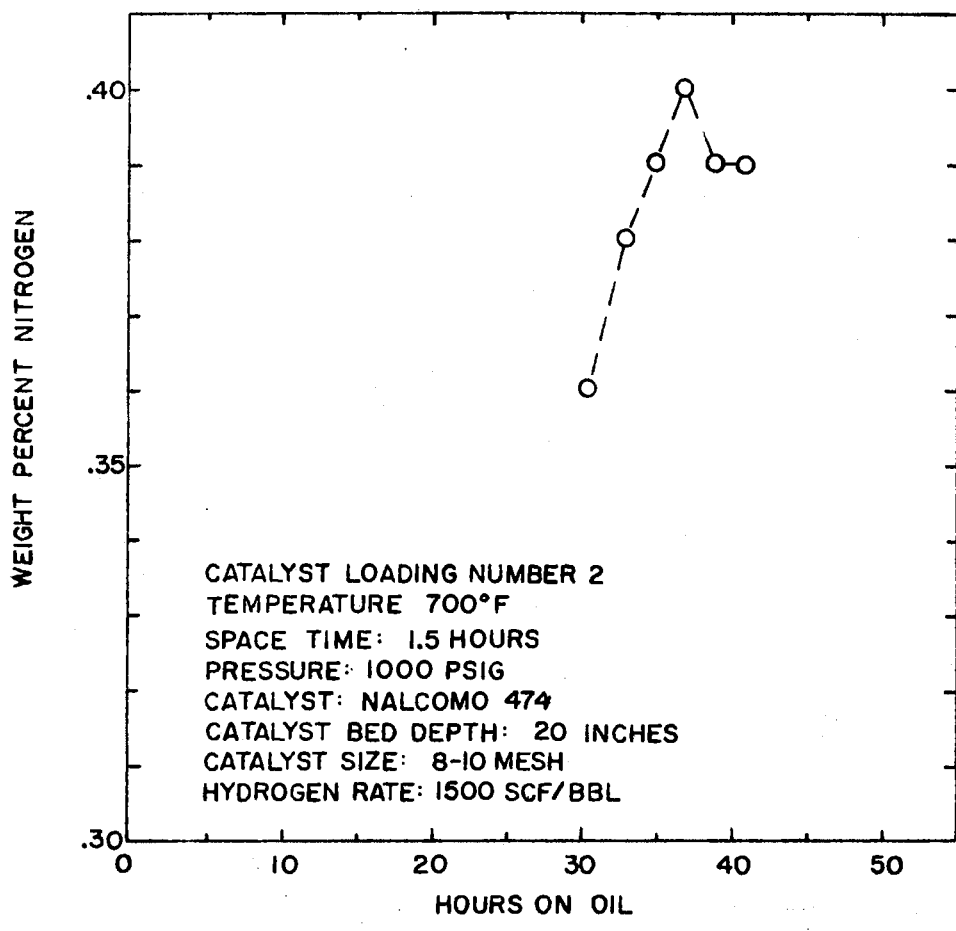
Figure 18. Catalyst Activity Stabilization
for Catalyst Loading Number 2
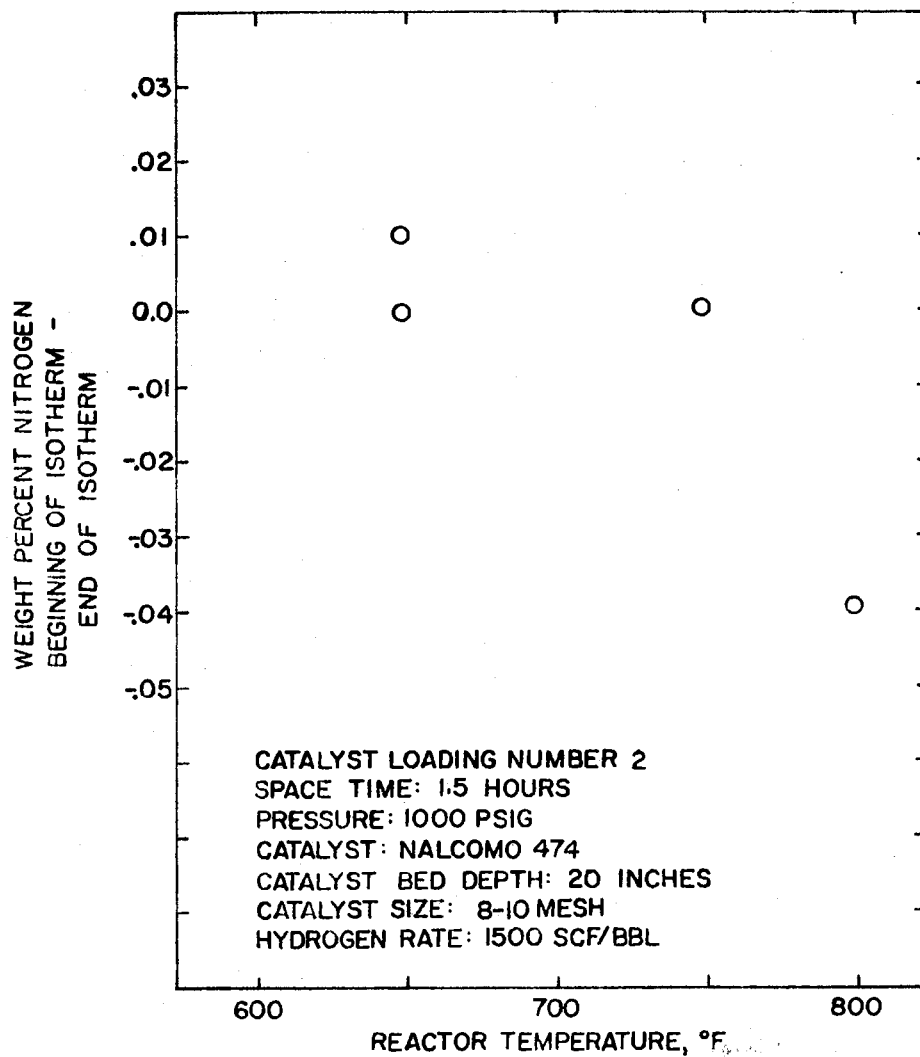
Figure 19. Catalyst Deactivation from Catalyst
Loading Number 2

analyze with reactor operating conditions more severe than 700°, 1000

psig, and a space time of .75 hours. In order to gain kinetic information

tion for desulfurization, 600 and 650°F isotherms were run. Figure

20 is a plot of the weight percent nitrogen in the reactor product as

a function of space time with parameters of reactor operating tempera-

ture.

The effect of increasing the hydrogen rate from 1500 to 20,000

standard cubic feet per barrel was determined by comparing consecutive

runs at the two hydrogen rates. Table IX summarizes the results. The

data presented in Table IX indicate that increasing the hydrogen

rate from 1500 to 20,000 standard cubic feet per barrel had a negli-

gible effect on the conversion of total nitrogen in the product oil.

TABLE IX

EFFECT OF HYDROGEN RATE

Reactor Temperature, °F	Reactor Pressure psig	Volume Hourly Space Time	Hydrogen Rate, SCF/Bbl.	Weight Percent Nitrogen	Run Number
700	1000	1.5	1500	.53	51
700	1000	1.5	1500	.53	52
700	1000	1.5	20000	.54	53
700	1000	1.5	20000	.53	54
650	1000	1.5	1500	.64	61
650	1000	1.5	1500	.65	62
650	1000	1.5	20000	.68	63
650	1000	1.5	20000	.68	64
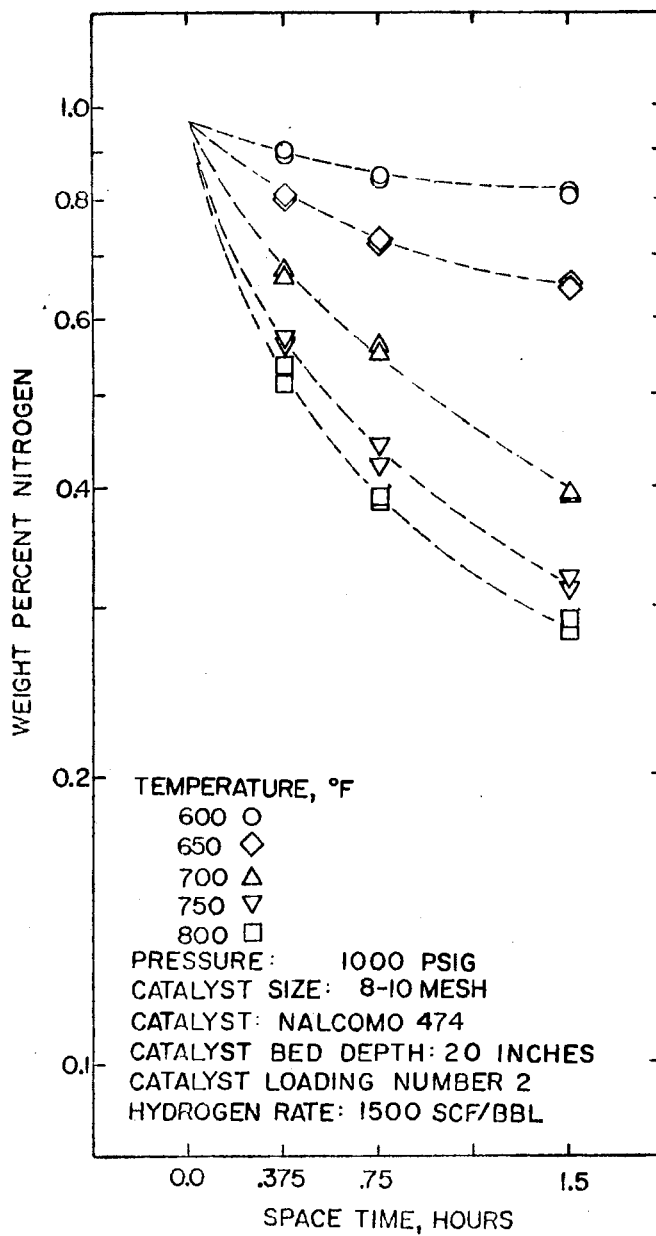
Figure 20. Denitrogenation Kinetics
from Catalyst Loading 2

Reproducibility Check

Experimental reproducibility was checked by reloading the reactor with fresh Nalcomo 474 catalyst and using the same pretreatment procedure as in the previous catalyst loading. Figure 21 is a plot of the weight percent nitrogen in the reactor product as a function of the number of hours of continuous operation at these conditions. The general negative slope of the plot indicates that the catalyst is becoming more active with time. The catalyst activity stabilization plot for Catalyst Loading 2 (Figure 18) indicated that the catalyst activity was decreasing with time. After thirty-five hours of continuous operation, the weight percent nitrogen in the product was within 0.01 of 0.40 for Catalyst Loading Number 3. After thirty-five hours of continuous operation, the product weight percent nitrogen was within 0.01 of 0.39 in Catalyst Loading Number 2. Therefore, the two separate catalyst loadings results reproduced within the precision of the individual runs.

The reproducibility of the weight percent nitrogen in the reactor product oil was also tested by attempting to reproduce the $700^{\circ}F$ isotherm. These data are presented in Figure 22. The weight percent in the product oil lie in a 0.03 weight percent nitrogen range for both catalyst loadings.

Pressure Effect Runs

After completing the reproducibility runs, Catalyst Loading 3 was continued to determine the effect of reactor operating pressure on the weight percent nitrogen level in the reactor product oil.

CATALYST LOADING NUMBER 3
TEMPERATURE 700°F
SPACE TIME: 1.5 HOURS
PRESSURE: 1000 PSIG
CATALYST: NALCOMO 474
CATALYST BED DEPTH: 20 INCHES
CATALYST SIZE: 8-10 MESH
HYDROGEN RATE: 1500 SCF/BBL
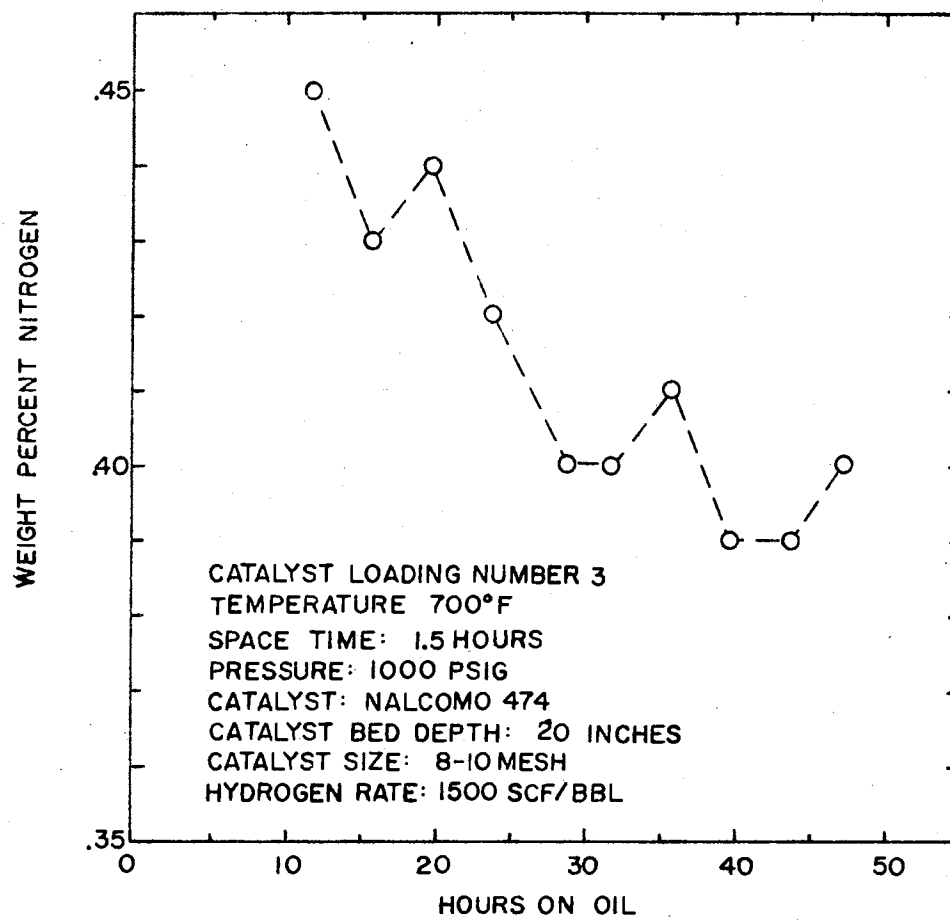
Figure 21.   Catalyst Activity Stabilization for
Catalyst Loading Number 3
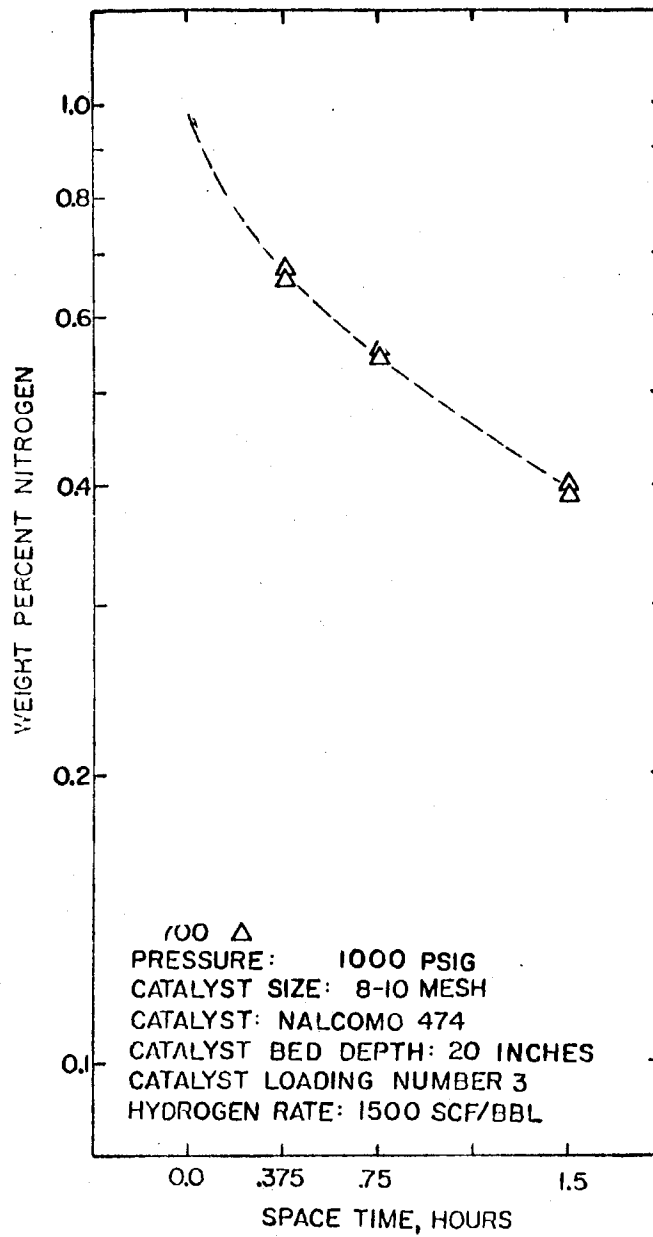
Figure 22. 700°F Isotherm from
Catalyst Loading
Number 3

Figures 23, 24, and 25 are plots of the logarithm of weight percent nitrogen in the product oil as a function of space time with parameters of reactor operating temperature at 500, 1000, and 1500 psig, respectively.

Figure 26 is a plot of the difference between the weight percent nitrogen in the product oil obtained at the beginning and the end of a series of isothermal and isobaric runs as a function of reactor operating temperature. The general negative slope of this plot indicates that catalyst deactivation becomes more severe with increasing temperature. Figure 27 is a plot of the difference between the weight percent nitrogen obtained at the beginning of the isotherm and the end as a function of reactor operating pressure. If the catalyst stability is a function of reactor operating pressure at these conditions, the effect is the same order of magnitude as the scatter in the data presented in Figure 27.

Effect of Catalyst Particle Size

The reactor was reloaded with 40-48 mesh Nalcomo 474 catalyst, as compared to the 8-10 mesh size used in the reference runs. A reactor start-up procedure identical to Catalyst Loading 2 and 3 was used. Figure 28 is a plot of the weight percent nitrogen in the reactor product oil as a function of the number of hours on continuous operation at the same conditions as used in Catalyst Loadings 2 and 3. The 0.42 weight percent nitrogen obtained at the end of the catalyst conditioning run is greater than the .39 and .40 weight percent nitrogen obtained in Catalyst Loadings 2 and 3, respectively. One would normally expect that the reduction of the catalyst particle
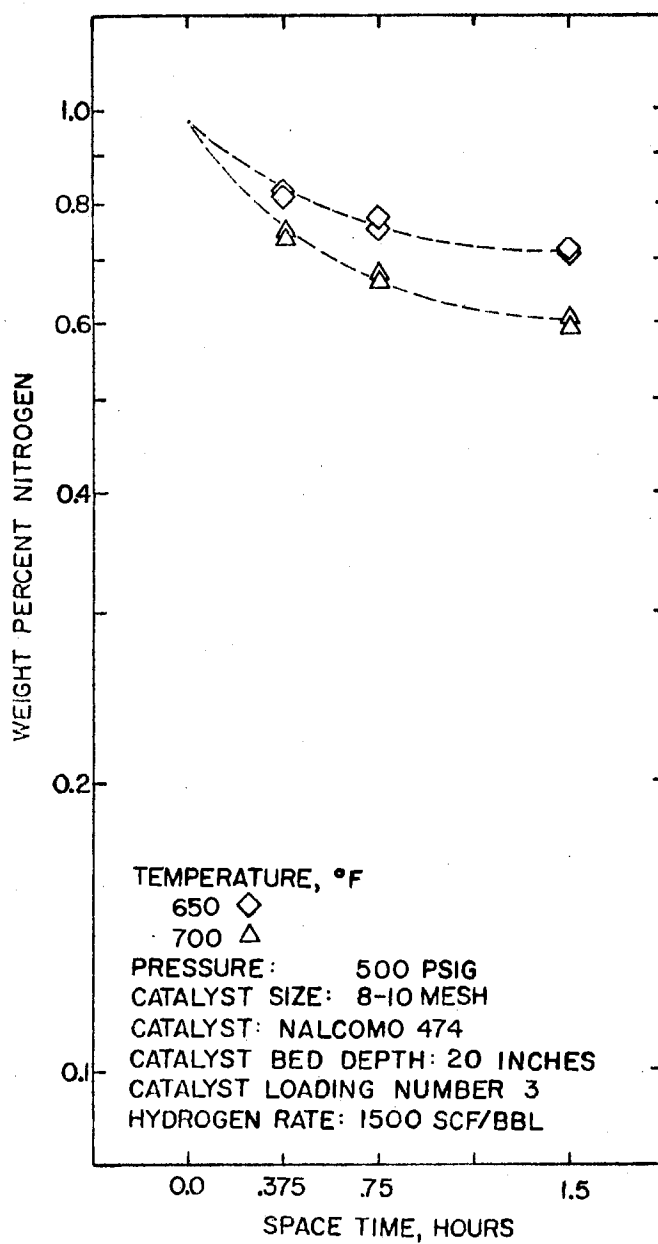
Figure 23. Denitrogenation Kinetics
from Catalyst Loading
Number 3 at 500 psig
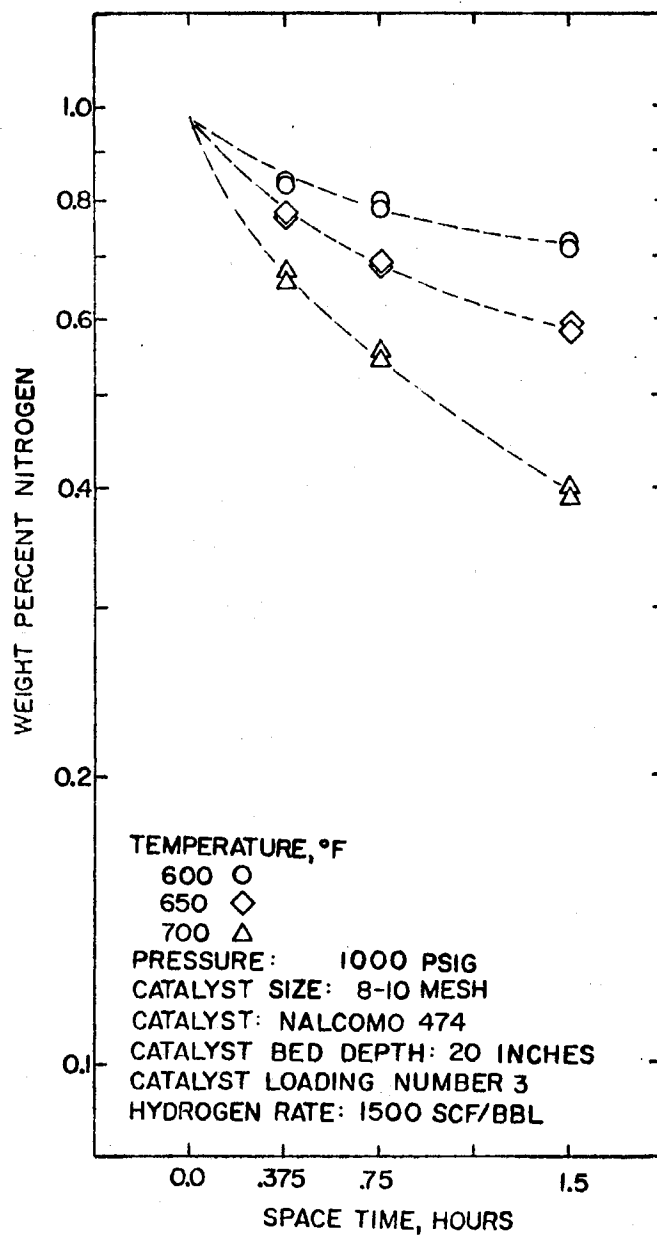
Figure 24.   Denitrogenation Kinetics
from Catalyst Loading
Number 3 at 1000 psig

Figure 25. Denitrogenation Kinetics from Catalyst Loading Number 3 at 1500 psig
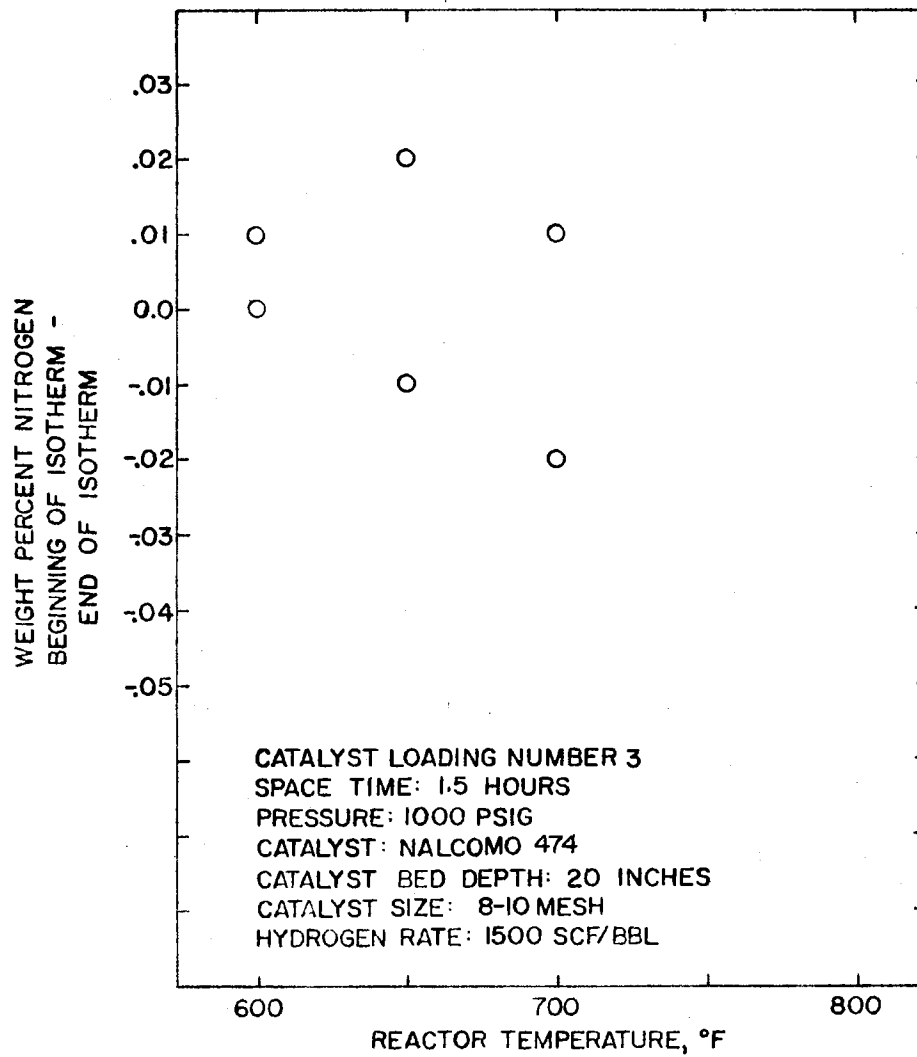
Figure 26.   Catalyst Deactivation from
Catalyst Loading Number 3
as a Function of Temperature
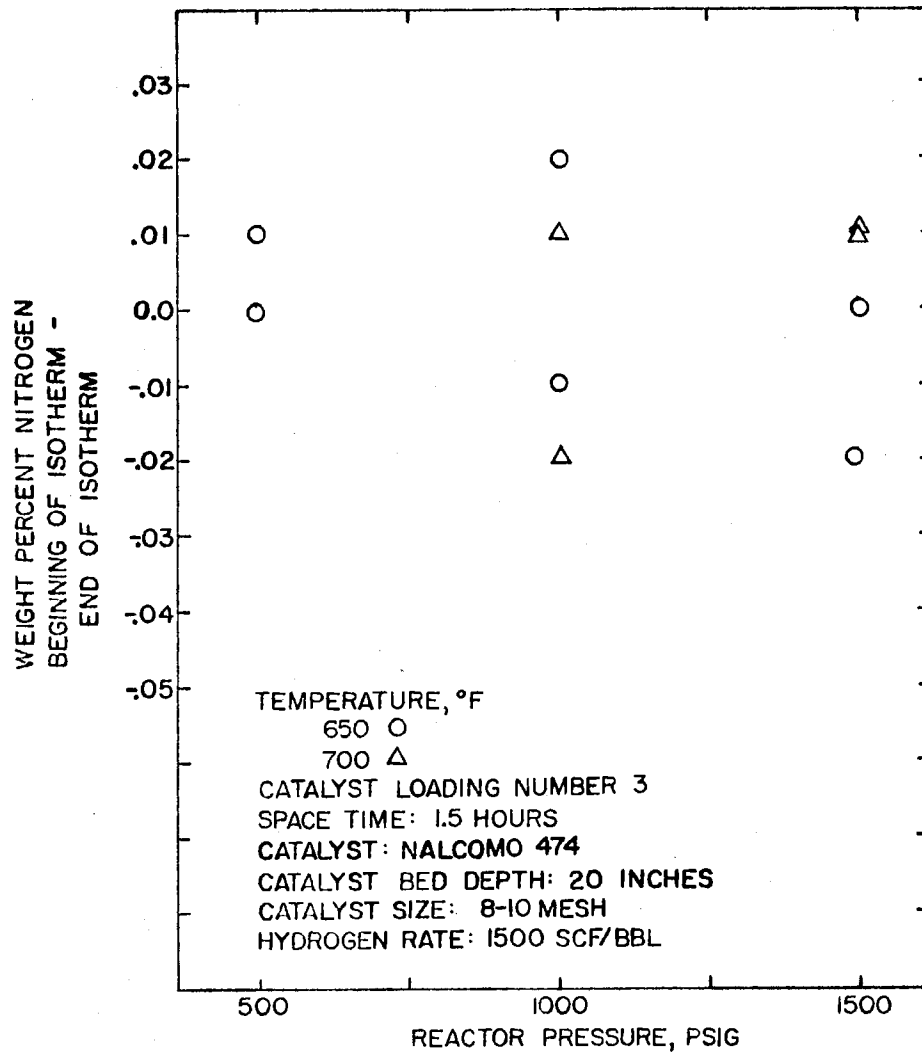
Figure 27. Catalyst Deactivation from
Catalyst Loading Number 3
as a Function of Pressure
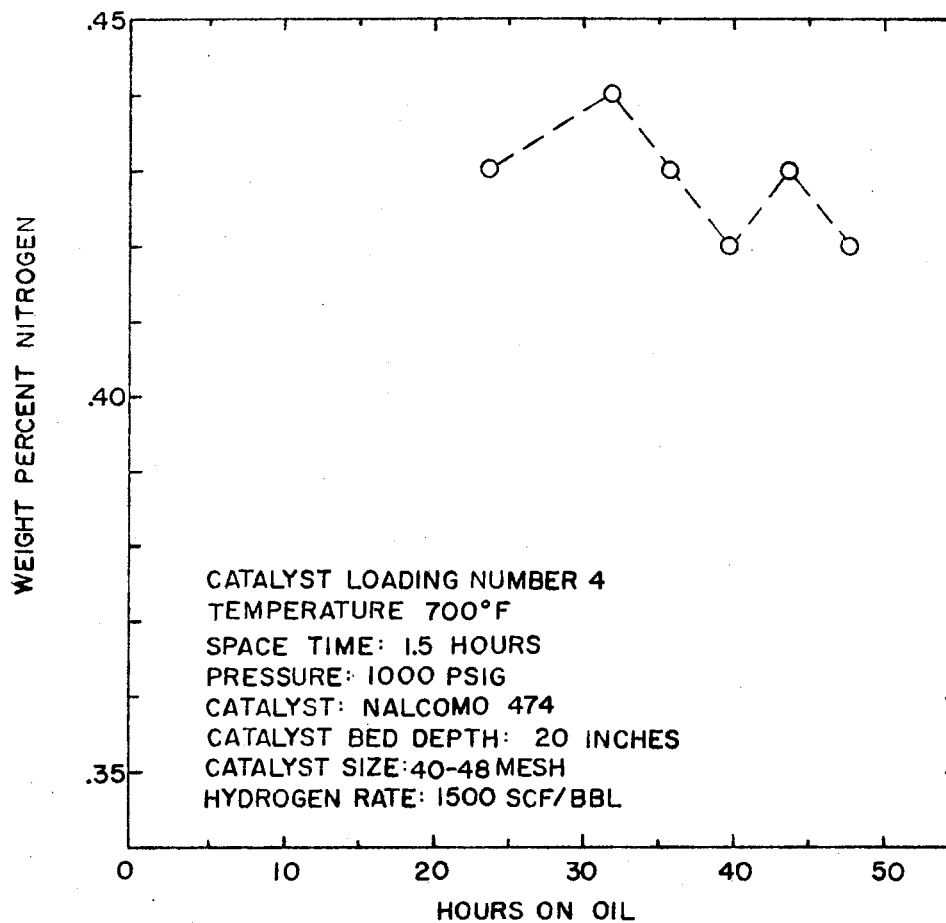
Figure 28. Catalyst Activity Stabilization
for Catalyst Loading Number 4

size would decrease the product nitrogen content by decreasing the catalyst intraparticle diffusion resistances.

Figure 29 is a plot of the logarithm of the weight percent nitrogen in the reactor oil product as a function of space time with parameters of reactor operating temperature. A comparison of of Figures 20 and 29 shows that at 750°F, the smaller catalyst size resulted in greater conversion of organonitrogen species. In fact, the 750°F conversion of Catalyst Loading 4 was higher than the 800°F conversion of Catalyst Loading 2.

Figure 30 is a plot of the difference between the weight percent nitrogen measured at the beginning and end of an isotherm as a function of reactor operating temperature. The data indicate that catalyst deactivation tends to be more important at the higher reactor operating temperatures for the 40-48 mesh Nalcomo 474 catalyst.

<div align="center">

Effect of Reactant Flux at

Constant Space Time

</div>

The reactor was reloaded with 10 inch catalyst bed depth, rather than 20 inch deep catalyst bed as in previous catalyst loadings, to test the effect of reactant flux at constant space time. The remainder of the reactor was filled with inert packing, crushed beryl saddles.

Figure 31 is a plot of weight percent nitrogen in the reactor product as a function of hours of continuous operating at 650°F, 1000 psia, 0.75 space time, and a hydrogen rate of 1500 SCF/bbl. The results of earlier catalyst conditioning runs, Figure 18 and 21, indicated that about thirty hours on oil were required to obtain a
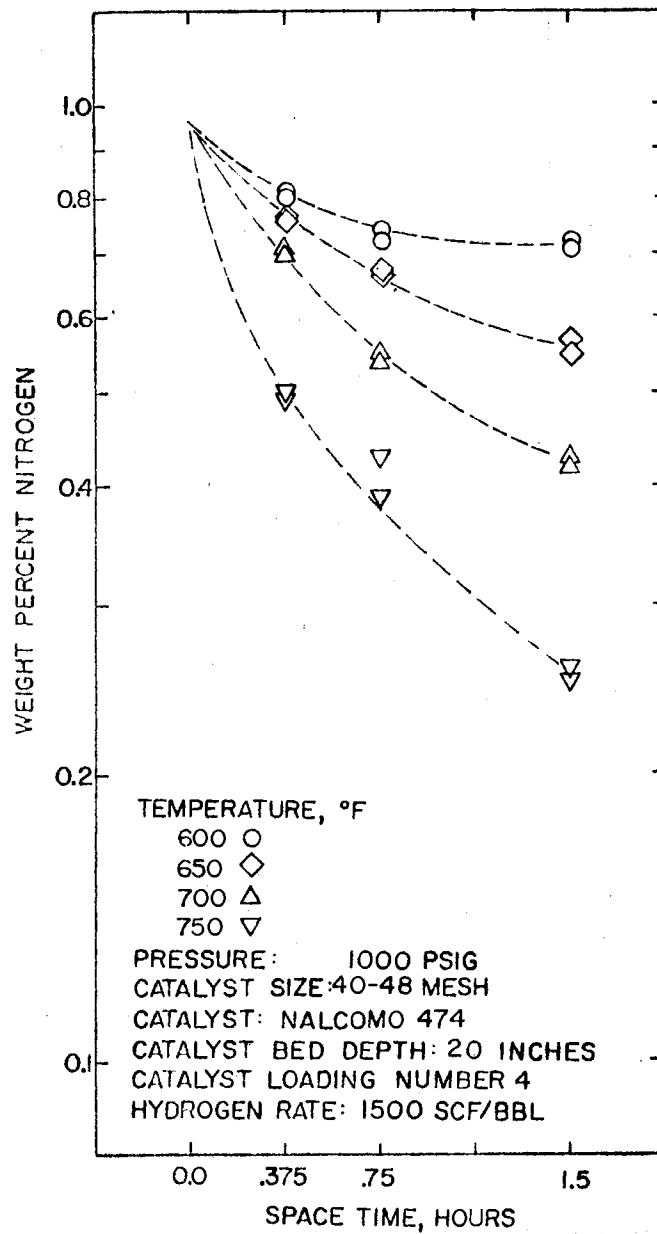
Figure 29. Denitrogenation Kinetics
from Catalyst Loading
Number 4

CATALYST LOADING NUMBER 4
SPACE TIME: 1.5 HOURS
PRESSURE: 1000 PSIG
CATALYST: NALCOMO 474
CATALYST BED DEPTH: 20 INCHES
CATALYST SIZE 40-48 MESH
HYDROGEN RATE: 1500 SCF/BBL
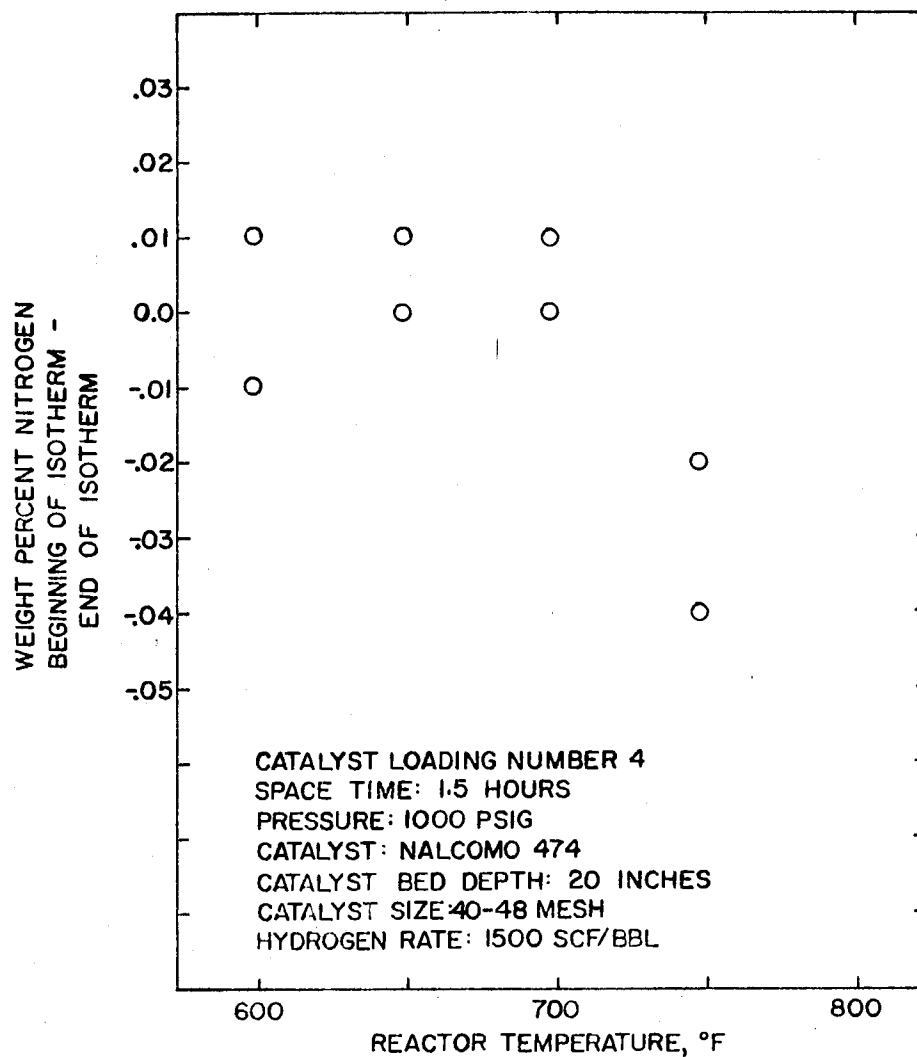
Figure 30. Catalyst Deactivation from
Catalyst Loading Number 4

CATALYST LOADING NUMBER 5
TEMPERATURE 650°F
SPACE TIME: .75 HOURS
PRESSURE: 1000 PSIG
CATALYST: NALCOMO 474
CATALYST BED DEPTH: 10 INCHES
CATALYST SIZE: 8-10 MESH
HYDROGEN RATE: 1500 SCF/BBL
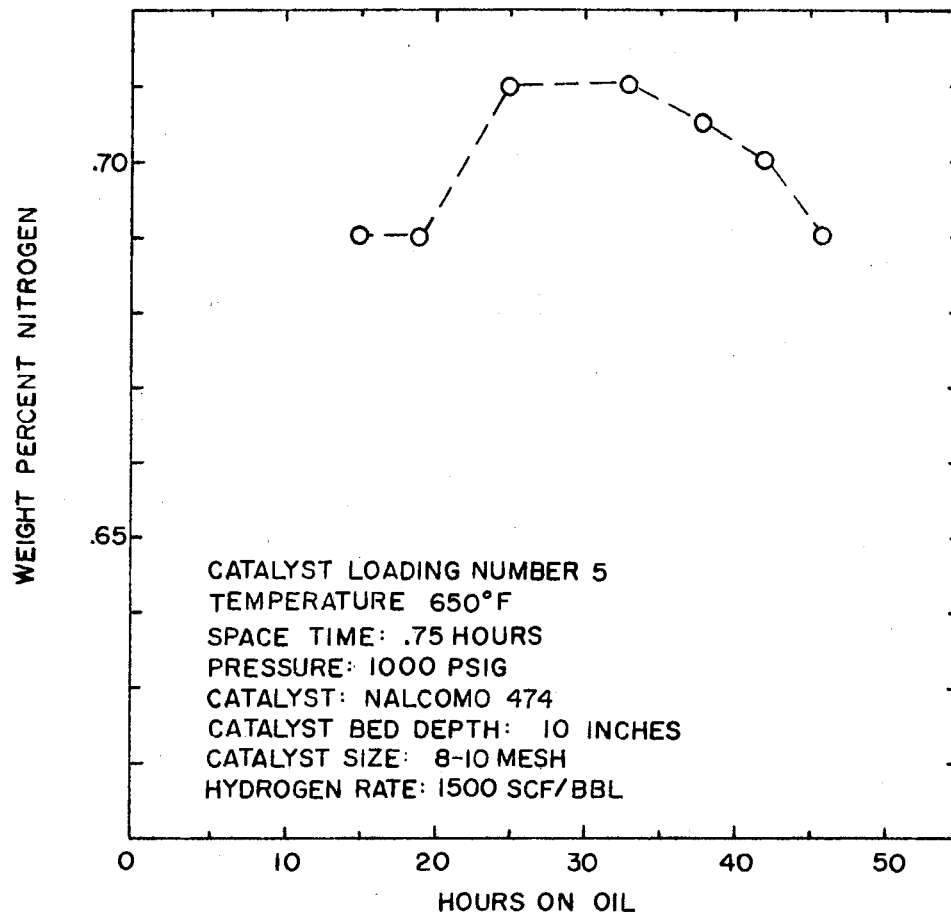
Figure 31.   Catalyst Activity Stabilization
for Catalyst Loading Number 5

relatively stable catalyst activity. However, Figure 31 indicates that the measured weight percent nitrogen in the reactor product oil at fifteen hours on oil was equal to the nitrogen level at 48 hours on oil. This may indicate that the reduction of reactor operating temperature from 700°F to 650°F and space time from 1.5 to 0.75 hours resulted in obtaining a relatively stable catalyst activity more rapidly.

Figure 32 is a plot of the logarithm of the weight percent nitrogen in the reactor product oil as a function of space time with parameters of temperature. The effect of catalyst bed depth can be estimated by comparing Figures 20 and 24 with Figure 32. Inspection of these data indicates that decreasing the bed height by a factor of two resulted in a modest decrease in the apparent catalyst activity.

Figure 33 is a plot of the difference between the weight percent nitrogen obtained at the beginning and end of an isotherm as a function of reactor operating temperature. These data are consistent with the earlier observation that higher reactor operating temperatures tend to favor catalyst deactivation.

Catalyst Activity as a Function of

Pore Diameter Distribution

Three catalysts were obtained from the Nalco Chemical Company, Nalcomo 474, Nalco 72-4710A, and 72-4710B. The metals content and support material were identical (see Table VIII). Nalco attempted to vary the pore diameter distribution without changing the intrinsic
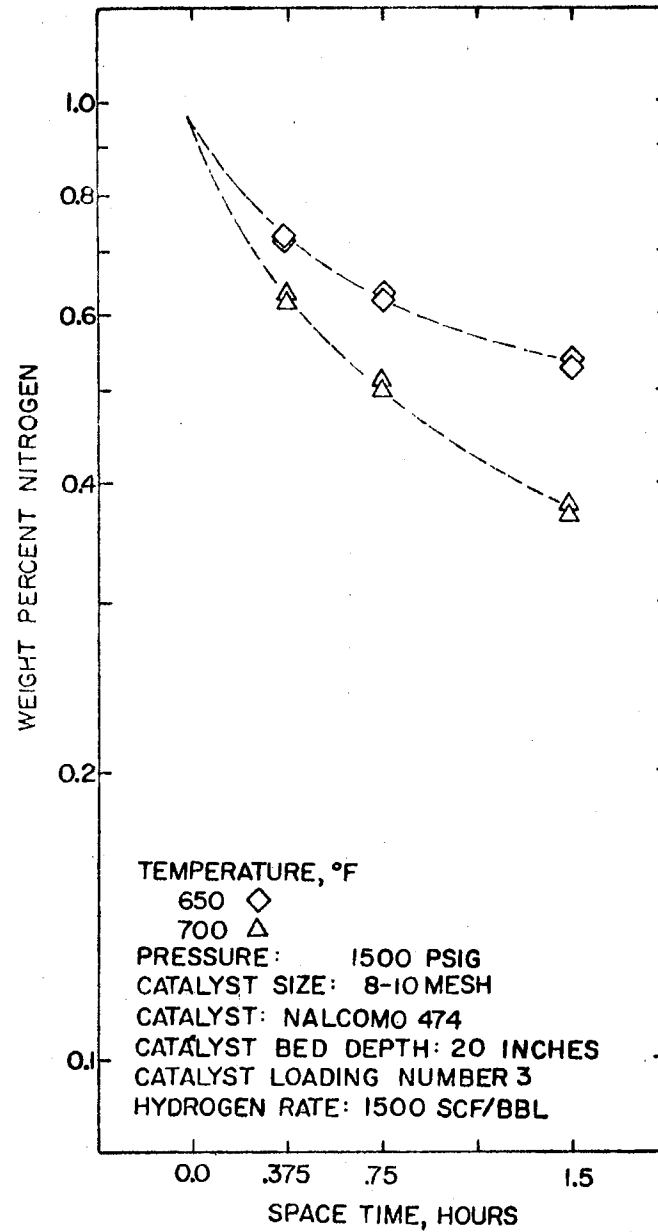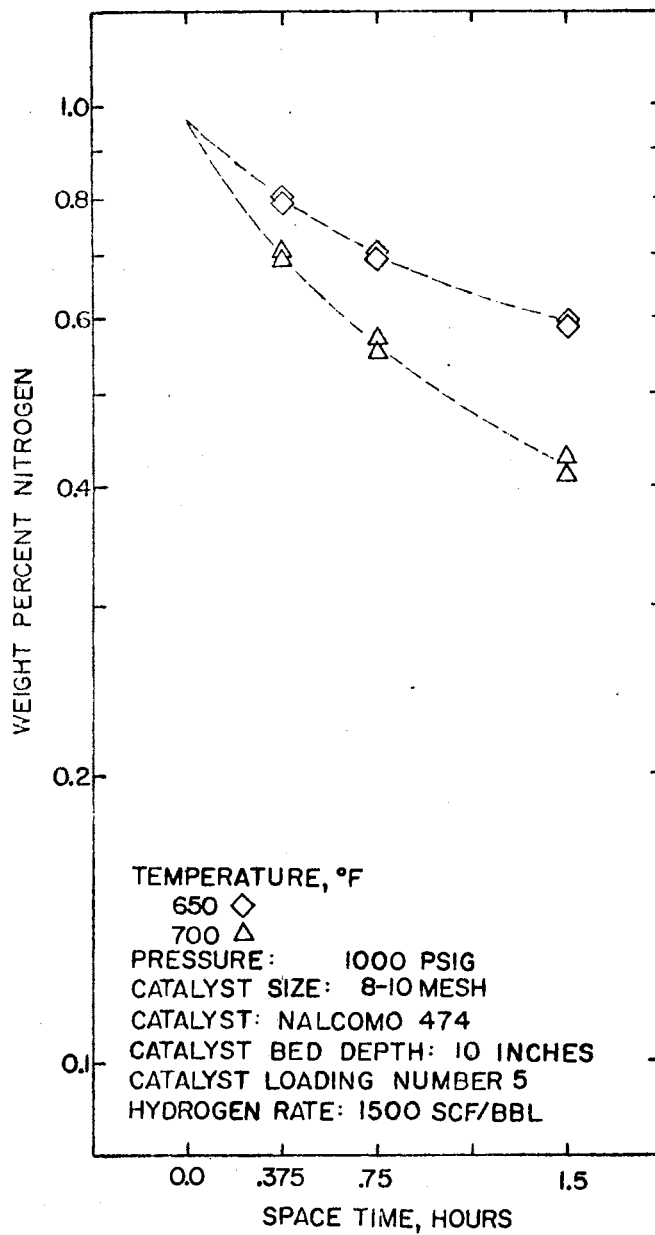
Figure 32. Denitrogenation Kinetics
from Catalyst Loading
Number 5
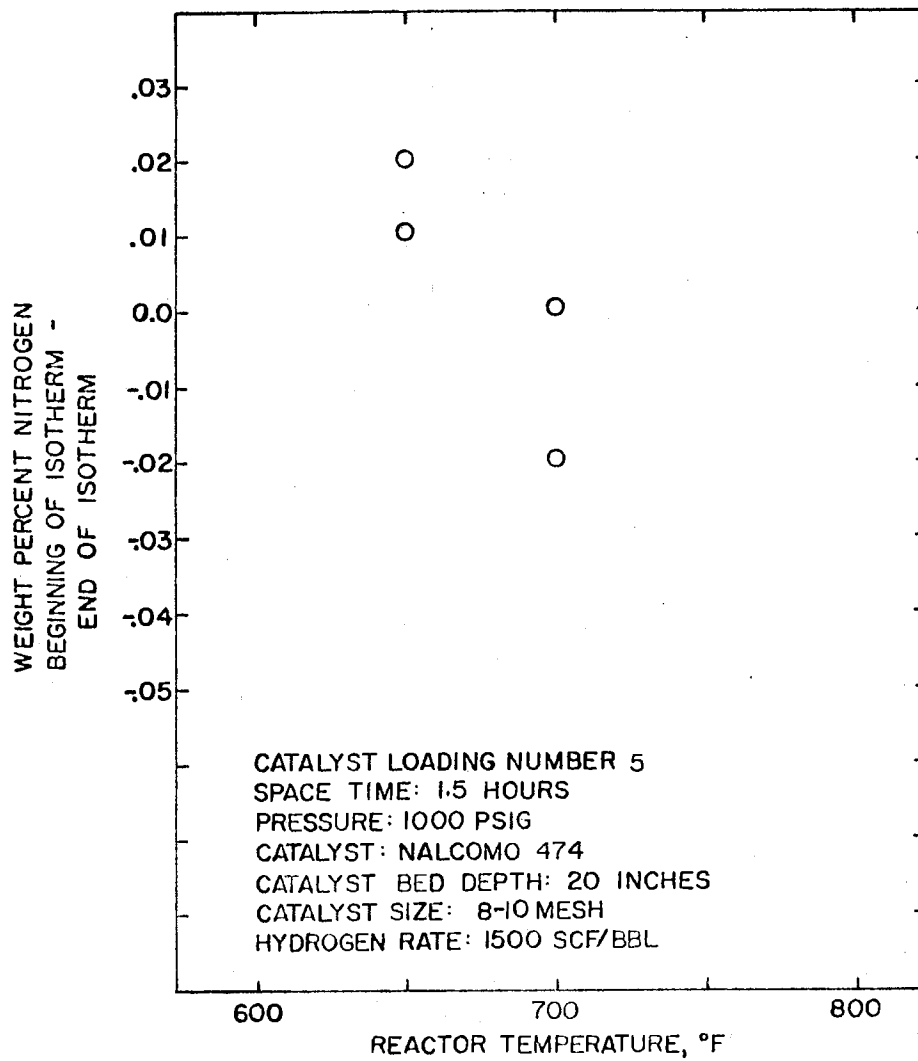
Figure 33.   Catalyst Deactivation from
Catalyst Loading Number 5

activity of the catalyst. First, the pore radius distribution will be
characterized and then the activity of the three catalyst will be
evaluated.

The cumulative pore volume as a function of pore radius was
determined using mercury posimetry (20) by the American Instrument
Company. The measured mercury intrusion per gram of catalyst as a
function of the applied pressure for all three catalysts is presented
in Appendix A. The relative frequency of pore diameters can be esti-
mated (20) by plotting $\Delta V / \Delta \ln r$. Where V is the volume of mercury
that has penetrated the catalyst pellet and r is the pore radius.
Figures 34, 35, and 36 are plots of the relative frequency of pore
radius as a function the logarithm of pore radius for Nalcomo 474,
Nalco 72-4710A, and Nalco 72-4710B, respectively. Figures 37, 38, and
39 are plots of the weight percent nitrogen in the reactor product as
a function of hours of continuous operation for Nalco 474, Nalco
72-4710A, and Nalco 72-4710B, respectively. Figures 40, 41, and 42
are plots of the logarithm of the nitrogen content in the reactor
product oil as a function of space time with parameters of reactor
operating temperature for Nalcomo 474, Nalco 72-4710A, and Nalco
72-4710B, respectively. Figures 43, 44, and 45 are plots of the
difference between the weight percent nitrogen at the beginning and
end of an isotherm as a function of reactor operating temperature for
Nalcomo 474, Nalco 72-4710A, and Nalco 72-4710B. Figures 46, 47,
and 48 are plots of the logarithm of the weight percent nitrogen as
a function of boiling point at fifty millimeters of mercury for Nalcomo
474, Nalco 72-4710A, and Nalco 72-4710B. A full discussion of the
data presented in this chapter will be given in the following chapter.
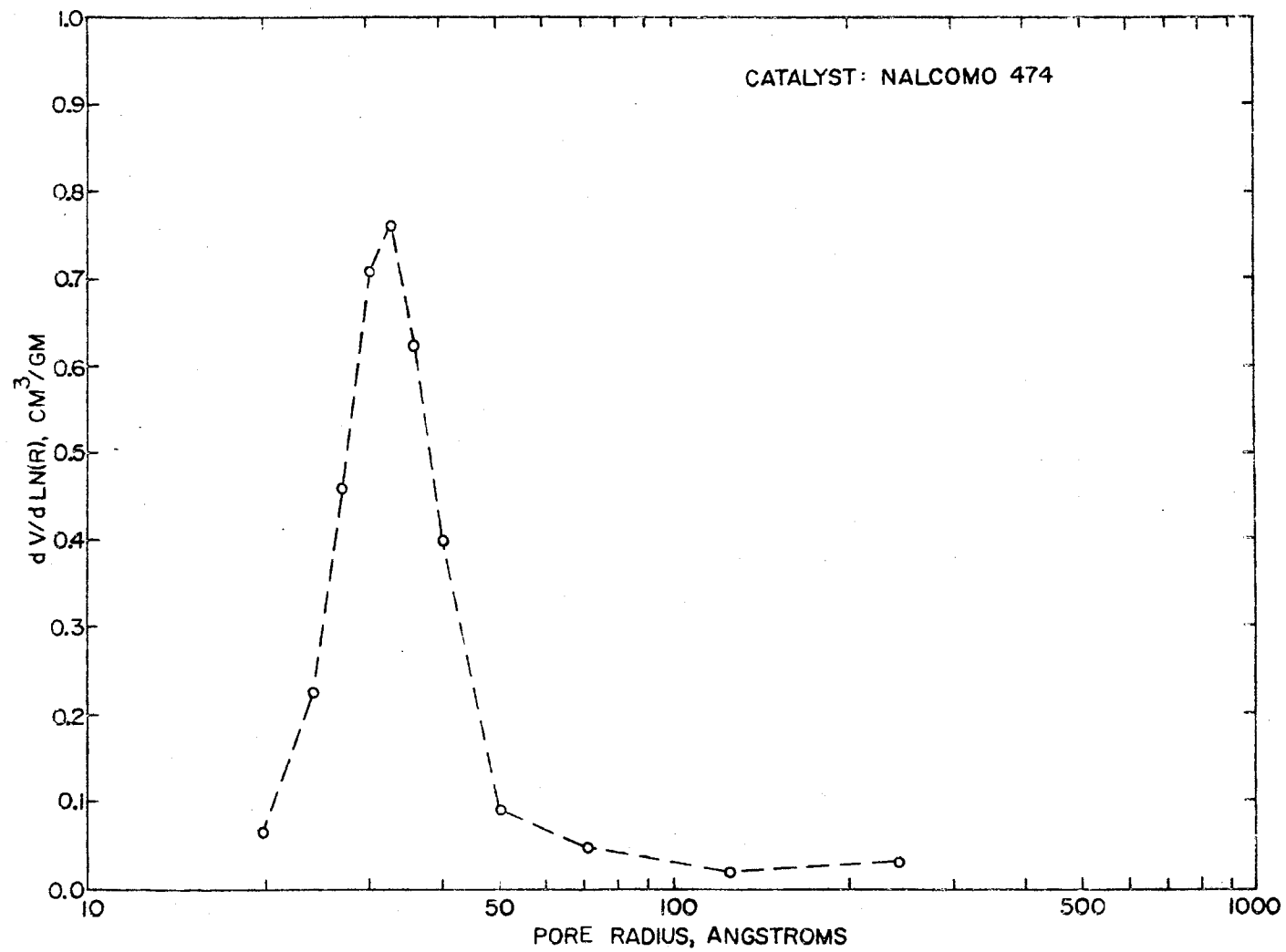
Figure 34. Pore Radius Distribution for Nalcomo 474
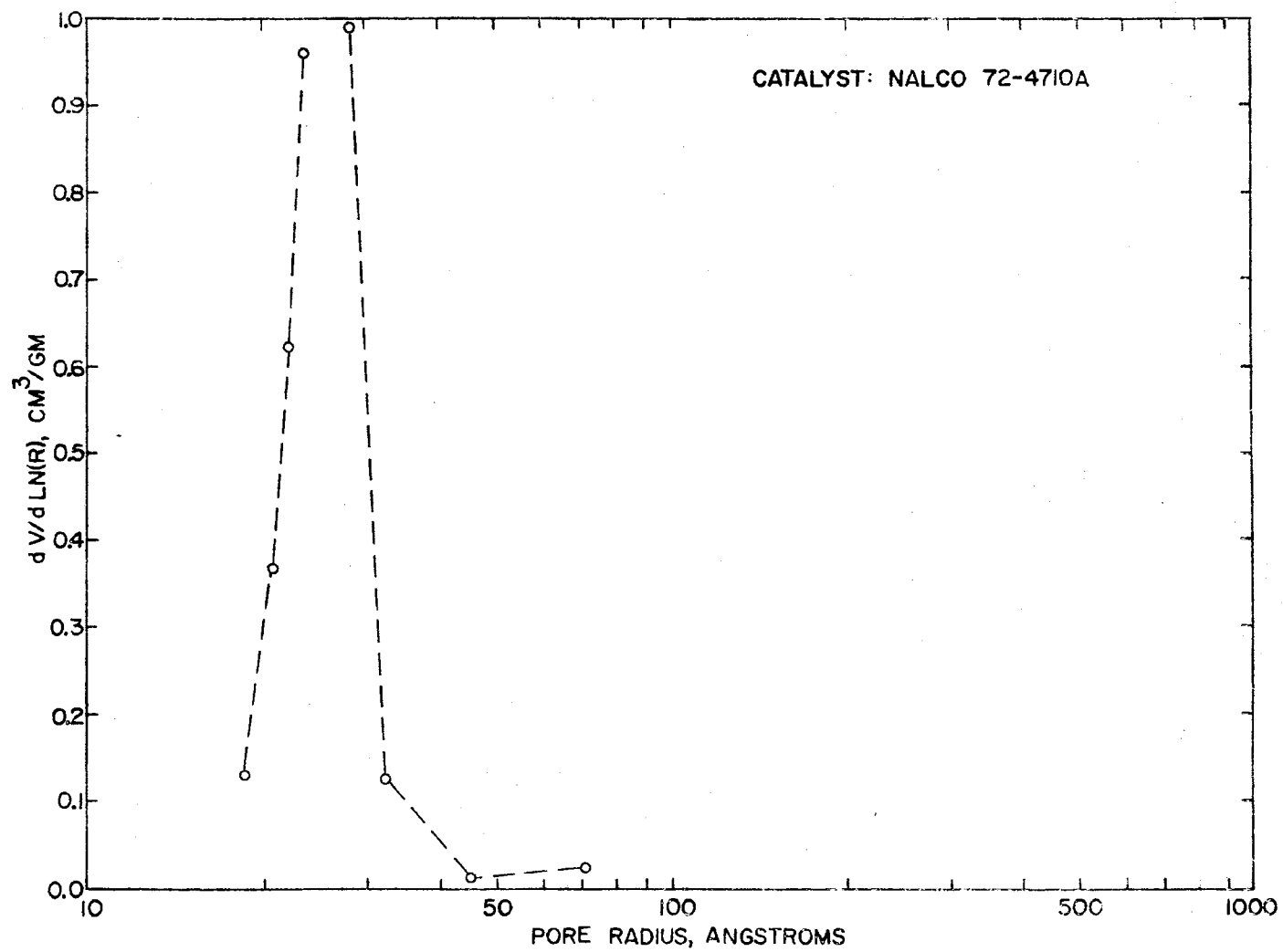
Figure 35. Pore Radius Distribution for Nalco 72-4710A
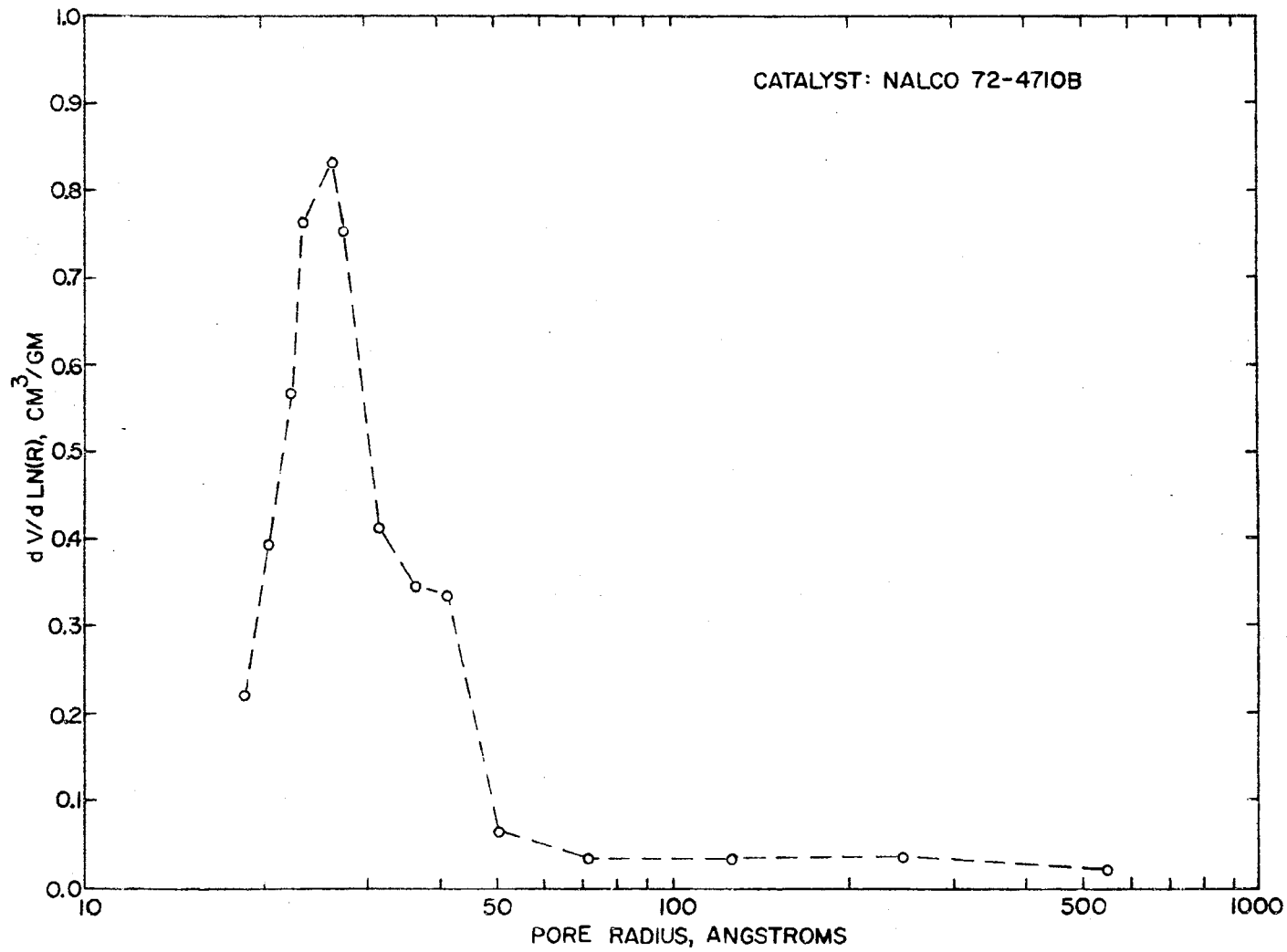
Figure 36. Pore Radius Distribution for Nalco 72-4710B
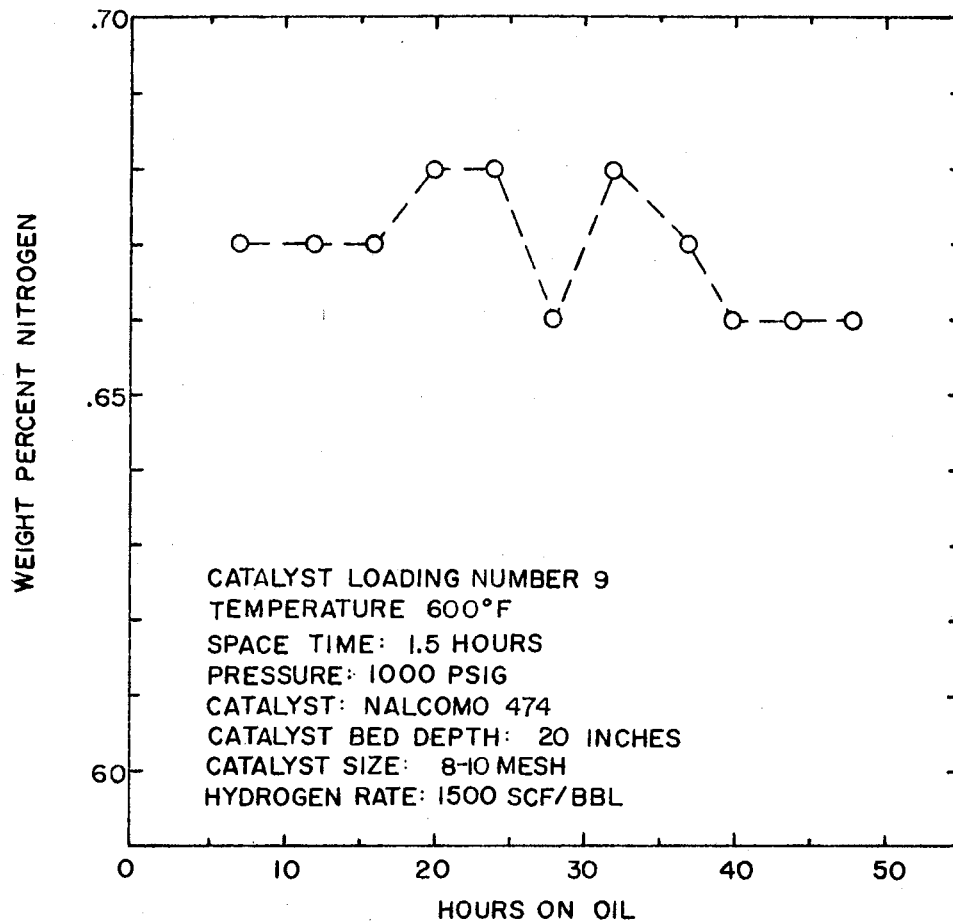
Figure 37. Catalyst Activity Stabilization
for Catalyst Loading Number 9
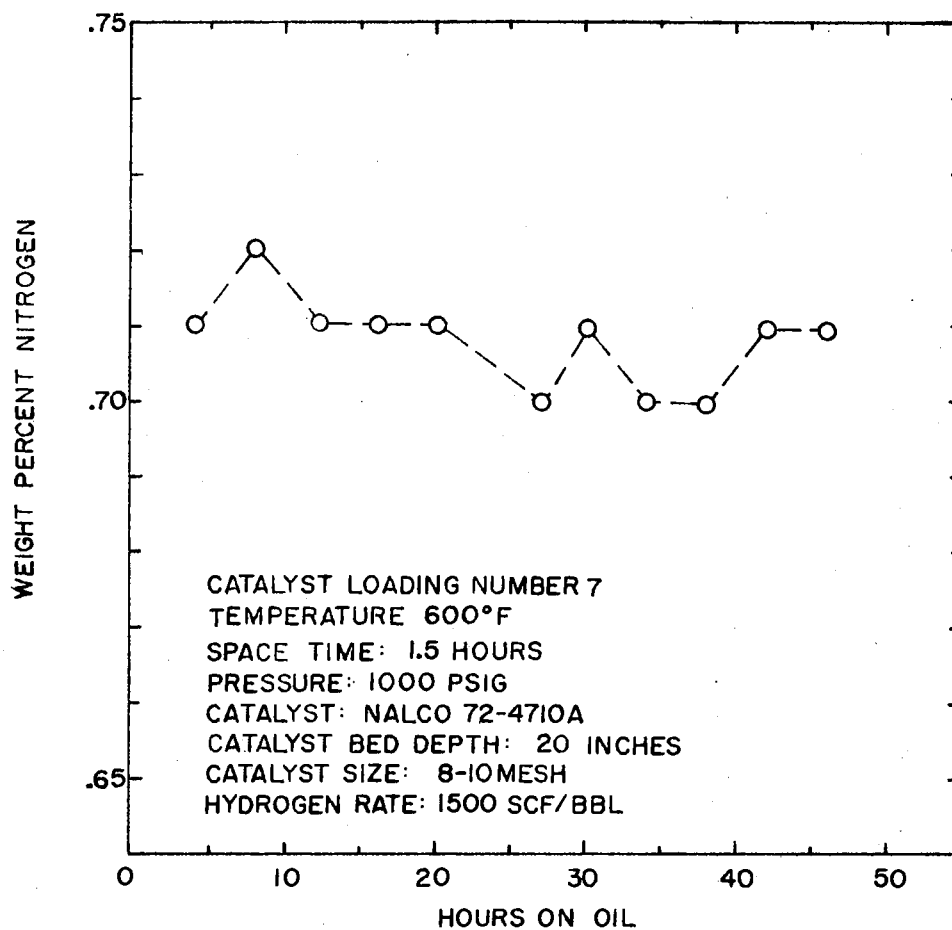
Figure 38. Catalyst Activity Stabilization
for Catalyst Loading Number 7
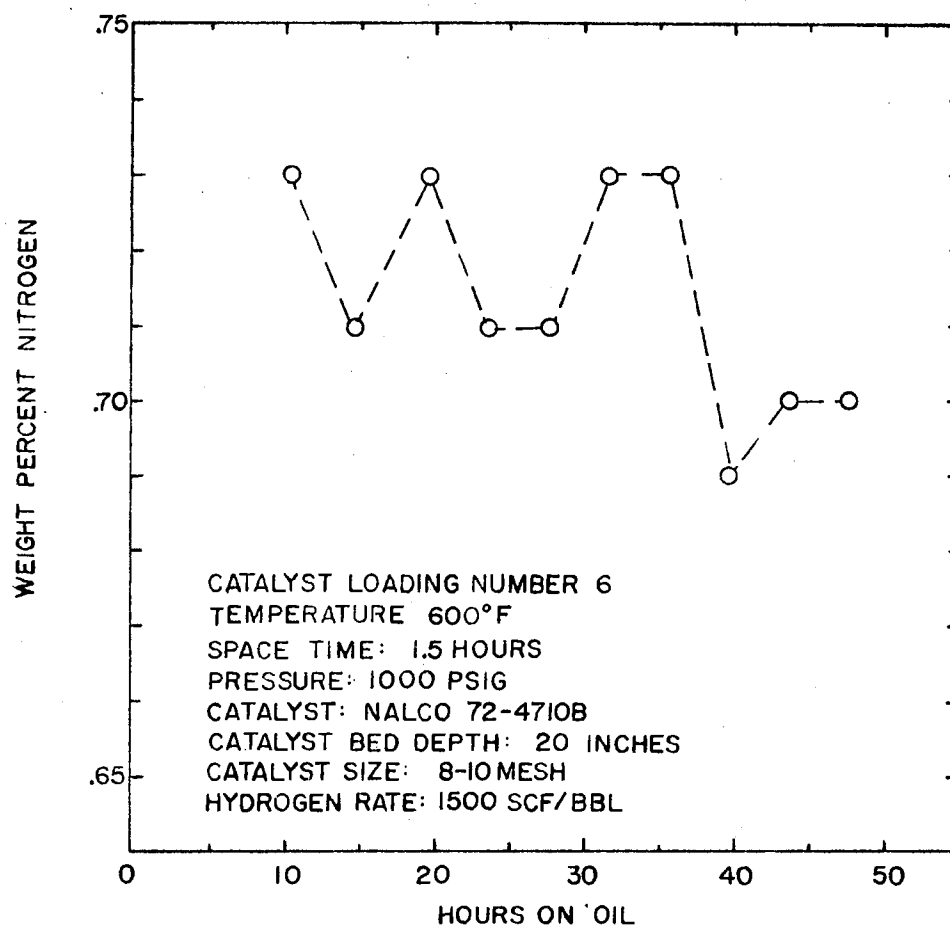
Figure 39. Catalyst Activity Stabilization
for Catalyst Loading Number 6

TEMPERATURE, °F
  600 ○
  650 ◇
  700 △
  750 ▽
PRESSURE: 1000 PSIG
CATALYST SIZE: 8-10 MESH
CATALYST: NALCOMO 474
CATALYST BED DEPTH: 20 INCHES
CATALYST LOADING NUMBER 9
HYDROGEN RATE: 1500 SCF/BBL
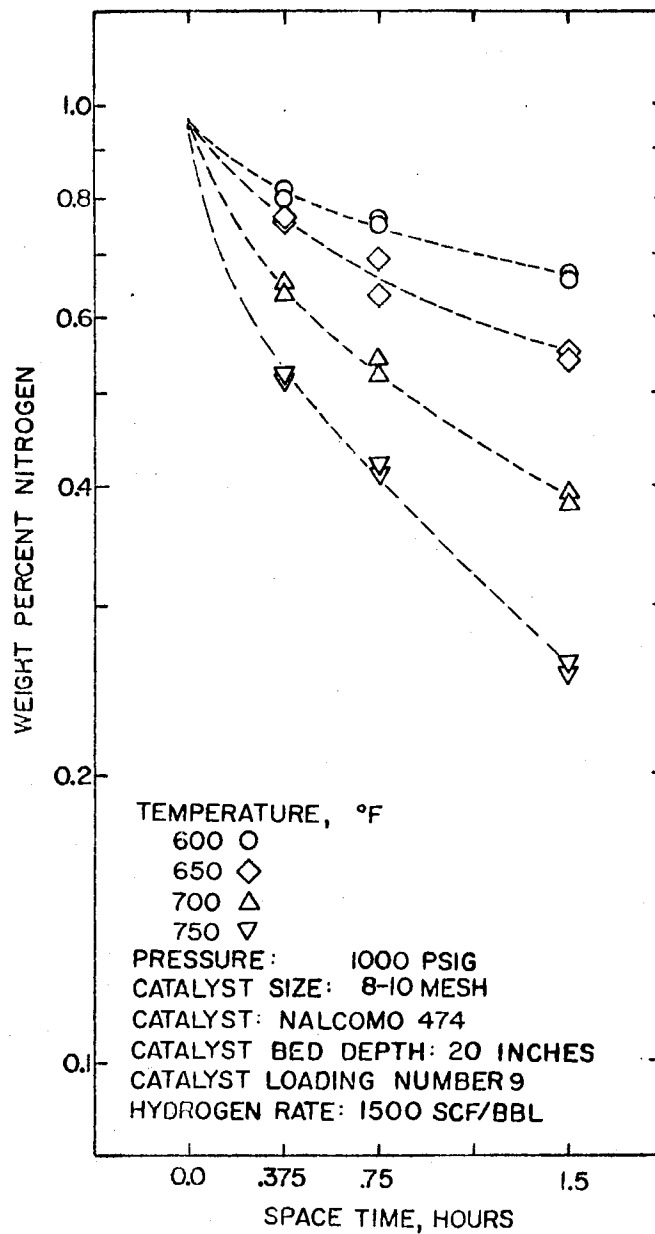
Figure 40.   Denitrogenation Kinetics
                 from Catalyst Loading
                 Number 9
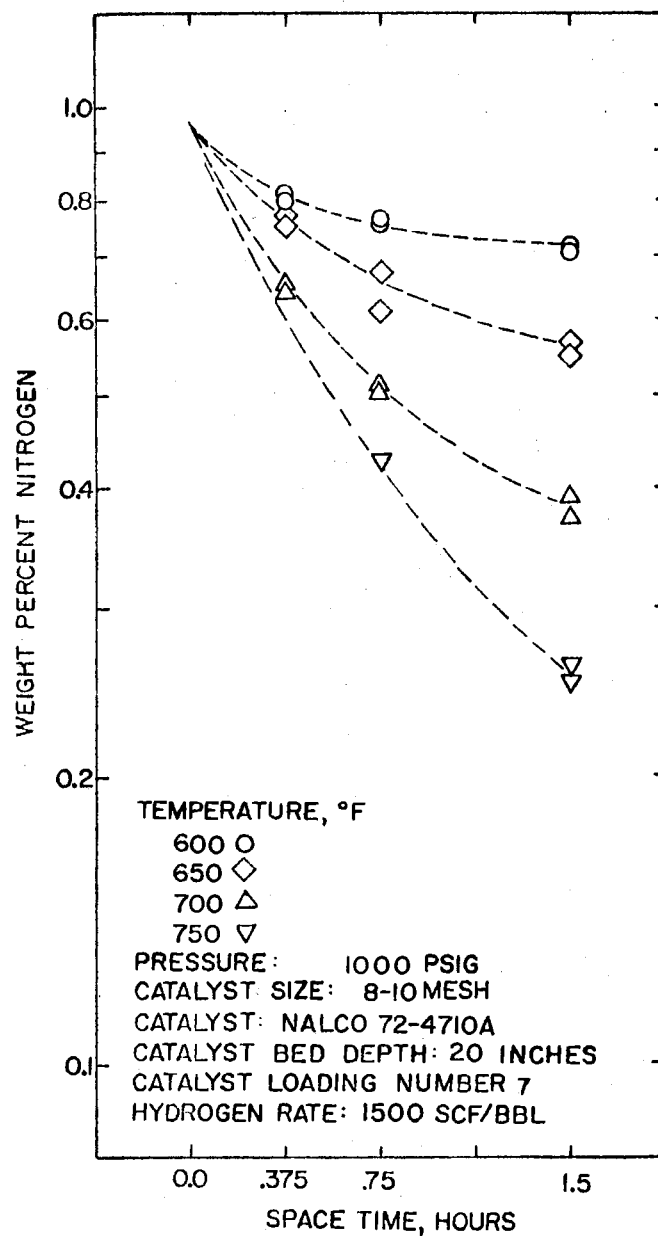
Figure 41. Denitrogenation Kinetics
          from Catalyst Loading
          Number 7
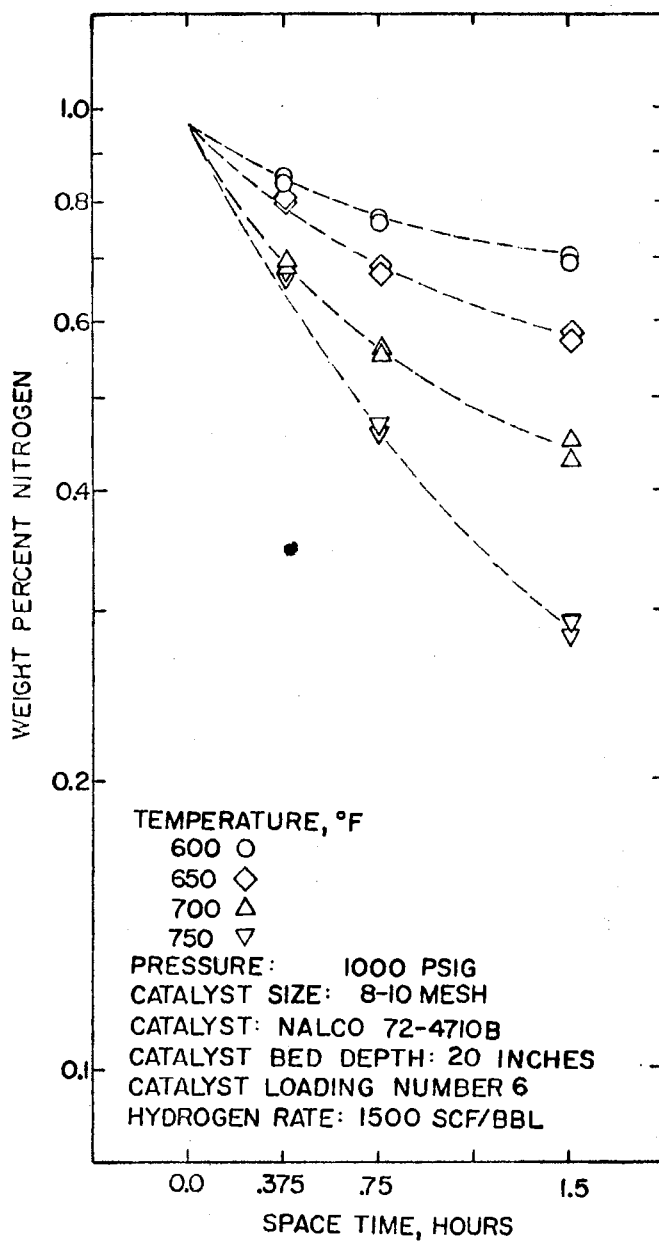
Figure 42. Denitrogenation Kinetics
from Catalyst Loading 6
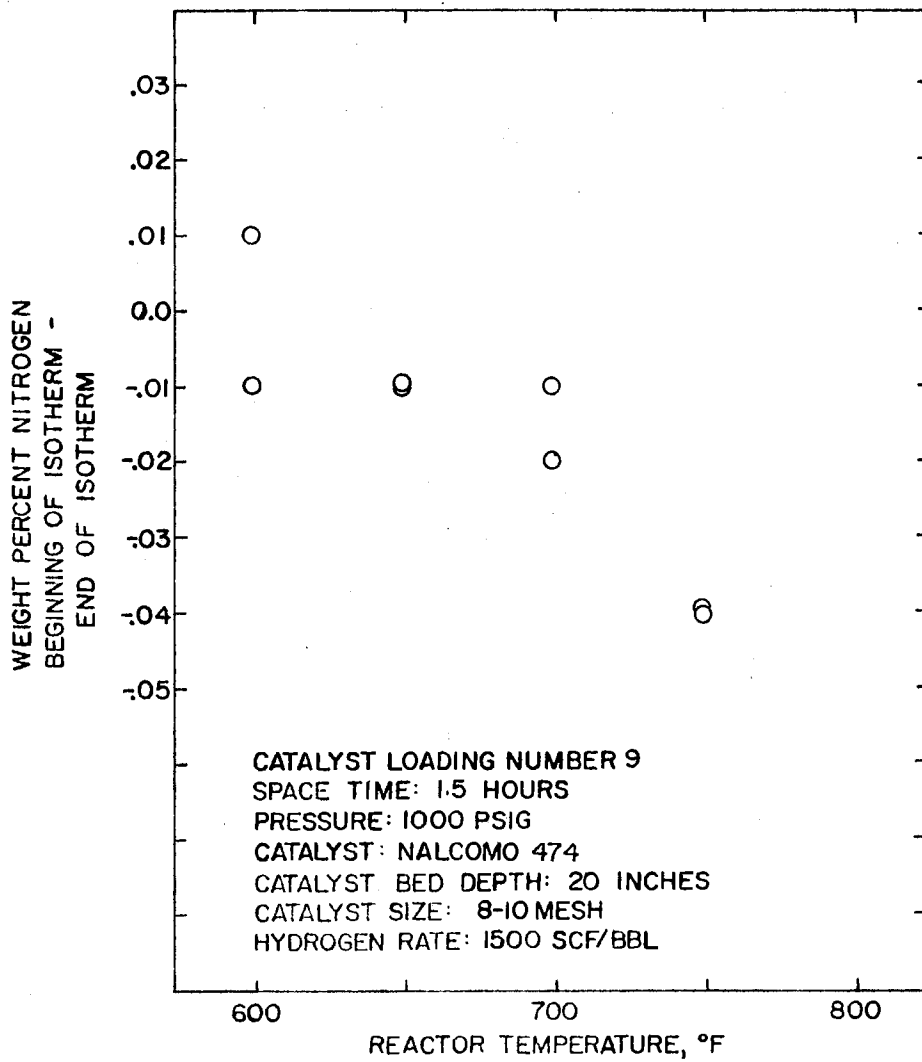
Figure 43. Catalyst Deactivation from Catalyst Loading Number 9

Chart details:

Y-axis: WEIGHT PERCENT NITROGEN BEGINNING OF ISOTHERM - END OF ISOTHERM

Y-axis values: .03, .02, .01, 0.0, -.01, -.02, -.03, -.04, -.05

X-axis: REACTOR TEMPERATURE, °F

X-axis values: 600, 700, 800

CATALYST LOADING NUMBER 9
SPACE TIME: 1.5 HOURS
PRESSURE: 1000 PSIG
CATALYST: NALCOMO 474
CATALYST BED DEPTH: 20 INCHES
CATALYST SIZE: 8-10 MESH
HYDROGEN RATE: 1500 SCF/BBL
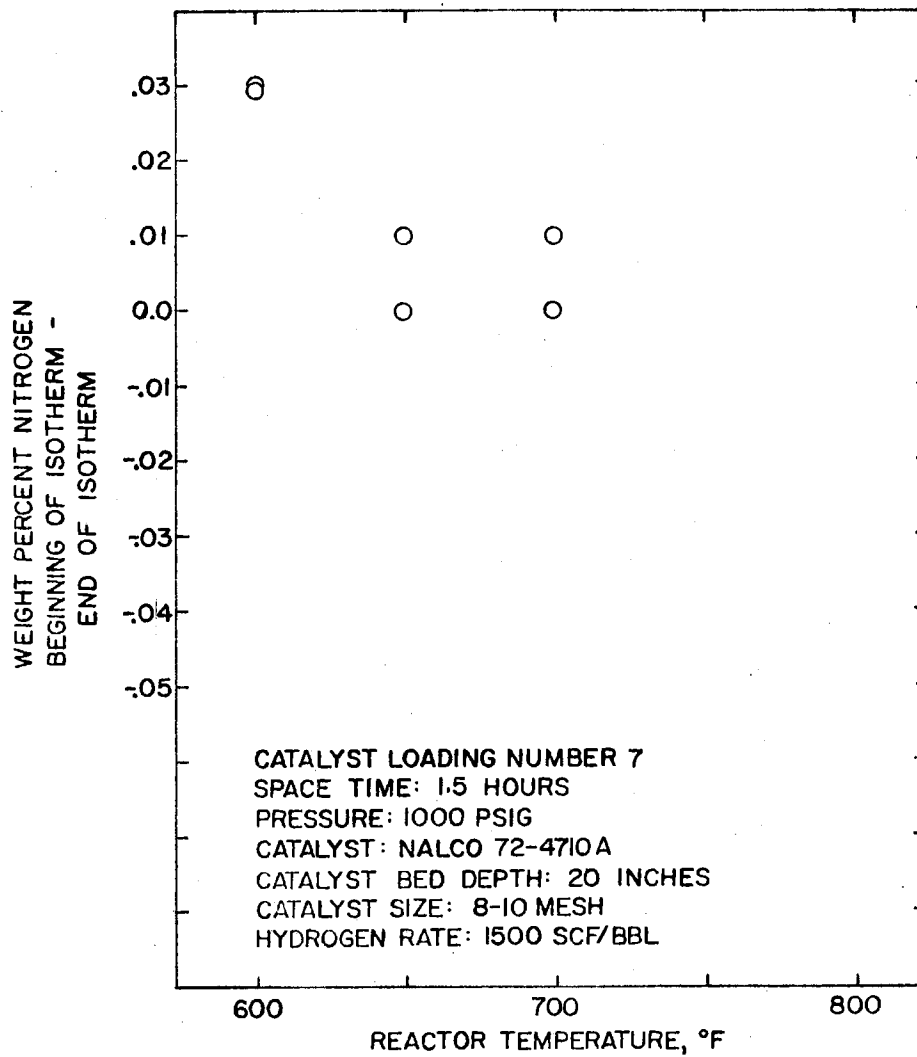
Figure 44.   Catalyst Deactivation from
                   Catalyst Loading Number 7
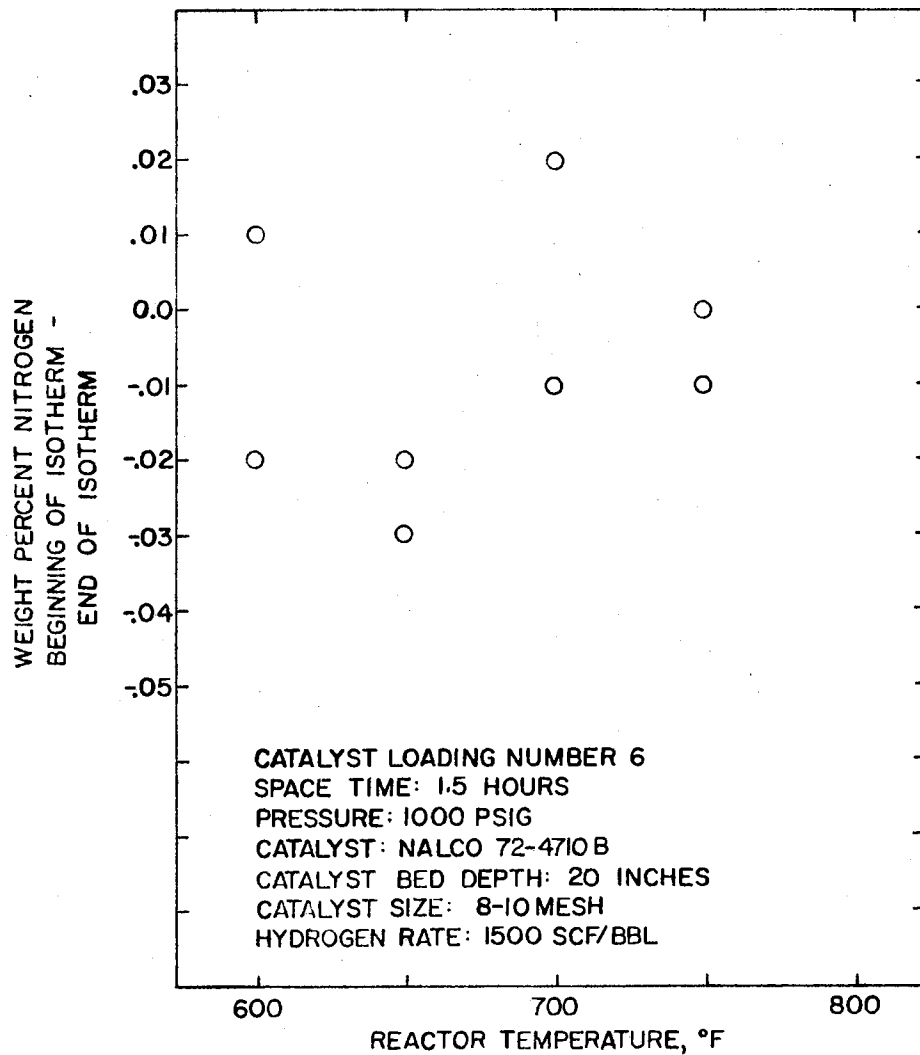
Figure 45. Catalyst Deactivation from
Catalyst Loading Number 6
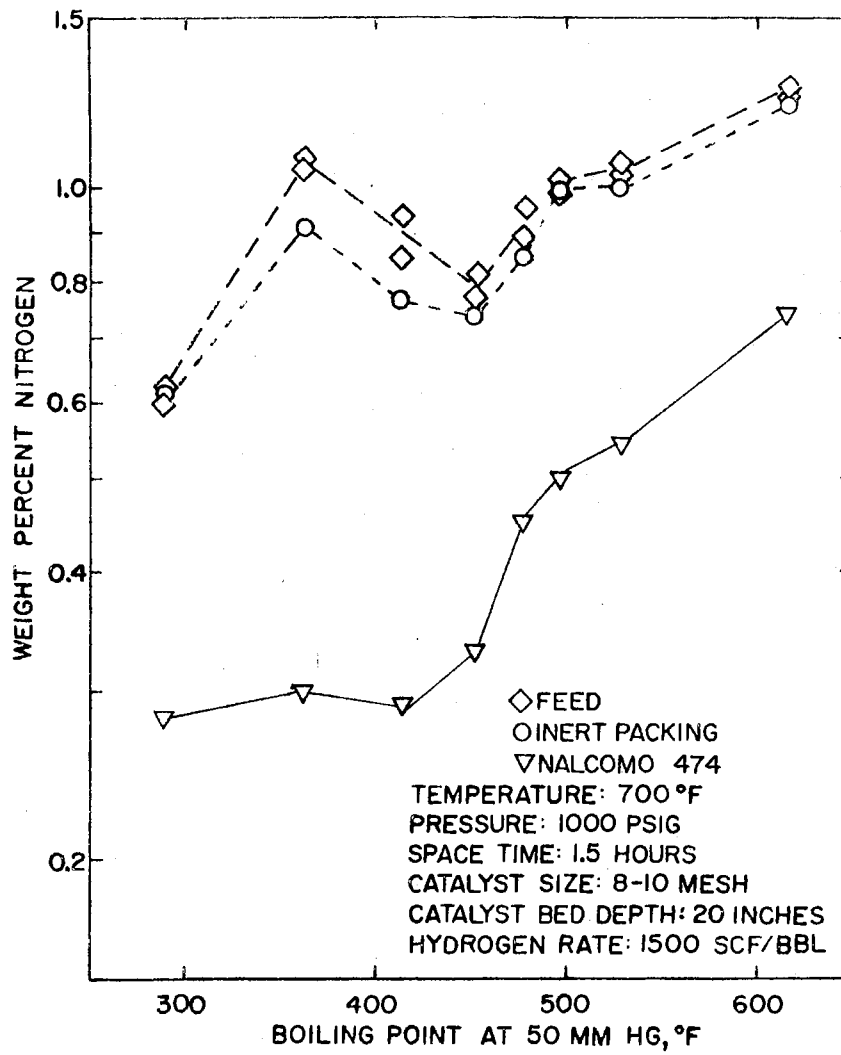
Figure 46. Denitrogenation as a Function of
Boiling Point at 50 mm Hg Using
Nalcomo 474 Catalyst
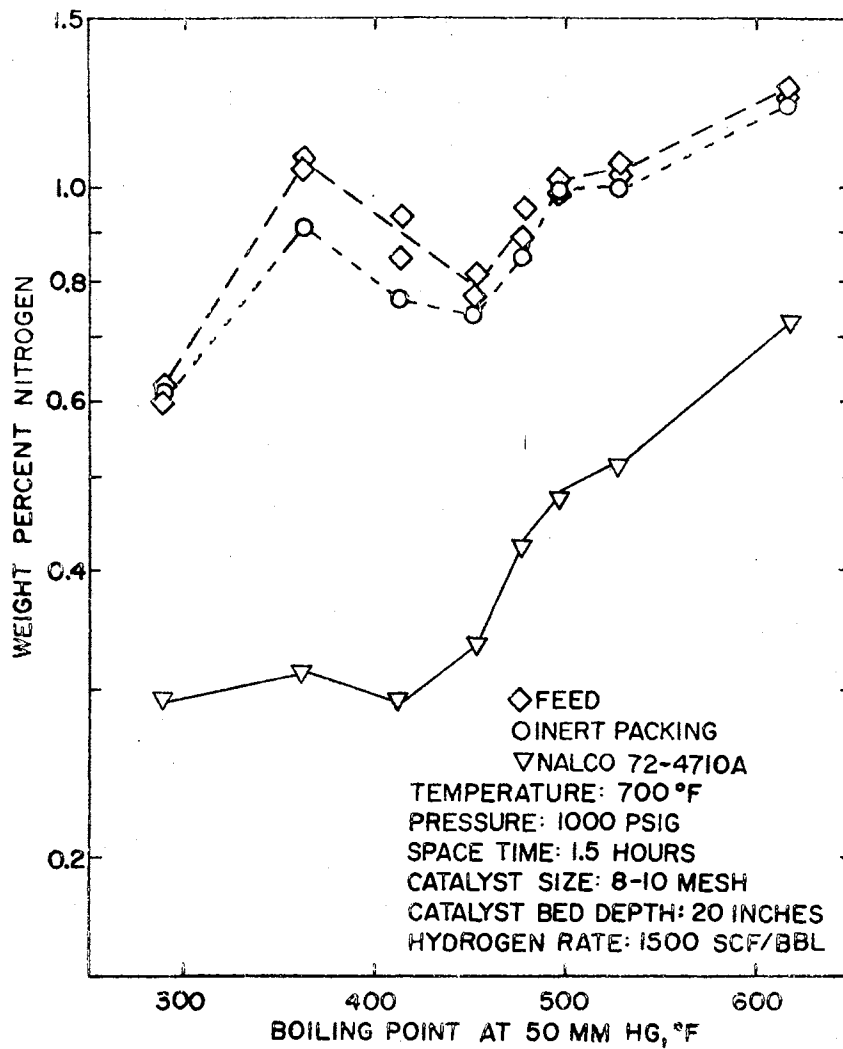
Figure 47. Denitrogenation as a Function of
Boiling Point at 50 mm Hg Using
Nalco 72-4710A Catalyst
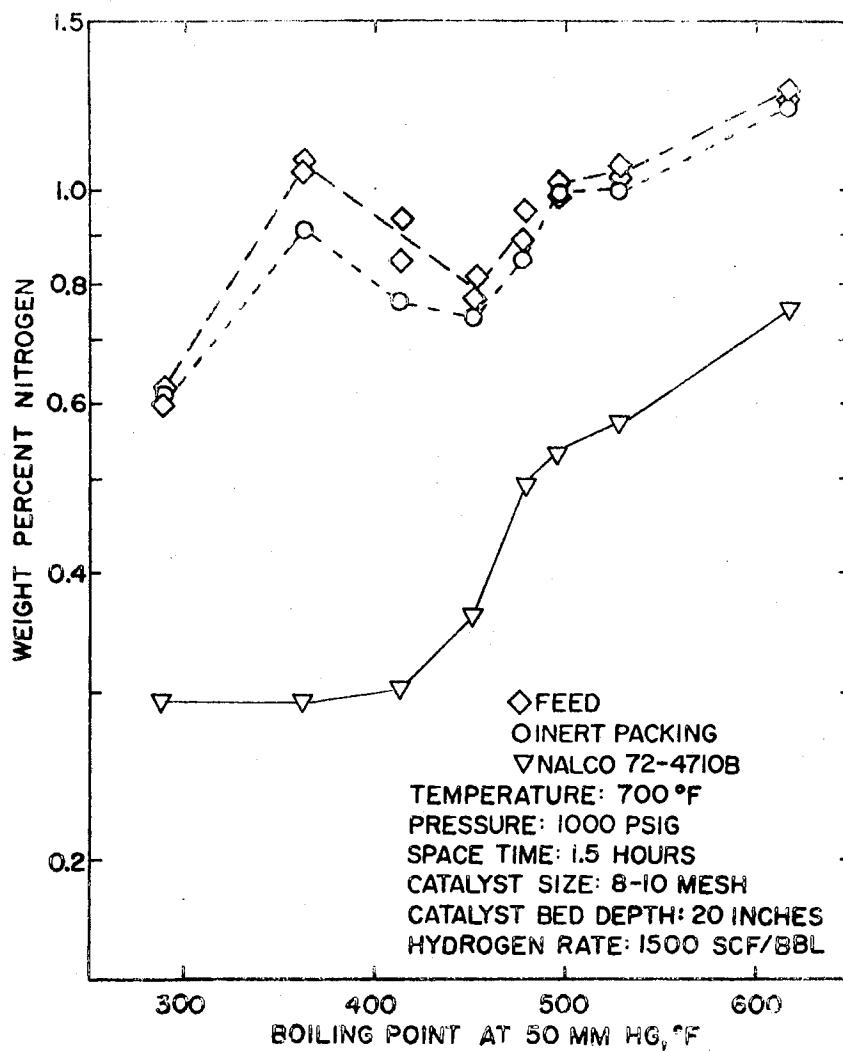
Figure 48. Denitrogenation as a Function of
Boiling Point at 50 mm Hg Using
Nalco 72-4710B

CHAPTER VI

DISCUSSION

The results, presented in the previous chapter, will be analyzed
in detail in this chapter. First, semi-quantative arguments will be
used to develop a basis for a kinetic model for denitrogenation. Then,
the data will be analyzed in terms of the kinetic model. The following
topics will be considered:

1. First Estimate of Precision of the Data

2. Factors Affecting Data Precision

3. Effect of Catalyst Particle Size

4. Kinetic Model Development

5. Effect of Reactor Operating Temperature

6. Effect of Reactor Operating Pressure

7. Catalyst Activity as a Function of Pore Size

8. Denitrogenation Selectivity as a Function of Pore Size

First Estimate of Precision of the Data

A discussion of the precision of only the analytical methods
used in this work was presented in Chapter IV. In this section,
a first estimate of the data's precision will be made to serve as a
basis for the kinetic model development. Later, a detailed error
analysis will be made in terms of the kinetic model. Most of the

97

conclusions of this work will be based on comparisons of reactor

performance from separate catalyst loadings. As a result, at least an

estimate of the effect of errors in

1. loading of catalyst,

2. catalyst activation,

3. catalyst conditioning to obtain a stable activity,

4. and reactor operation

on the observed reactor performance is required.

The precision of the reactor start-up and operation was tested by

loading Nalcomo 474 catalyst from the same catalyst batch, using the

activation procedure presented in Chapter III and conditioning the

catalyst at $700^{\circ}F$, 1000 psia, a hydrogen rate of 1500 SCF/bbl, and

a volumetric space time of 1.5 hours for 48 hours of continuous

operation. Figure 49 is a plot of the weight percent nitrogen in the

reactor product oil as a function of the number of hours of continuous

operation for Catalyst Loadings 2 and 3. The plot shows that the

activity of the catalyst in Catalyst Loading Number 3 increased for

the first 28 hours on oil. Then, the product nitrogen level stabilized

at 0.4 (+.01) weight percent nitrogen. The results for catalyst

Loading Number 2 show that the catalyst activity tended to decrease

with time. However, the catalyst activity seems to have stabilized

at the same level, 0.4 (+0.01) weight percent nitrogen, for both

catalyst loadings. The difference in the initial catalyst activity

is probably due to slight differences in the manner in which the

catalysts were activated. Figure 49 indicates that the effect of

initial activity can be minimized by allowing the catalyst to operate

continuously for 38 hours at the operating conditions studied.
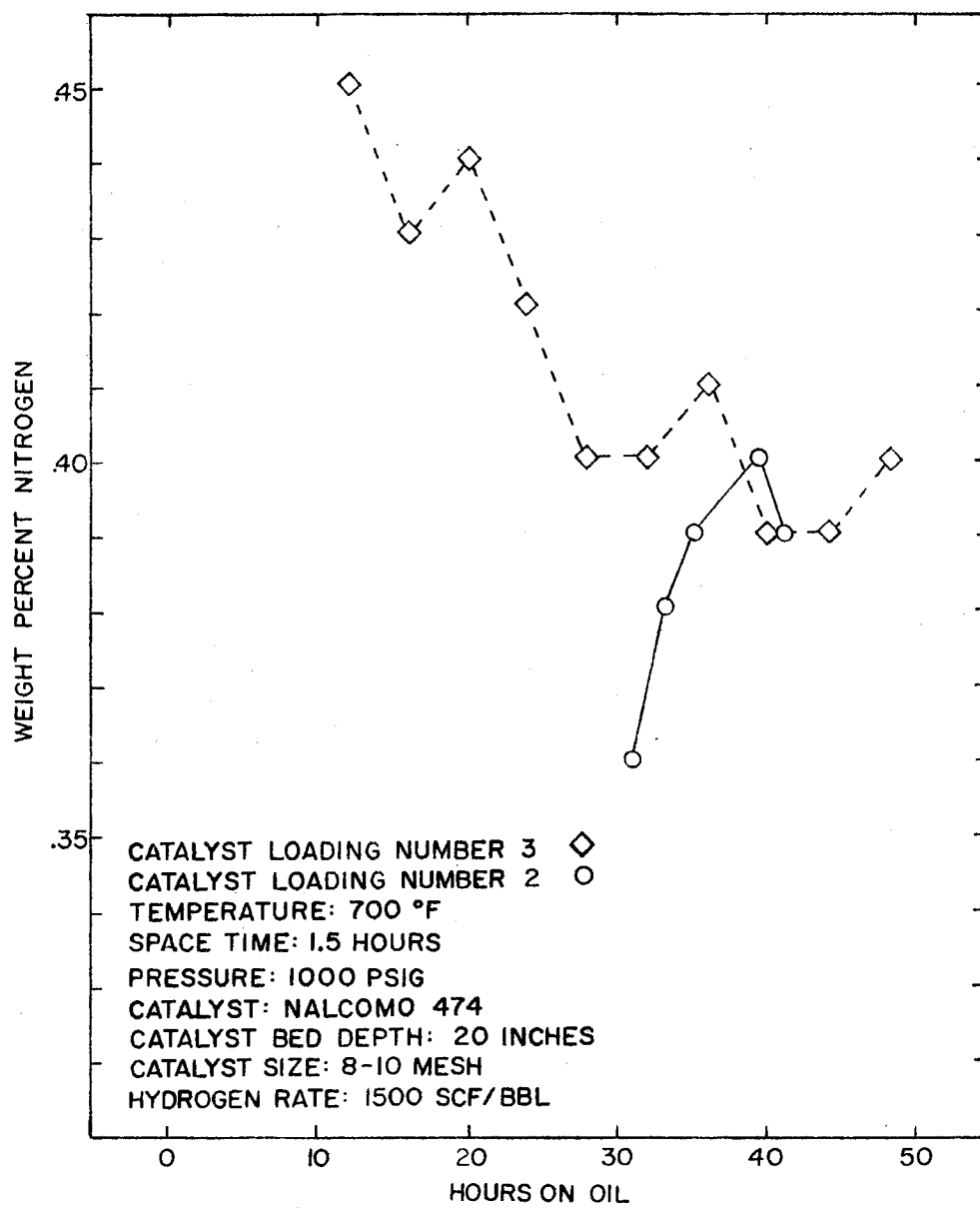
Figure 49. Catalyst Activity Stabilization
for Catalyst Loadings 2 and 3

Figure 50 is a plot of the weight percent nitrogen in the reactor product oil as a function of space time for Catalyst Loadings Number 2 and 3. The plot shows that the product nitrogen levels lie in a 0.03 range of weight percent nitrogen for all space times and both catalyst loadings.

Factors Affecting Data Precision

In this section, factors affecting the precision of the data not amenable to an error analysis will be considered. These factors fall into two general areas:

1. Effect of reactant mass flux at constant space time

2. Effect of operational history on catalyst activity

The effect of errors in the reactor operating temperature, pressure, space time, and hydrogen rate on the precision of the data will be estimated using a formal error analysis.

Liquid hourly space time, the total catalyst bed volume divided by the oil reactant volumetric flow rate, is usually used to design hydrotreating reactors. A weight hourly space time can also be used. The space time concept is based on the assumption that the conversion from a hydrotreating reactor is independent of catalyst bed depth at constant space time. Theoretically, if both the oil reactant volumetric flow rate and the catalyst bed depth were halved at constant reactor cross sectional area, the conversion should be unchanged.

Figure 51 is a plot of the weight percent nitrogen in the reactor product oil as a function of space time with a 10 inch deep catalyst bed. The bars are the range of conversions obtained from Catalyst Loadings 2 and 3 at the same reactor operating conditions but using a
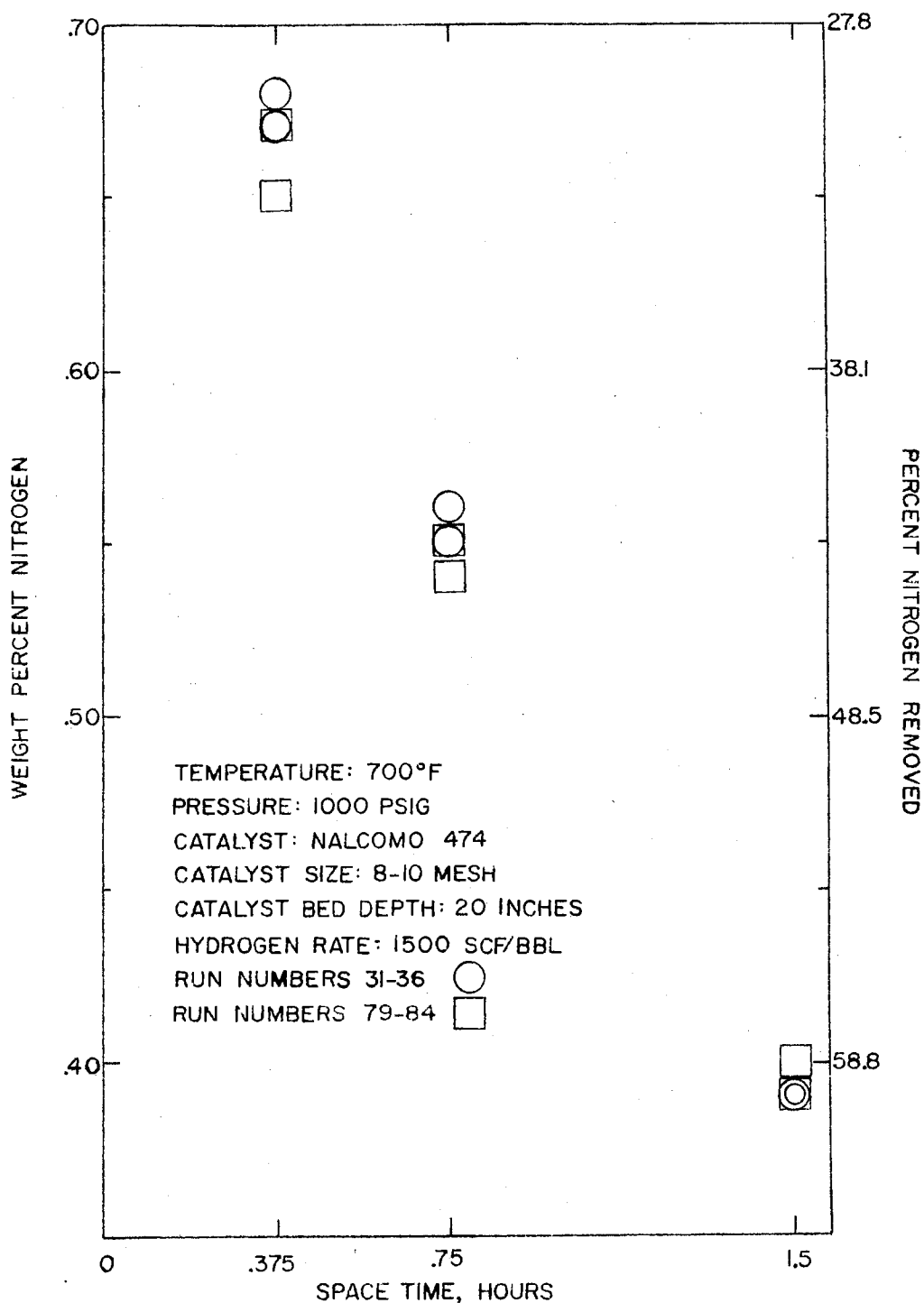
Figure 50. Comparison of 700°F Isotherm from Catalyst Loadings 2 and 3
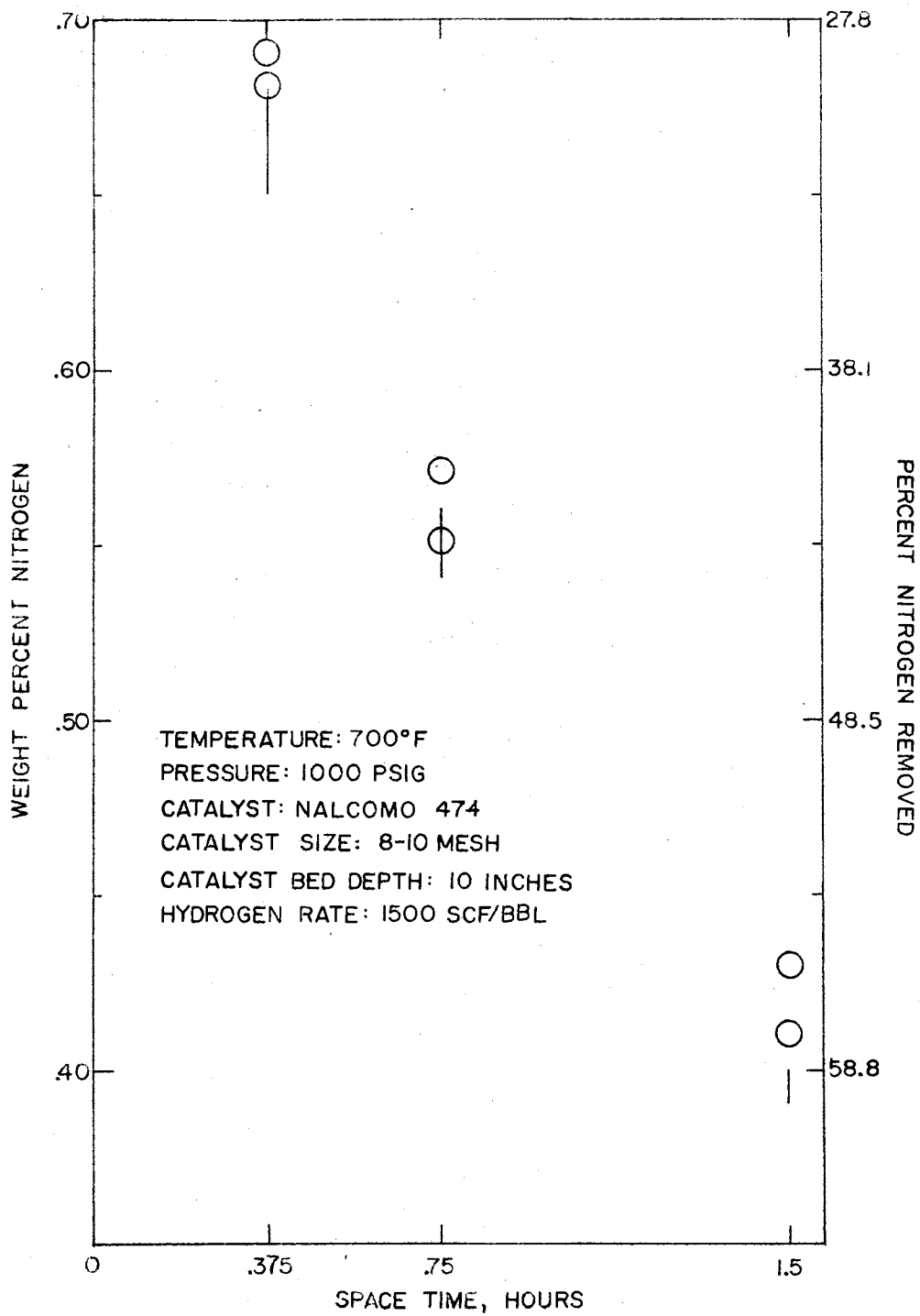
Figure 51. Comparison of 700°F Isotherm from
Catalyst Loading Number 5 with
the Range of Product Nitrogen
Levels from Catalyst Loadings
2 and 3

20 inch deep catalyst bed. The weight percent nitrogen in the product from the 10 inch bed tended to be higher (lower conversion of organo-nitrogen species) than the range of values for the 20 inch catalyst bed. These results indicate that the conversion of organo-nitrogen species is a function of bed height at the operating conditions studied. The general approach used in this work will be to develop a kinetic model assuming that the effect of catalyst bed height is negligible, and then interpret the results in light of the uncertainty introduced by reactant flux through the reactor.

The effect of catalyst history on the catalyst activity was very difficult to analyze when a large number of operating conditions were investigated in each catalyst loading. Typically, the activity of the catalyst decreases with increasing number of hours of continuous operation. Therefore, the activity of the catalyst at any time is a function of the hours on oil and the previous operating conditions. Therefore, the catalyst deactivation can be divided into two types:

1. Deactivation as a result of continuous operation at a given set of operating conditions.

2. Deactivation due to a change in operating conditions.

Since reactor performance is typically most sensitive to changes in the reactor operating temperature, the deactivation of the catalyst will be analyzed in terms of the reactor temperature and changes in the reactor temperature.

The effect of catalyst deactivation at all temperature levels was evaluated by comparing a 1.5 space time run made at the beginning of a series of isothermal and isobaric runs with the results of the 1.5 space time run at the end. Since, approximately 24 hours were

required to complete each isotherm, catalyst deactivation was measured over about a day of continuous operation. Figure 52 is a plot of the average difference between the reactor product oil weight percent nitrogen level at the beginning and end of a series of isothermal runs for all the isotherms in this study. If this quantity is negative, then deactivation was observed; a positive value indicates the catalyst activity increased. The plot shows that deactivation tends to increase with temperature. The effect is very small at temperature of $700^{\circ}F$ and below, possibly too small to be measured with the precision of the experimental technique used in this work. At $800^{\circ}F$, the catalyst deactivation was severe. As a result of the poor catalyst stability observed at $800^{\circ}F$, $750^{\circ}F$ was the maximum temperature used in subsequent runs. At reactor operating temperatures of $750^{\circ}F$ and below, the effect of catalyst deactivation was too small to evaluate with reasonable precision using the techniques of this work. Therefore, there will be no attempt to adjust the data to account for the effect of catalyst deactivation. The approach used in this work will be to develop a kinetic model assuming the effect of catalyst deactivation during an isothermal run is negligible. Then, the resulting kinetic model will be interpreted in light of the uncertainty introduced by catalyst deactivation. Next, the effect of thermal history on the catalyst activity will be considered.

The general approach for evaluating thermal history on catalyst activity will be to compare the catalyst activity when the reactor was previously operated at a higher or lower temperature with runs in which the catalyst was operated at only one temperature throughout its history. Figure 53 is a plot of the weight percent nitrogen in the

AVERAGE WEIGHT PERCENT NITROGEN
DIFFERENCE BETWEEN BEGINNING
AND END OF ISOTHERM

SPACE TIME: 1.5 HOURS
PRESSURE: 1000 PSIG
HYDROGEN RATE: 1500 SCF/BBL

REACTOR TEMPERATURE, °F
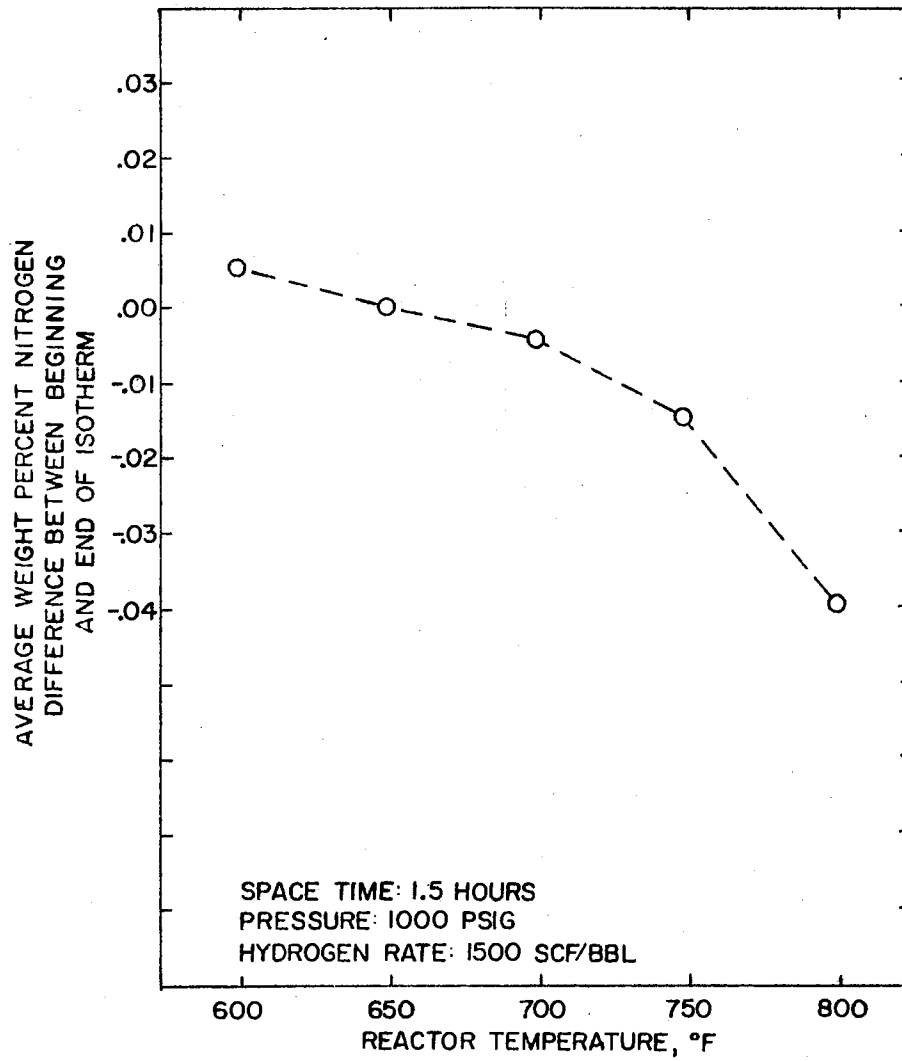
Figure 52.   Catalyst Deactivation as a Function
of Reactor Operating Temperature
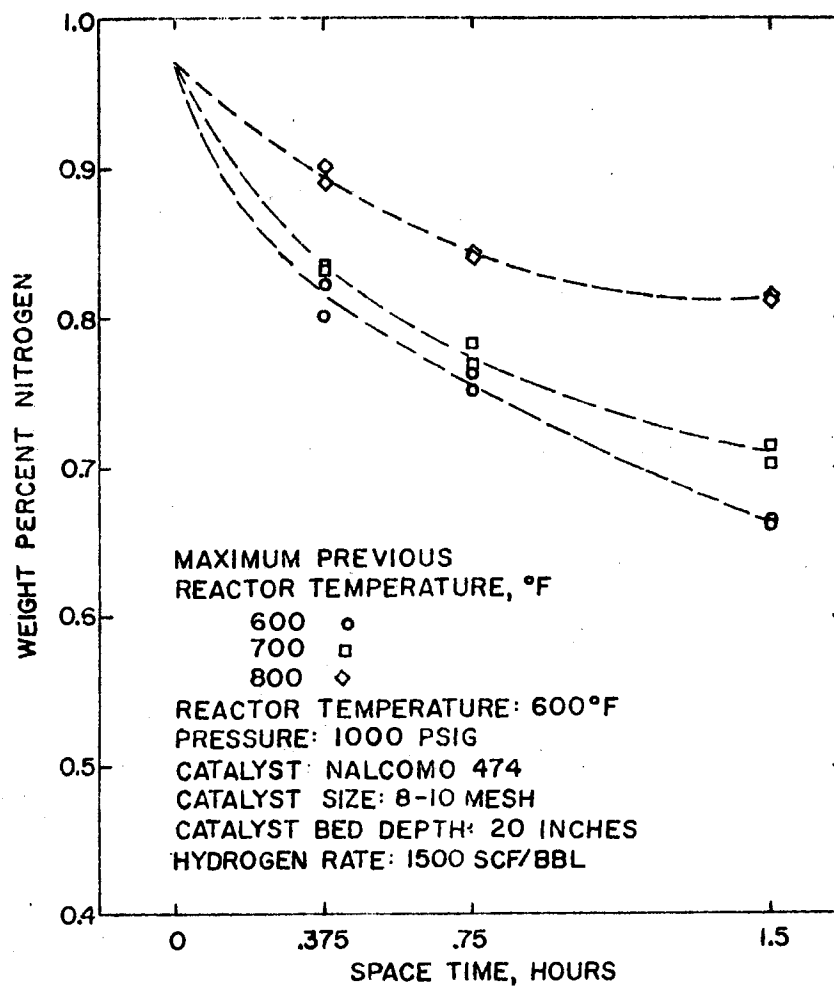
Figure 53. Effect of Previous Maximum
Operating Temperature on
Catalyst Activity at 600°F

product oil as a function of space time with parameters of maximum previous operating temperature in the catalyst loading. The data in Figure 53 are for the reactor operating at 600°F, 1000 psig, and a hydrogen rate of 1500 SCF/bbl. These results indicate that the higher the maximum previous reactor operating temperature, the lower the catalyst activity at 600°F. The decrease in activity at 600°F associated with higher previous reactor was the result of deactivation both during the isothermal runs and deactivation resulting from the change in reactor operating temperature. Previous analysis suggested that the deactivation associated with isothermal operation was much less than the loss of activity shown in Figure 53. Therefore, the deactivation associated with a change in reactor operating temperature was probably greater than the deactivation associated with isothermal operation at these conditions.

However, Figure 53 does not give any clues to whether the deactivation occurred when the reactor temperature was increased or decreased. In order to clarify the situation, the effect of an increase in the reactor operating temperature on the catalyst activity will be estimated. Figure 54 is a plot of the weight percent nitrogen as a function of space time with parameters of minimum previous reactor operating temperature. Since only deactivation resulting from isothermal operation and an increase in reactor operating temperature were involved, the effect of an increase in reactor operating temperature can be estimated. Figure 54 shows that previous miminum reactor operating temperature had a very small effect on the activity of the catalyst at 700°F and 1000 psig. These results imply that the
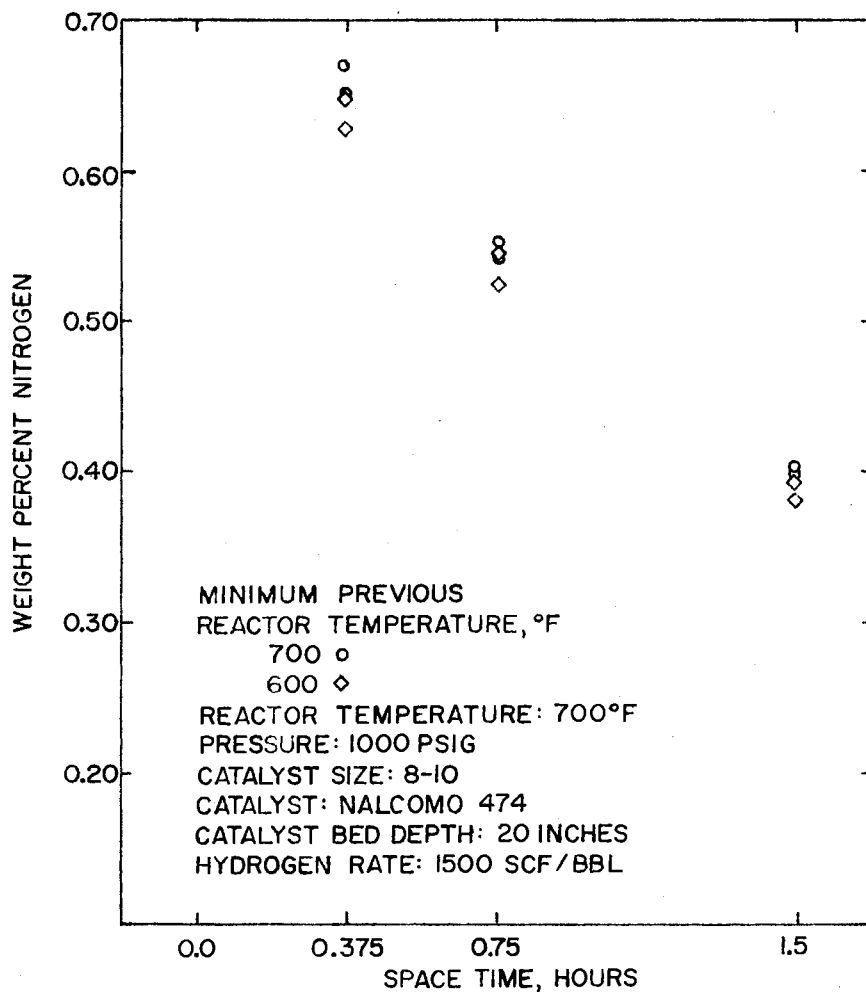
Figure 54. Effect of Previous Minimum Reactor
Operating Temperature on Catalyst
Activity at 700°F

catalyst deactivation associated with a reduction in reactor operating temperature was much greater than the deactivation resulting from isothermal operation or increase in reactor operating temperature.

This study will make no attempt to adjust the data to account for the effect of catalyst deactivation. The general approach was to operate the reactor such that the effect of catalyst deactivation was minimized, and then interpret the results in light of the uncertainty introduced by catalyst deactivation. All runs made after a reduction in reactor operating temperature from a temperature greater than $700^{O}F$ will be discarded. Only runs with the same previous temperature sequencing will be used for comparisons among the catalyst loadings. Since the catalyst activity was not stable at $800^{O}F$, the maximum reactor operating temperature was set at $750^{O}F$.

Effect of Catalyst Particle Size

Diffusion resistances to reaction in a trickle flow reactor can be divided into two types:

1. Resistances encountered in the liquid film surrounding the catalyst pellet

2. Resistances encountered in the pores of the catalyst

Pore diffusion resistances cause a decrease in the reactant concentration from the catalyst particle outer boundary to the center of the catalyst, which in turn decreases the rate of reaction in the interior of the catalyst pellet. Since the effect of diffusion resistances on the rate of reaction is of primary importance, the role of pore diffusion will be discussed in terms of the effectiveness factor.

The effectiveness factor is defined as the ratio of the actual measured reaction rate to that which would be observed if all the surface throughout the inside of the catalyst pellet were exposed to the catalyst outer boundary reactant concentration and temperature. Normally, the effectiveness factor is estimated by comparing the catalyst performance for two or more catalyst particle sizes. A rate expression for the reaction under investigation is required for an estimate of the effectiveness factor from catalyst performance of two particle sizes. However, the two limiting cases can be evaluated without knowledge of the rate expression. If the effectiveness factor is one, then the rate is independent of the particle diameter. If the effectiveness factor is zero, then the rate of reaction is proportional to the catalyst external surface area, which is also proportional to the catalyst particle diameter. A qualitative estimate of the effectiveness factor will be made by comparing the results of this work with the results that would be expected if the effectiveness factor were zero or one. After the kinetic model development, a quantitative estimate of the effectiveness factor will be made.

Figure 55 is a plot of the logarithm of the weight percent nitrogen for the 40-48 mesh particle size as a function of the logarithm of the nitrogen content for the 8-10 mesh particle size at the same reactor operating conditions. The line for an effectiveness factor of one was located by drawing a line through the feed nitrogen level with a slope of -1. The line for an effectiveness factor of zero was located by drawing a line through the feed nitrogen concentration with a slope equal to the ratio of the catalyst particle diameters.

The data indicate that the effectiveness factor is much closer to one than zero. This result implies that the rate of overall reaction is predominately controlled by the rate of surface reaction. Subsequent model development will assume that the surface reaction was the rate controlling step. After the kinetic model has been developed, the effectiveness factor will be estimated using the data in Figure 55 and the kinetic model.

Kinetic Model Development

The development of a kinetic model will begin by reviewing the basis for the kinetic model presented in previous sections of this chapter.

1. Catalyst bed height at constant space time will be assumed to have a negligible effect on kinetics of denitrogenation.

2. Catalyst deactivation during a series of isothermal runs will be assumed to be negligible.

3. Only runs with essentially the same thermal history will be compared.

4. The overall rate of reaction will be assumed to be controlled by the rate of surface reaction.

Development of Model 1

A simple "power law" rate express, Equation 6.1, will be used in the initial model development.

$$\frac{dN}{d\Theta} = - k_{6.1} N^b \qquad (6.1)$$
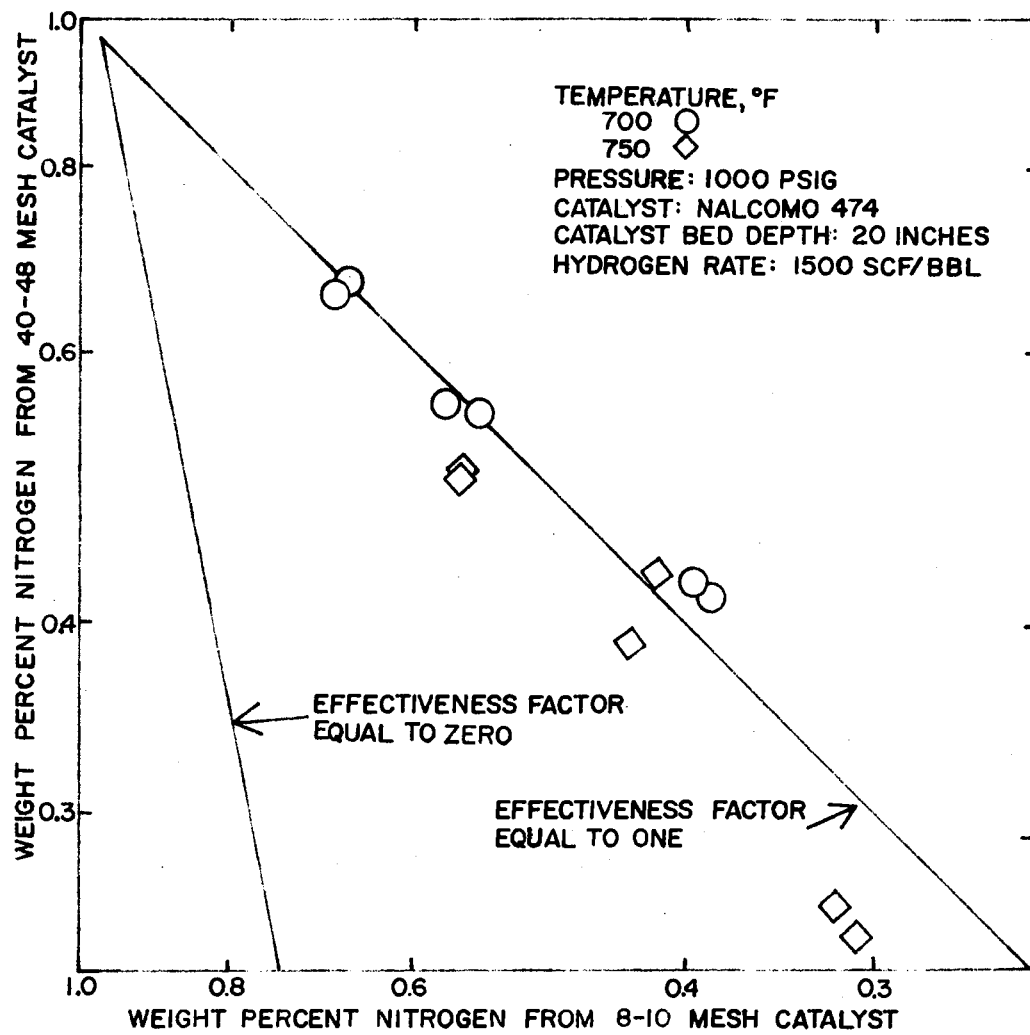
Figure 55. Estimate of Effectiveness Factor for
Nalcomo 474 Catalyst

Where, b is an arbitrary constant to be evaluated by regression of the data.

The value of b will be evaluated by choosing integer values of b, integrating Equation 6.1, and then fitting the integrated form of Equation 6.1 to the data of this work. Figure 56 is a plot of the sum of squares of the error, the sum of the square of the difference between the weight percent nitrogen observed and obtained by regression of Equation 6.1, as a function of the reaction order, the value of b. This plot indicates that a third order reaction gives the best fit of the data. This is much higher than the first order kinetics reported in some pure component studies (24, 26, 27).

One explanation of a high apparent reaction order is that the various organonitrogen species in the mixture have a wide range of reactivities. Denitrogenation of the more reactive species tends to occur at relatively low space times, resulting in a high apparent initial rate constant. At high space times, relatively small quantities of the very reactive organonitrogen species remain. As a result the apparent rate constant is smaller than at lower space times. The only way a rate expression such as Equation 6.1 can compensate for this effect is to have a large reaction order. The model development will continue by assuming that the feedstock studied contained organonitrogen species with a wide range of reactivities. Then, the reactivity distribution will be estimated and incorporated into the model.

Development of Model 2

Flinn and Beuther (27) showed that the reactivity of organonitrogen species from petroleum feedstocks was a function of boiling point.
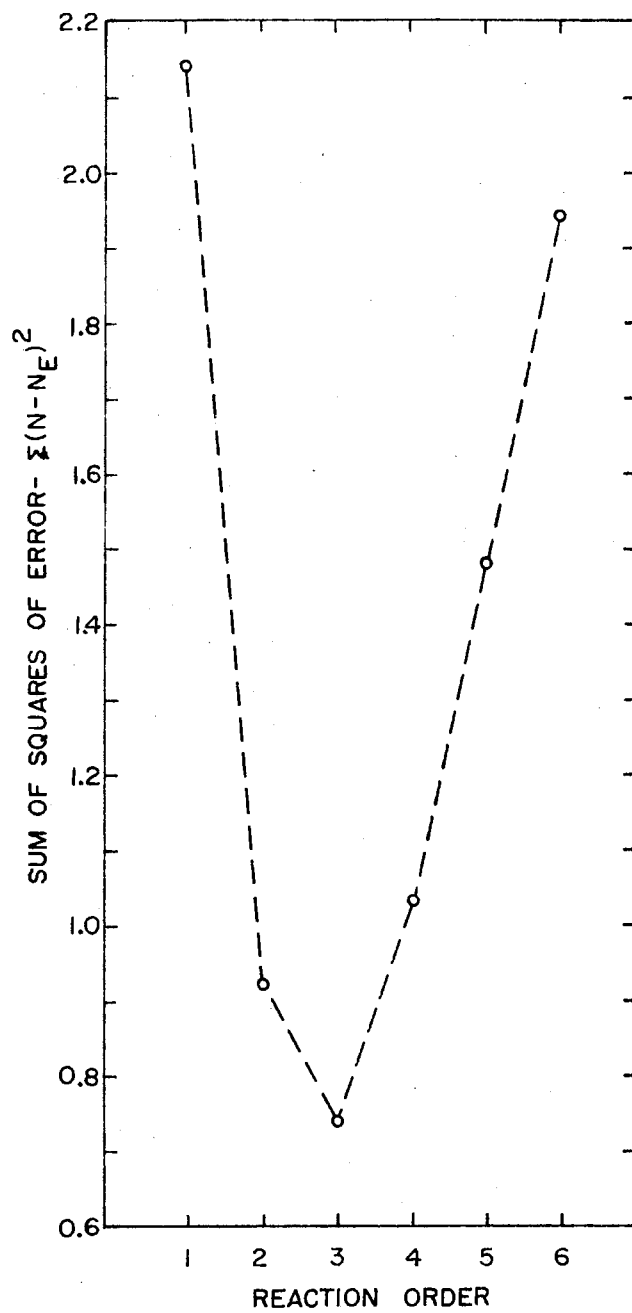
Figure 56. Reaction Order Selection
for Model 1

The reactivity of the organonitrogen species in the feed used in this study was estimated by analyzing boiling point ranges of the feed and product oils for organonitrogen level. Figure 57 is a plot of the logarithm of the weight percent nitrogen in the feed and product as a function of the average boiling point measured at fifty millimeters of mercury. In order to make the reactivity as a function of boiling poing more apparent, the data in Figure 57 were replotted in Figure 58. Figure 58 is a plot of the weight percent nitrogen remaining as a function of boiling point at fifty millimeters of mercury. The percent nitrogen remaining is defined as the weight percent nitrogen in a boiling range of reactor product divided by that of the feed all multiplied by a hundred. If denitrogenation were first order with respect to organonitrogen level and the first order rate constant was independent of the boiling point, then the plot on Figure 58 should form horizontal line. If the first order rate constant tended to decrease, as a previous work (27) indicated, then the percent nitrogen remaining would tend to increase with increasing boiling point. In general, the weight percent nitrogen remaining, shown in Figure 58, did tend to increase with increasing boiling point. However, the percent remaining in the lowest boiling range was much greater than one would expect based on the results for the other boiling ranges.

One is tempted to dismiss the low conversion for the lowest boiling range material as an experimental blunder. The weight percent nitrogen of the feed as a function of boiling point was determined a second time with essentially the same result. The conversion of organonitrogen species in the lowest boiling range for all three
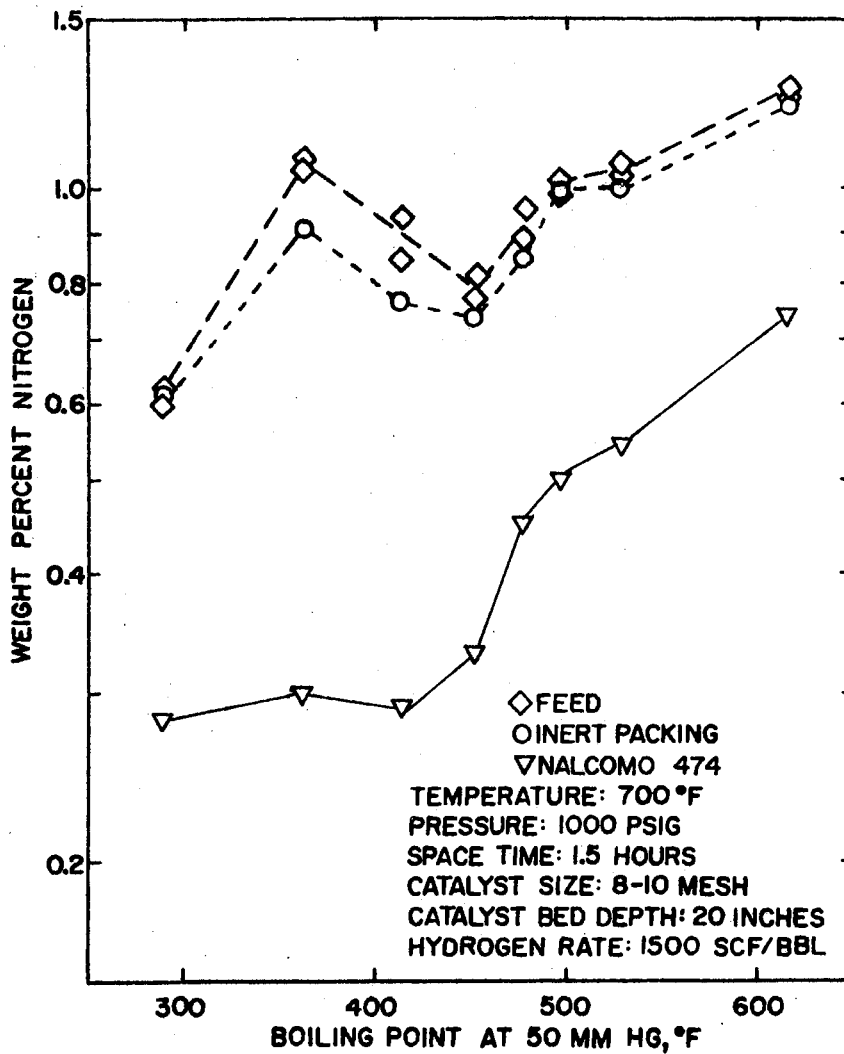
Figure 57. Organonitrogen Specie Reactivity as
a Function of Boiling Point

TEMPERATURE: 700°F
PRESSURE: 1000 PSIG
CATALYST: NALCOMO 474
CATALYST SIZE: 8-10 MESH
CATALYST BED DEPTH: 20 INCHES
HYDROGEN RATE: 1500 SCF/BBL
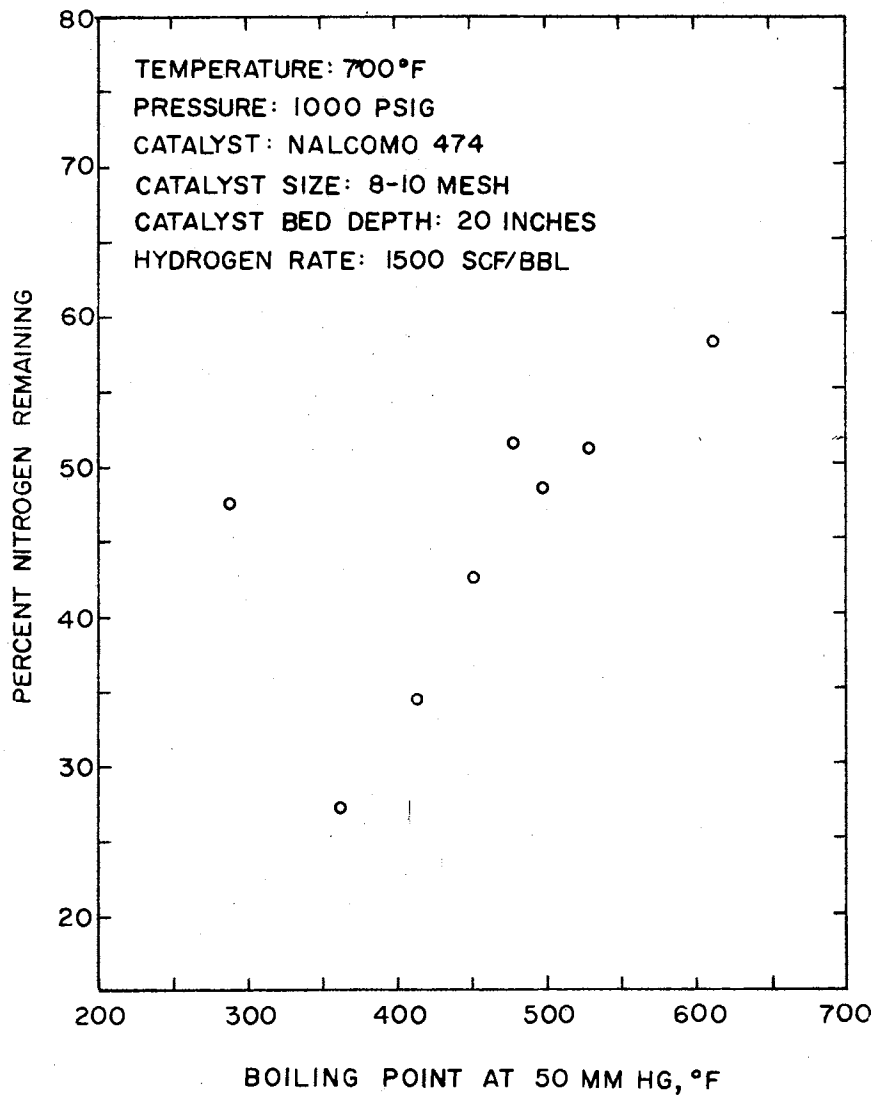
Figure 58. Organonitrogen Specie Reactivity
as a Function of Boiling Point

catalysts studied was much less than one would have expected based on the results from the other ranges. Therefore, the low conversion obtained in the lowest boiling range was not an experimental blunder.

One implicit assumption of comparing weight percent nitrogen as a function of boiling point in Figure 58 is that all species remain in the same boiling range in the reactor product as it occupied in the feed oil. However, a substantial amount of cracking, reduction of the molecular weight and boiling point of the oil, was observed (See Table XXI). Therefore, the results in Figure 58 in fact couple the effect of denitrogenation reactivity and hydrocracking.

The low conversion in the lowest boiling range can be rationalized in terms of the effect of hydrocracking. The weight percent nitrogen in the second lowest boiling range (328 to 394°F at 50 mm Hg), 1.07, is much higher than in the lowest boiling range (less than 328°F at 50 mm Hg), 0.60. The low conversion of organonitrogen species in the lowest boiling range could have been the result of cracking of organonitrogen species into the lowest boiling range before denitrogenation occured.

If hydrocracking reactions can effectively mask the apparent conversion of organonitrogen species, as the above analysis suggests, then one would like a method of uncoupling the effect of reactivity of organonitrogen species and hydrocracking reactions before attempting to estimate the reactivity of organonitrogen molecules as a function of boiling point from the data in Figure 58.

Flinn (27) found that the assumed first order denitrogenation rate constant was approximately a linear function of the boiling point

with a petroleum feedstock. Figure 59 is a plot of the pseudo first order rate constant calculated using the data presented in Figure 57 and Equation 6.2.

$$k_i = \frac{\ln (N_{fi}/N_{pi})}{\theta_v} \qquad (6.2)$$

The variable k_i is the pseudo first order rate constant for boiling range number i (the boiling ranges are numbered from the lowest average boiling point to the highest). N_{fi} and N_{pi} are the weight percent nitrogen in the feed and product in boiling range i. θ_v is the hourly volumetric space time. Figure 59 shows that the pseudo first order rate constant is roughly a linear function of boiling point if the lowest boiling range is excluded.

This work will assume that the pseudo rate constant, any order, is actually a linear function of the boiling point. Then the value of the rate constant as a function of boiling point will be estimated by curve fitting the data in Figure 57 assuming the rate constant is a linear function of boiling point excluding the results from the lowest boiling range. Equation 6.2 will be used to determine the pseudo first order rate constants and Equation 6.3 will be used for n^{th} order rate constants where n is greater than one.

$$k_i = \frac{1}{n-1} \left[\left(\frac{1}{N_{pi}}\right)^{n-1} - \left(\frac{1}{N_{fi}}\right)^{n-1} \right] \frac{1}{\theta_v} \qquad (6.3)$$

Equation 6.3 was obtained by integrating a simple "power law" rate expression of order n. Where, n is not equal to one.

The ratio of the k_i's will be assumed to be independent of the reactor operating temperature and pressure. This assumption will be
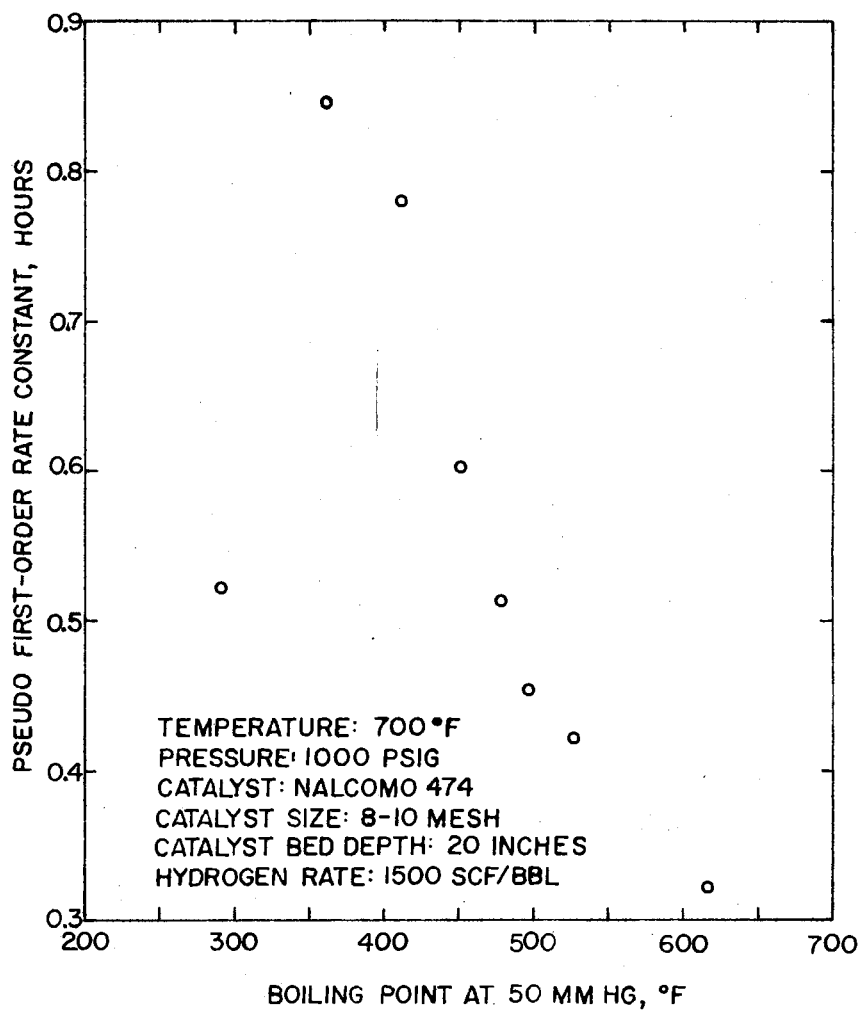
Figure 59. Pseudo-First Order Rate Constant
as a Function of Feedstock
Boiling Point

checked later in the model development. The activity ratio will be defined by Equation 6.4.

$$r_i = k_i / k_8 \qquad (6.4)$$

Since the rate constant for the eighth, and highest boiling range, has the lowest rate constant, the activity ratio for all cuts has a value equal to or greater than one.

The next step will be to put Equations 6.2, 6.3, and 6.4 in a form that can easily be curve fitted. Solving for the reactor outlet weight percent nitrogen level in Equations 6.2 and 6.3 yields Equations 6.5 and 6.6.

$$N_{pi} = N_{fi} / d^{k_i \theta_v} \qquad (6.5)$$

$$N_{pi} = \frac{1.0}{[k_i (n-1) \theta_v + (1.0/N_{fi})^{n-1}]^{1.0/(n-1)}} \qquad (6.6)$$

Equation 6.5 is used when the assumed reaction order is one and Equation 6.6 is used for all other reaction orders. The weight percent nitrogen of the individual boiling point ranges were related to the overall nitrogen level by Equation 6.7.

$$N_p = \sum_i w_i N_{pi} \qquad (6.7)$$

Where N_p, N_{pi}, and w_i are the weight percent nitrogen in the reactor product, the weight percent nitrogen in boiling range i in the product, and the mass fraction of material in boiling range i. The model will assume that denitrogenation occurs before hydrocracking.

The next step will be to combine Equations 6.5, 6.6, and 6.7 to give Equations 6.8 and 6.9.

$$N_p = \sum_i w_i \, N_{fi} \, e^{-k_i \theta_v} \qquad (6.8)$$

$$N_p = \sum_i \frac{w_i}{[k_i(n-1)\,\theta_v + (1.0/N_{fi})^{n-1}]^{1/(n-1)}} \qquad (6.9)$$

Equation 6.8 is used when n equaled one and Equation 6.9 was used for other values of n. Combining Equations 6.4, 6.8, and 6.9 give Equations 6.10 and 6.11.

$$N_p = \sum w_i \, N_{fi} \, e^{-(r_i \, k_8 \, \theta_v)} \qquad (6.10)$$

$$N_p = \sum \frac{w_i}{[k_8 \, r_i \,(n-1)\theta_v + (1/N_{fi})^{n-1}]^{1/(n-1)}} \qquad (6.11)$$

Equations 6.10 and 6.11 are the working equations for fitting Model 2 to the isothermal data of this work using a first order and n order rate expressions, respectively. The next step will be to determine the reaction order that yields the best fit to the data using Equations 6.10 and 6.11.

Table X gives the values of w_i, N_{fi}, and $\overline{T}_i$ (the average boiling point at 50 mm Hg of boiling range i). The next step will be to estimate the values of r_i in Equations 6.10 and 6.11 using the data presented in Figure 57 and Equations 6.2, 6.3, and 6.4.

TABLE X

FEED CHARACTERIZATION

Boiling Point Range Number	w_i	N_{fi}	$\bar{T}_i, {}^\circ F$
1	.105	.59	289
2	.106	1.07	361
3	.110	.93	411
4	.112	.81	450
5	.120	.90	478
6	.110	.99	496
7	.127	1.03	527
8	.210	1.21	614

The first step in estimating the activity ratios, r_i, is to assume a reaction order. Then, the k_i's can be estimated by fitting Equation 6.2, for a first order reaction, or Equation 6.3, for a nth order reaction, to the data presented in Figure 57 assuming that k_i is a linear function of boiling point and excluding the results from the lowest boiling range. The activity ratios are calculated using Equation 6.4. Table XI presents activity ratios for several assumed reaction orders.

TABLE XI

ACTIVITY RATIOS (r_i)

Boiling Point Range Number	Reaction Order		
	1	2	3
1	3.86	11.66	12.34
2	3.22	9.30	9.82
3	2.78	7.66	8.08
4	2.44	6.38	6.72
5	2.20	5.46	5.75
6	2.04	4.87	5.12
7	1.76	3.85	4.04
8	1.00	1.00	1.00

The reaction order that yields the best fit of the model to the hydrodenitrogenation data in Appendix A was determined using the following procedure:

1. Assume a reaction order.

2. Determine the activity ratios using Equation 6.4.

3. Fit all the hydrodenitrogenation data in Appendix A isotherm by isotherm to Equation 6.10 or 6.11 using k_8 as the only adjustable parameter.

4. The reaction order will be selected based on the minimization of the sum of squares of the error.

Figure 60 is a plot of the sum of squares of error as a function of the reaction order. The sums of squares of error for the second and third order reaction are nearly equal. The second order reaction was chosen over the third order for the following reasons:

1. The second order rate expression described the data taken with a reactor temperature greater than 700°F better than the third order rate expression. A commercial reactor would probably operate at a temperature greater than 700°F.

2. The second order rate expression is more reasonable on physical grounds.

The next step will be to compare the performance of Model 1 and Model 2.

Comparison of Models 1 and 2

The primary measure of the performance of either kinetic model is the sum of squares of the error. Figure 61 is a plot of the sum of squares of the error as a function of the assumed reaction order for kinetic Model 1 and 2. The minimum sum of squares of the error for Model 1 is about six times that of Model 2. Since both models have only one freely adjustible parameter, the rate "constant," a direct comparison of the sum of squares of error is a reasonable measure of the model's performance; however, it is not the only measure of the performance of the model.

Later, the effect of reactor operating conditions, temperature, pressure, and space time, will be described in terms of the model. Therefore, it is important that the model accurately represent the
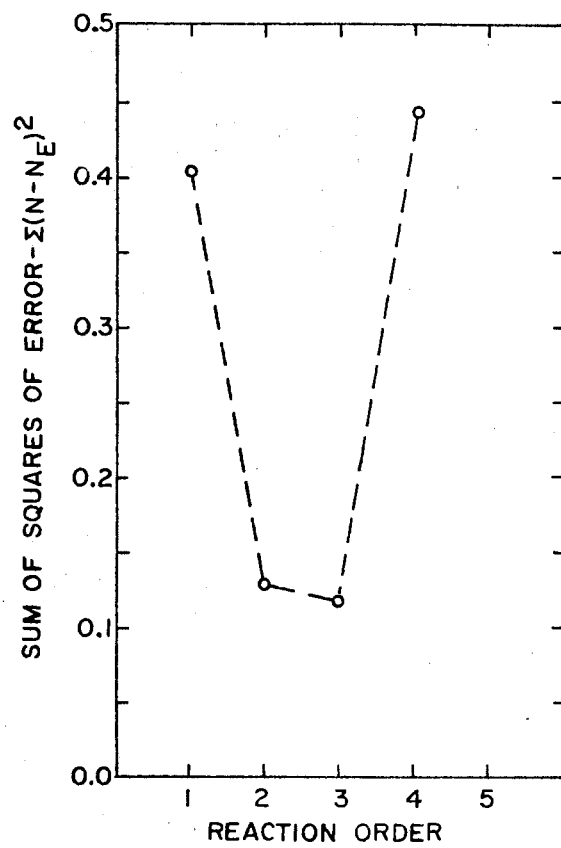
Figure 60. Reaction Order Selection
for Model 2
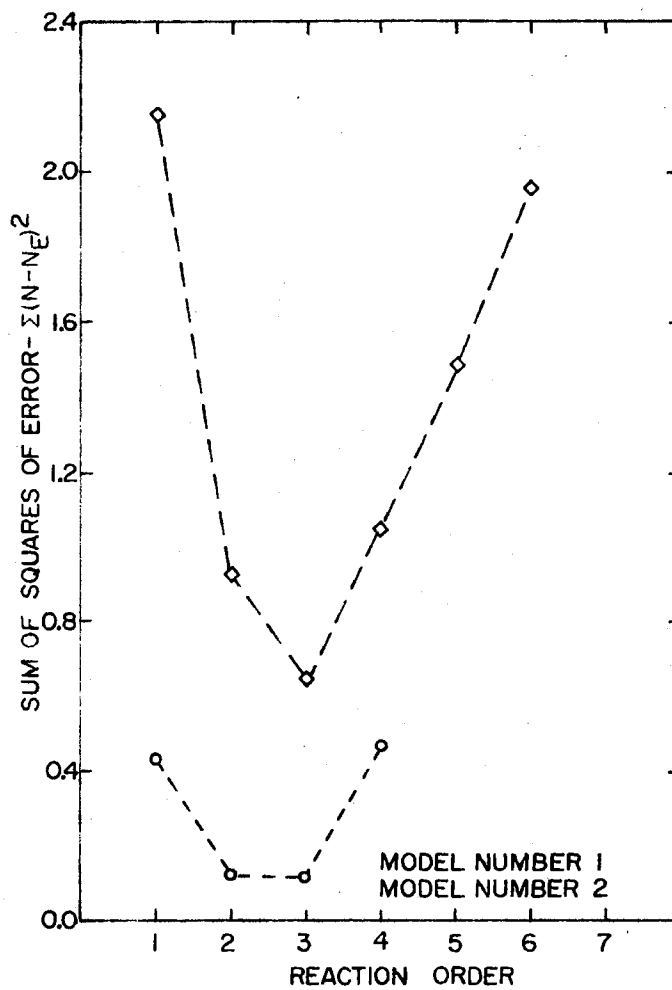
Figure 61. Comparison of the Sum of
Squares of the Error
for Model 1 and Model
2

effect of reactor operating temperature, pressure, and space time. Figure 62 is a plot of the average deviation (the sum of the experimentally determined weight percent nitrogen in the reactor product less the weight percent nitrogen by regression, the quantity divided by the number of data points) as a function of the reactor operating temperature. If the model showed no bias with respect to the reactor temperature, then the plot would be a horizontal line with a zero average deviation. Figure 62 shows that Model 2 describes the effect of reactor operating temperature on the weight percent nitrogen in the reactor product oil with much less bias than Model 1. Figure 63 is a plot of the average deviation of weight percent nitrogen in the reactor product oil as a function of reactor operating pressure. The plot shows that Model 1 shows less bias with respect to reactor operating pressure than Model 2.

Figure 64 is a plot of the average deviation of weight percent nitrogen in the reactor product oil as a function of space time. The plot shows that Model 1 shows less bias with respect to changes in space time than Model 2.

In summary, Model 2 is superior to Model 1 since the minimum sum of squares of the error Model 1 is about six times the corresponding quantity for Model 2. However, the bias with respect to reactor operating pressure and space time for Model 2 was greater than for Model 1. Model 2 only showed less bias than Model 1 with respect to reactor operating temperature.

One would like to improve the performance of Model 2 with respect to prediction of the weight percent nitrogen in the reactor effluent
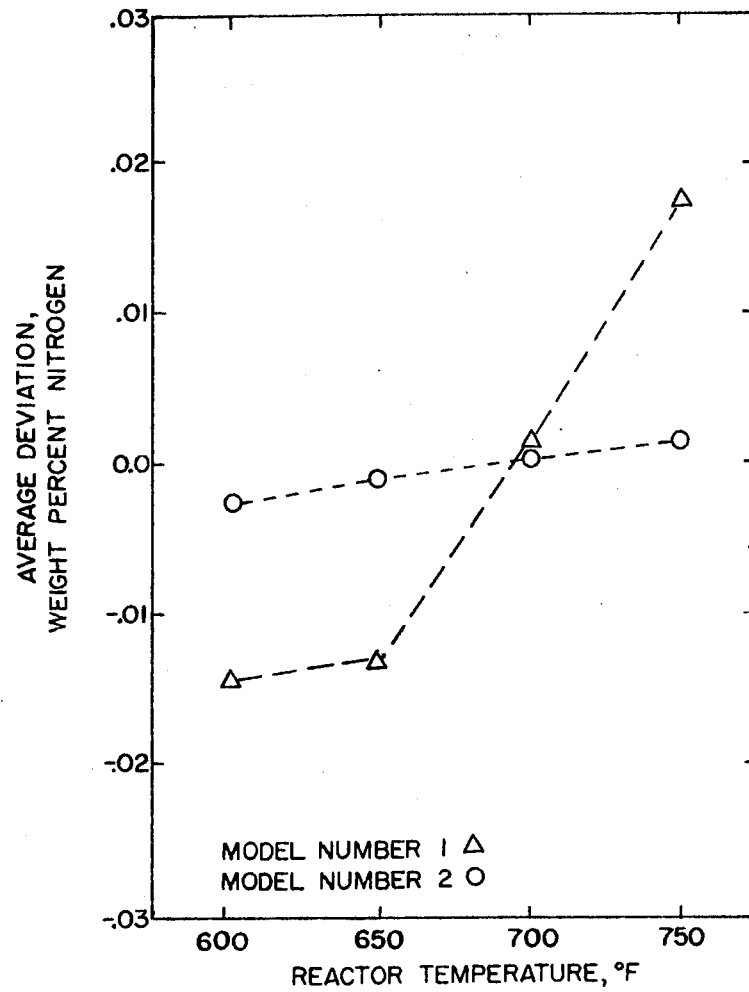
Figure 62. Average Deviation for Models
1 and 2 as a Function of
Temperature
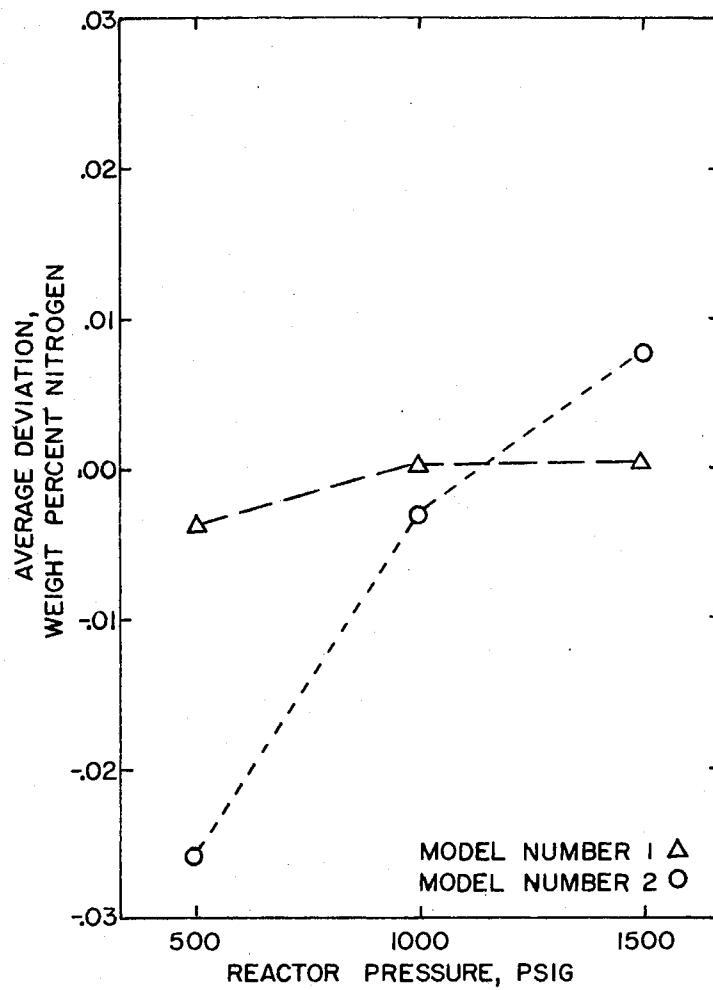
Figure 63. Average Deviation for
            Models 1 and 2 as a
            Function of Pressure
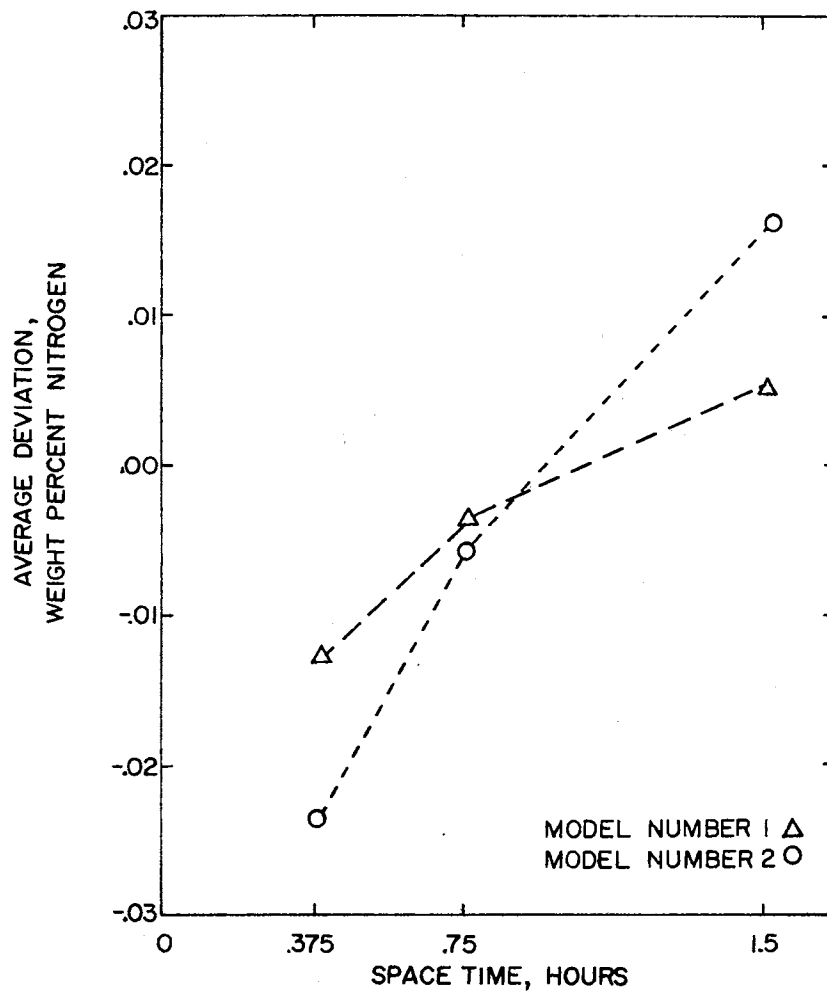
Figure 64. Average Deviation for
            Models 1 and 2 as a
            Function of Space
            Time
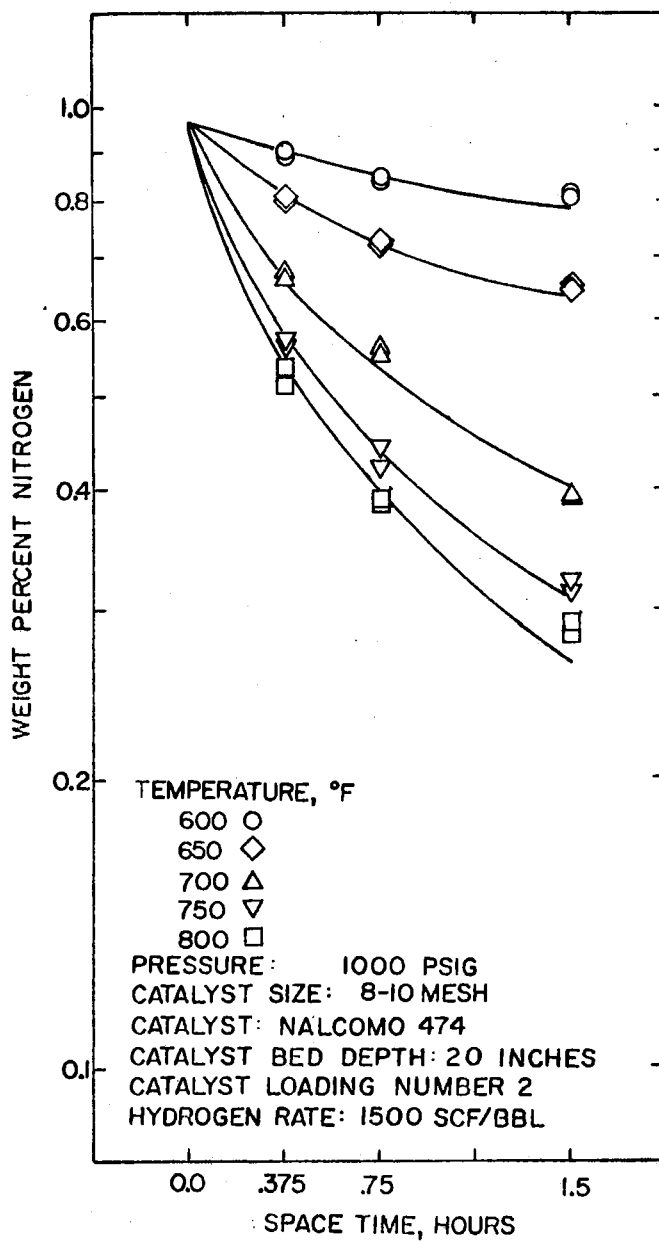
Figure 65. Fit of Model 2 to Data
of Catalyst Loading
2
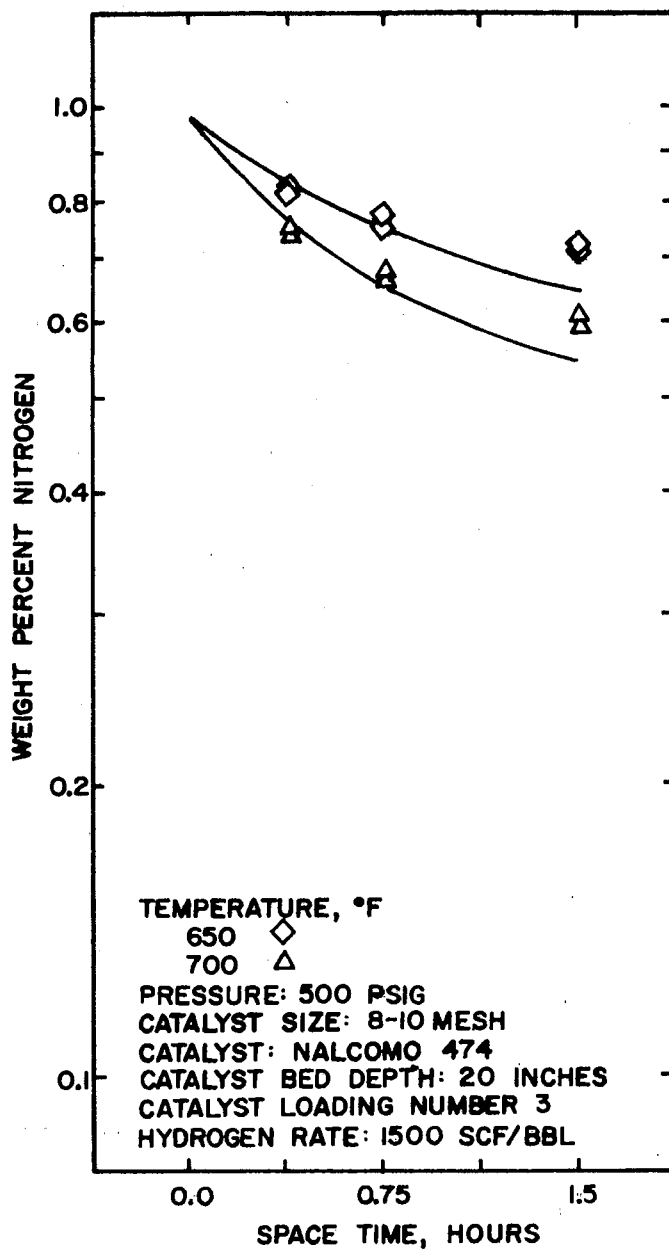
Figure 66.   Fit of Model 2 to Data
             of Catalyst Loading 3
             at 500 psig
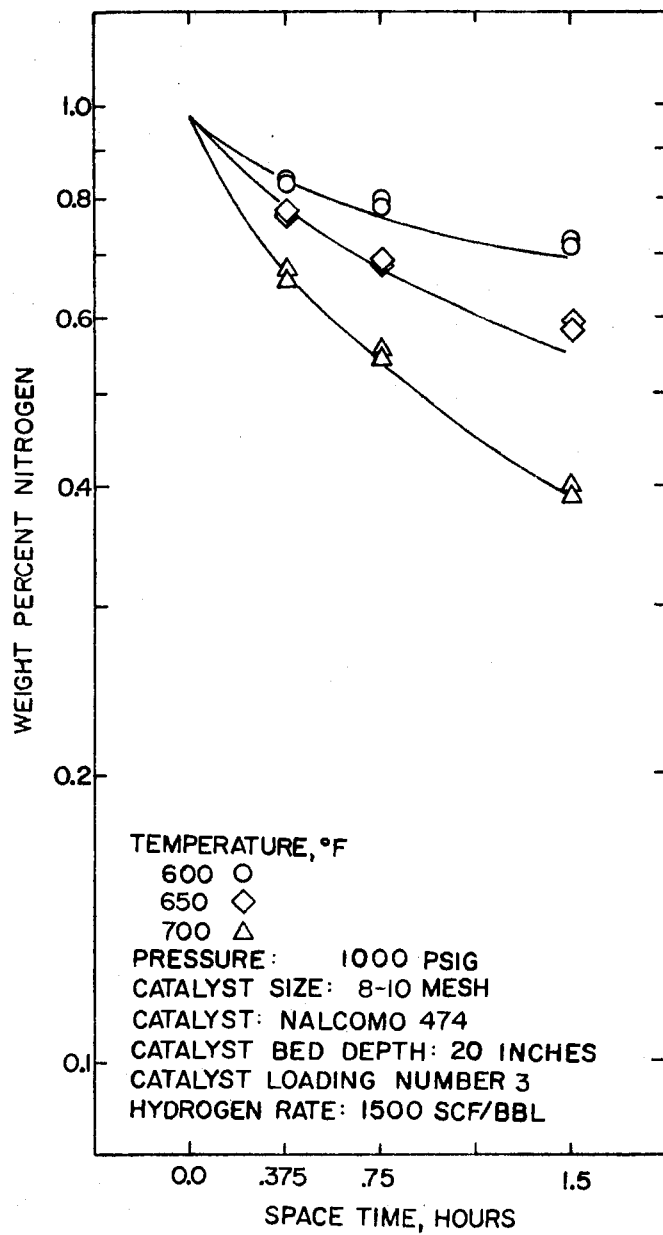
Figure 67. Fit of Model 2 to Data
of Catalyst Loading 3
at 1000 psig

WEIGHT PERCENT NITROGEN

SPACE TIME, HOURS

TEMPERATURE, °F
650 ◇
700 △
PRESSURE: 1500 PSIG
CATALYST SIZE: 8-10 MESH
CATALYST: NALCOMO 474
CATALYST BED DEPTH: 20 INCHES
CATALYST LOADING NUMBER 3
HYDROGEN RATE: 1500 SCF/BBL
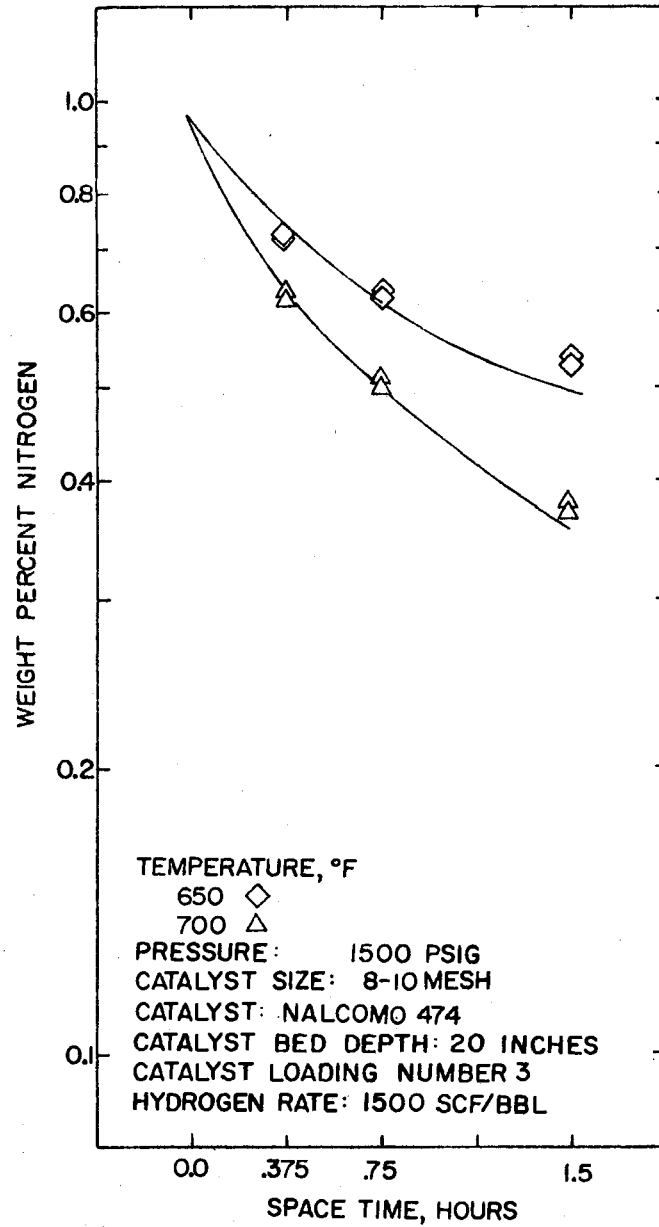
Figure 68. Fit of Model 2 to Data
of Catalyst Loading
3 at 1500 psig
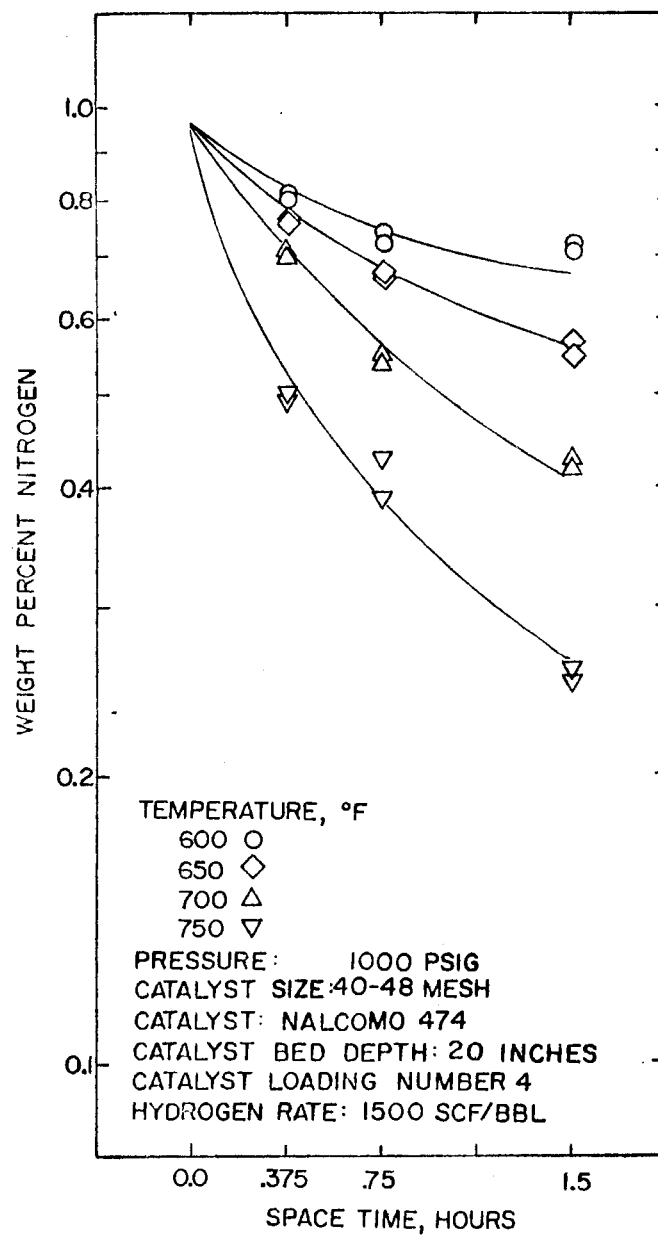
Figure 69. Fit of Model 2 to Data
of Catalyst Loading 4
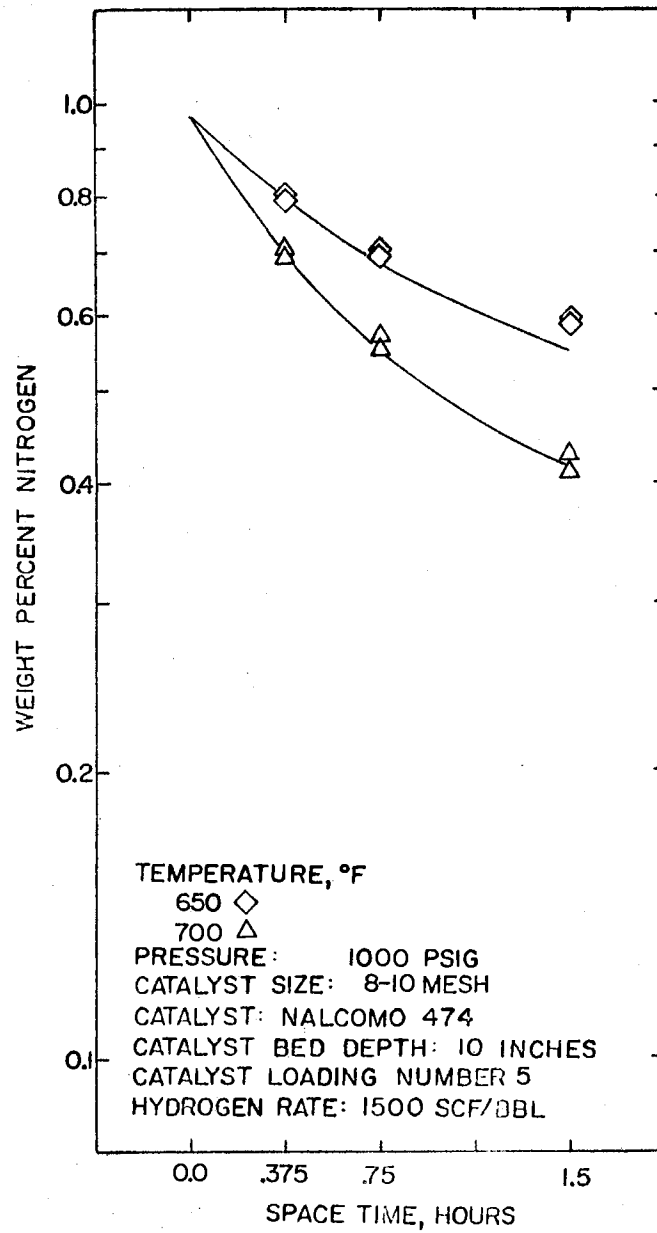
Figure 70. Fit of Model 2 to Data
of Catalyst Loading 5
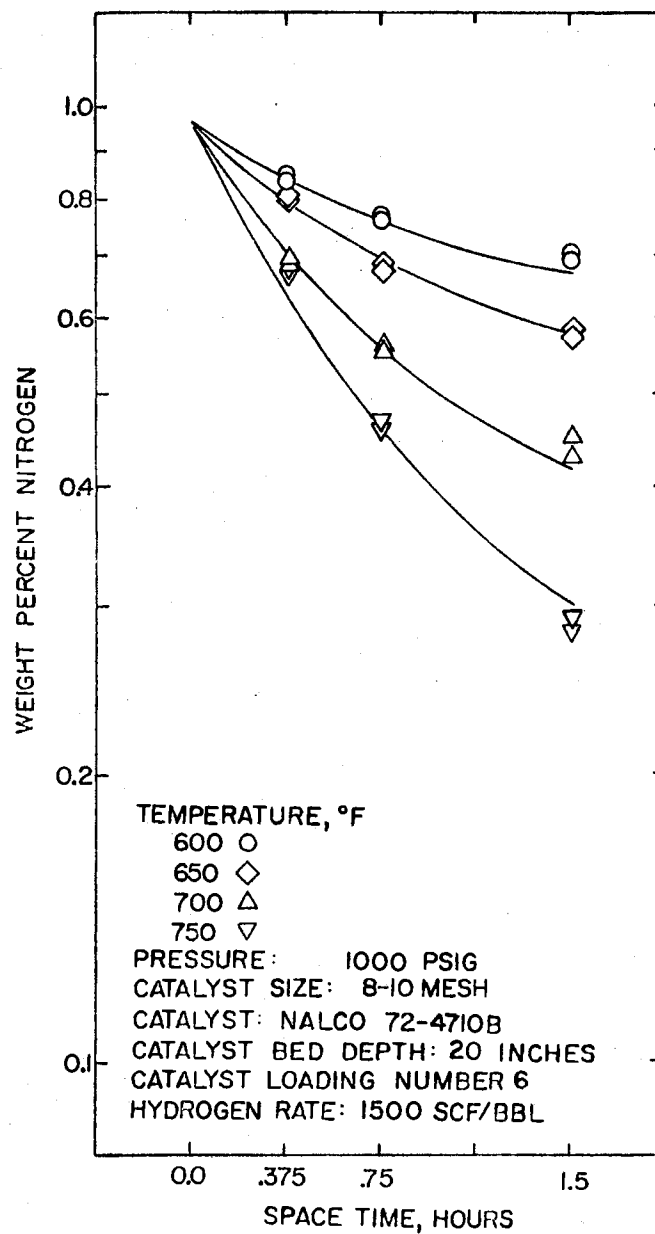
Figure 71. Fit of Model 2 to Data
of Catalyst Loading 6
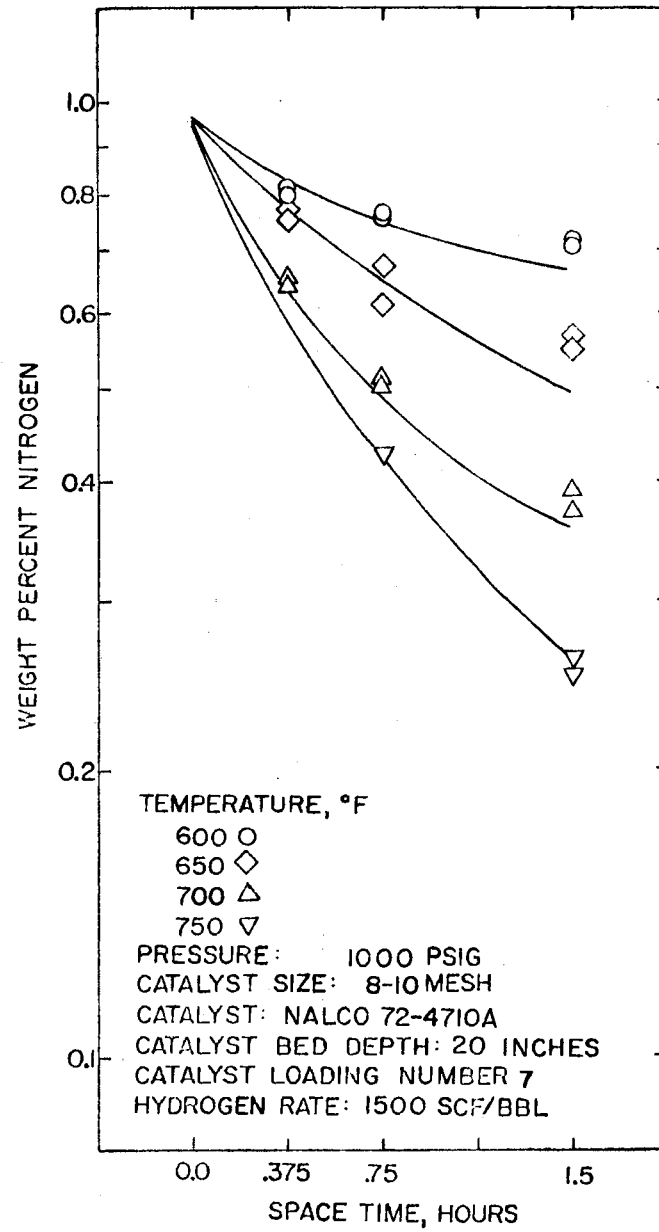
Figure 72. Fit of Model 2 to Data
of Catalyst Loading 7
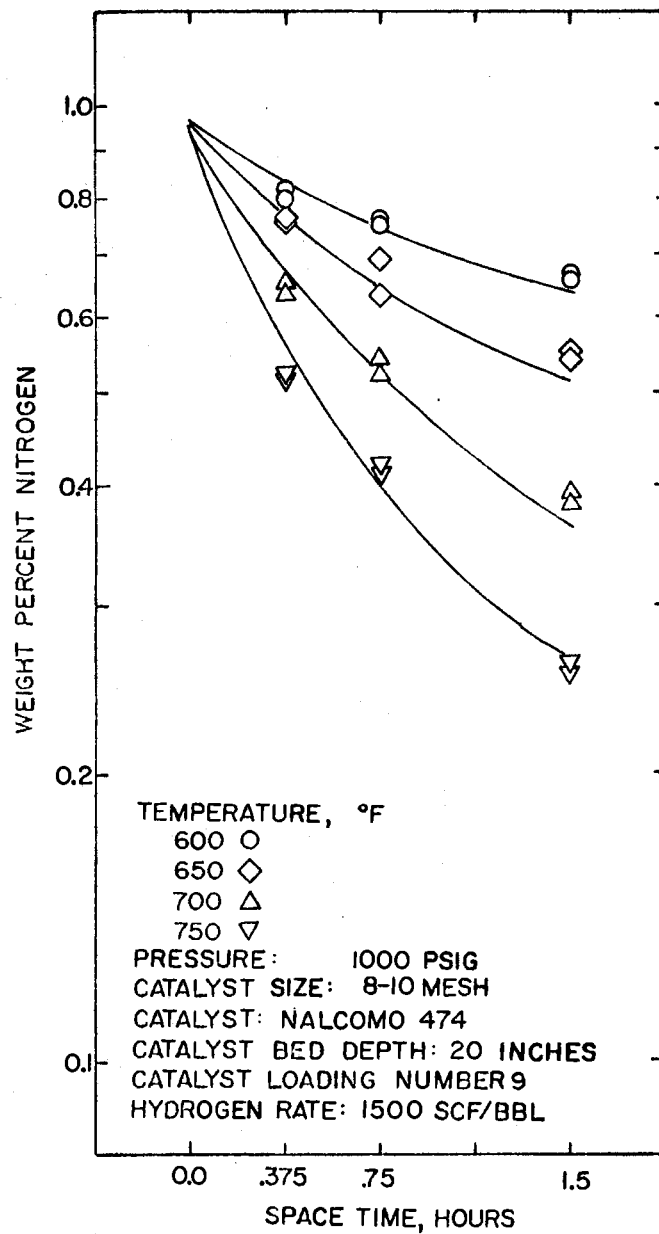
Figure 73. Fit of Model 2 to Data
of Catalyst Loading 9

as a function of space time. Flinn (27) also showed that the rate of denitrogenation was a function of specie type as well as boiling point. In general, amines were found to be the most reactive class. Organonitrogen species with the nitrogen in the aromatic ring tend to be the least reactive class. This suggests that the model should account for the rate constant as a function of specie type and boiling point. However, this approach would require the analysis of the feedstock with respect to the organonitrogen specie type. This is a very difficult task and is beyond the scope of this work. Therefore, Model 2, defined by Equation 6.14 with n set at a value of 2, will be used in the subsequent analysis of the data.

Figures 65-73 are plots of the logarithm of the weight percent nitrogen in reactor product oil as a function of space time. The lines on these plots are the results of fitting Equation 6.14 to the data in Appendix A isotherm by isotherm. The Figures are presented to give a graphical display of how well Model 2 fits the experimental data.

Effect of Reactor Operating Temperature

The effect of reactor operating temperature on the rate constant is usually expressed in terms of the Arrhenius equation, Equation 6.12.

$$k = A \exp(-E/RT) \tag{6.12}$$

Where, k, A, E, R, and T are the rate constant, frequency factor, activation energy, universal gas constant, and the absolute temperature. Taking the logarithm of both sides of Equation 6.12 yields Equation 6.13.

$$\log_e k = \log_e A - E/RT \qquad\qquad (6.13)$$

Equation 6.13 indicates that a plot of the logarithm of the experimental rate constant as a function of the reciprocal of the absolute reactor operating temperature should yield a straight line with slope of -E/R and an intercept of $\log_e$ A. Figure 74 is such a plot of the experimentally determined rate constant, k_8, as a function of the reciprocal of the absolute temperature. The line is a least squares best fit to the data. This line yields a value of 31,000 BTU/lb. mole for the activation energy, E, and a value of 2.1×10^5 hours^{-1} (weight percent nitrogen)$^{-1}$ for the frequency factor. Note that these values apply only for 1000 psia data and Nalcomo 474 catalyst.

One would like to know if the values for the frequency factor and activation energy are a function of the reactor operating temperature. Figure 75 is a plot of the logarithm of the experimentally determined rate constant, k_8, as a function of the reciprocal absolute temperature with parameters of reactor operating pressure. Unfortunately, experimental values for the rate constant were available only at 650 and 700°F at all three pressures. If the activation energy were independent of the reactor operating pressure, then all the lines on Figure 75 would be parallel. Table XII presents the activation energy as a function of the reactor operating pressure calculated from the data in Figure 75. Table XII shows that although there is considerable variation in the activation with changes in the reactor operating pressure, these variations do not seem to follow any simple trend. This indicates that the variation in the activation energy shown in Table XII is probably the result of error in the correlation
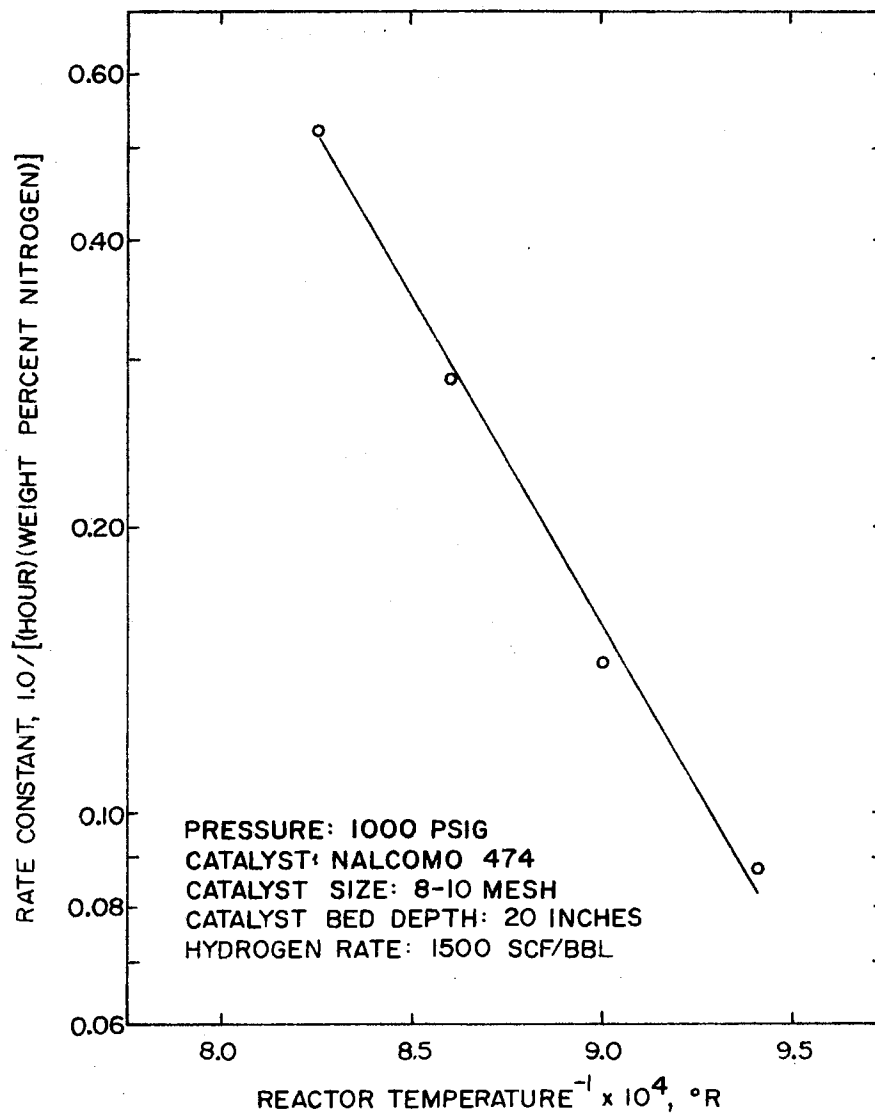
Figure 74. Arrhenius Plot for Nalcomo 474 at 1000 psig
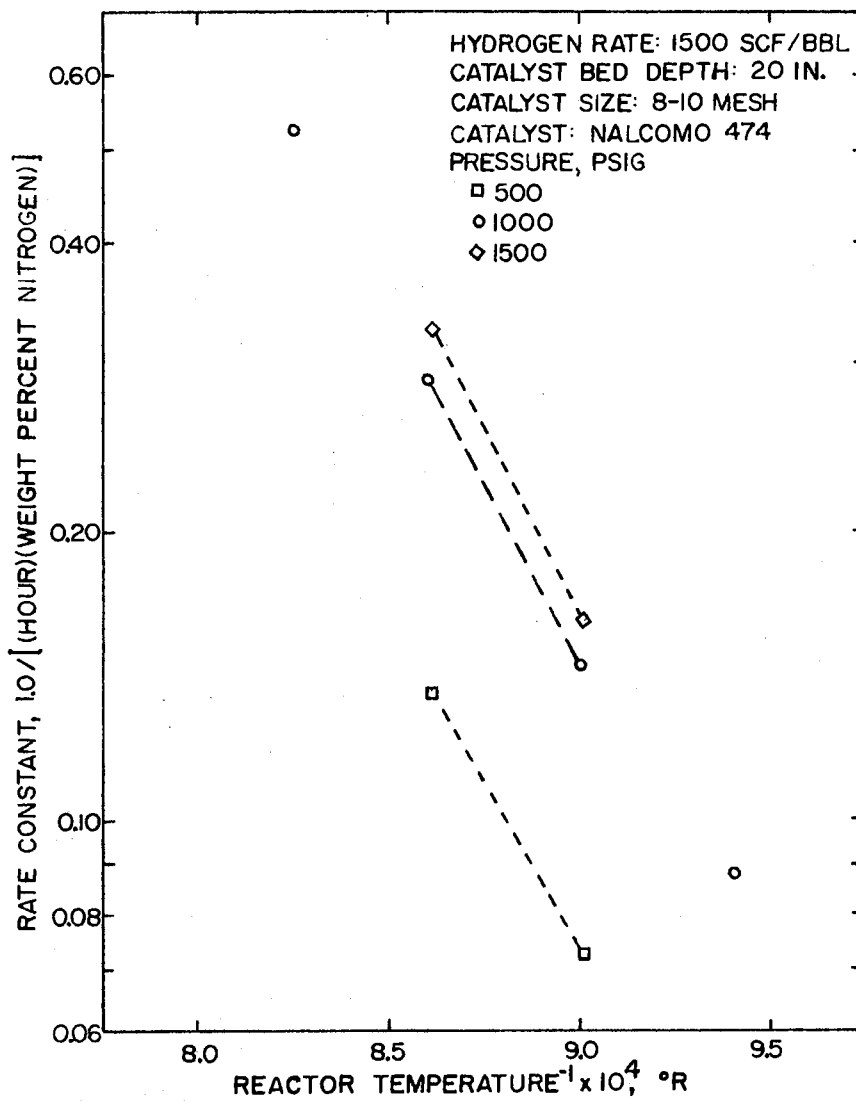
Figure 75. Arrhenius Plot for Nalcomo 474 Between 650 and 700°F at Pressures of 500, 1000, and 1500 psig

method and the data. Therefore, the activation energy is crudely

independent of the reactor operating pressure. The effect of pressure

on the frequency factor will be considered later in the analysis.

TABLE XII

ACTIVATION ENERGY AS A
FUNCTION OF PRESSURE

Pressure, Psig	Activation Energy, BTU/lb. mole	Frequency Factor, Hours^{-1} (Percent Nitrogen)$^{-1}$
500	30,800	8.9×10^{4}
1000	36,300	1.85×10^{6}
1500	34,000	8.6×10^{4}

In summary, the Arrhenius Equation, Equation 6.13, gives a

reasonable description of the effect of temperature on the rate con-

stant obtained from Model 2. Regression of the data using Nalcomo 474

catalyst at 1000 psig and over the temperature range of 600 to 750°F

indicates that the activation energy is in the region of 31,000 BTU/lb.

mole. The value of the activation energy is roughly independent of

the reactor operating pressure.

Effect of Reactor Operating Pressure

The effect of reactor operation pressure on the rate constant, k_8, is often expressed by an equation of the following form:

$$k \propto P^b \tag{6.14}$$

Where, P is the absolute reactor operating pressure and b is an arbitrary constant to be determined by regression of the data in Appendix A. Taking the logarithm of both sides of Equation 6.14 yields Equation 6.15.

$$\log k - b \log P + \text{constant} \tag{6.15}$$

Equation 6.15 indicates that if the logarithm of the rate constant, k_8, were plotted as a function of the logarithm of the reactor operating pressure, the data should form a straight line with slope of b. Figure 76 is such a plot at reactor operating temperatures of 650 and 700°F. These data yield values of .76 and .84 for reactor operating temperatures of 650 and 700°F.

Error Analysis

Combining Equations 6.11, 6.12, and 6.14 yields Equation 6.16.

$$N_p = \Sigma \frac{w_i \, N_{fi}}{0 \, 830. \, r_i \, P^{0.8} \, e^{-31,000/R \, T} \, N_{fi} + 1.0} \tag{6.16}$$

N_p is the total weight percent nitrogen in the reactor product. N_{fi} is the weight percent nitrogen in the reactor feed in the boiling
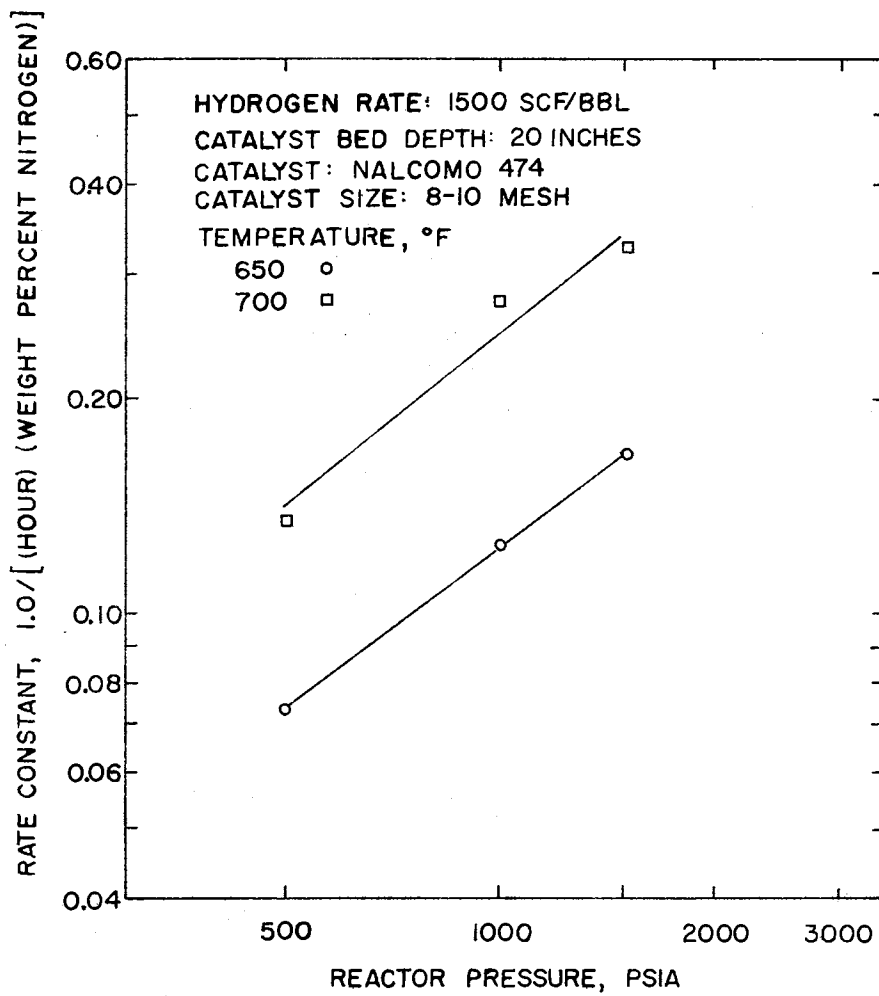
Figure 76. Effect of Reactor Operating
Pressure on the Rate of
Denitrogenation

range i. The values of N_{fi} and w_i for the feedstock used in this
work are tabulated in Table X. w_i is the weight fraction of
material boiling in boiling range i. Recall that r_i is the activity
ratio for boiling range i. The values of r_i are presented in Table
XI. P is the reactor operating pressure, psia. The exponent of .8
is the arithmetic average of the values obtained by regression of
the data in Figure 76. R is the universal gas constant. T is the
absolute reactor operating temperature. Θ is the space time, hours.
The maximum expected error in the weight percent nitrogen in the
reactor product due to errors in the measurement of the reactor tempera-
ture and pressure, space time, and nitrogen analysis will be estimated
using Equation 6.17.

$$N_p^T = \left| \frac{\partial N_p}{\partial T} \right| \Delta T + \left| \frac{\partial N_p}{\partial P} \right| \Delta P + \left| \frac{\partial N_p}{\partial \Theta} \right| \Delta \Theta + \left| \frac{\partial N_p}{\partial N_f} \right| \Delta N_f + \Delta N_p \qquad (6.17)$$

N_p^T is the total maximum expected error in the reactor product, weight
percent nitrogen. The bars indicate that the absolute values of the
partial derivatives are to be used. ΔT, ΔP, $\Delta \Theta$, ΔN_f, and ΔN_p are the
estimated errors in the reactor temperature, pressure, space time,
feed analysis, and product analysis. The estimated errors in the
reactor operating conditions are given in Table XIII. The partials
in Equation 6.17 were evaluated numerically using Equation 6.16.
This procedure is, of course, based on the assumption that the model
given by Equation 6.16 does indeed represent the time, temperature,
and pressure relationships for N, the weight percent nitrogen in the
reactor oil product. The error in the feed composition is assumed to
be uniformly distributed among the boiling point ranges. Since all the

errors in the operating conditions are positive in Equation 6.16 the

equation assumes that all the errors are additive. In addition, all

the errors are assumed to be uncorrelated.

TABLE XIII

ESTIMATED ERRORS IN THE REACTOR
OPERATING CONDITIONS

Temperature	$\pm$ 2°F
Pressure	$\pm$ 10 psia
Space Time	$\pm$ 1.5%
N_f	$\pm$ .005 Weight Percent Nitrogen
N_p	$\pm$ .005 Weight Percent Nitrogen

Since the experimental check of the overall reproducibility was

made at a temperature of 700°F and a pressure of 1000 psig, the results

of the error analysis for these operating conditions will be given in

detail. Table XIV presents the maximum expected error in the reactor

product nitrogen level due to errors in temperature, pressure, space

time, feed analysis, and product analysis. The results in Table XIV

indicate that errors in the product analysis and reactor operating

temperature make the largest contribution to the total error in the

weight percent nitrogen in the reactor product. The results

for the other reactor operating conditions used in this study
show the same trend. The results in Table XIV indicate that
the weight percent nitrogen from a reactor operating at 700°F, 1000
psig, and a space time of 1.5 hours should not differ by more than
.0314 percent nitrogen (one value could be .0172 weight percent
nitrogen above the correct value and the other .0172 below). Figure
49 shows that after 35 hours on oil, the difference between the product
nitrogen level between Catalyst Loadings 2 and 3 was not greater
than .02 weight percent nitrogen. Figure 50 shows that the product
nitrogen level for 700°F and 1000 psig lie in a range of 0.03 weight
percent nitrogen for Catalyst Loadings Number 2 and 3 at space times of
0.375, 0.75, and 1.5 hours. This observed error is less than the
maximum expected error presented in Table XIV. Therefore, the observed
error seems to be less than the maximum expected error predicted by
Equations 6.16 and 6.17.

TABLE XIV

ESTIMATE OF ERROR FOR 700°F AND 1000 PSIG OPERATION

Error Source	Product Error, Weight Percent Nitrogen Space Time, Hours		
	.375	.75	1.5
Reactor Temperature	.0045	.0048	.0044
Reactor Pressure	.0015	.0016	.0015
Space Time	.0029	.0031	.0029
Feed Analysis	.0033	.0026	.0019
Product Analysis	.0050	.0050	.0050
Total	.0172	.0171	.0157

The next step in the analysis will be to estimate the uncertainty of the value of the rate constant as a function of the reactor operating conditions. The following procedure will be used:

1. Determine the best value of k_8 using Equation 6.11 by a least squares regression of the data in the Appendix isotherm by isotherm.

2. Determine maximum expected error at each space time using Equations 6.16 and 6.17.

3. Calculate the minimum expected value of k_8 by doing a least squares regression of the sum of the weight percent nitrogen determined in Step 1 and the maximum expected error in the product nitrogen level, calculated in Step 2, using Equation 6.11.

4. Calculate the maximum expected value of k_8 by doing a least squares regression of the sum of the weight percent nitrogen determined in Step 1 and the maximum expected error in the product nitrogen level, calculated in Step 2, using Equation 6.11.

Figure 77 is a plot of the logarithm of the rate constant, k_8, as a function of the reciprocal of the absolute temperature. The bars on the plot indicate the range of the maximum expected error in the rate constant. Equation 6.13 predicts that a plot of the logarithm of the rate constant, k_8, as a function of the reciprocal of the absolute temperature should yield a straight line. Figure 77 shows that the Arrhenius Equation, Equation 6.13, describes the effect of temperature on the rate constant within the maximum expected error.
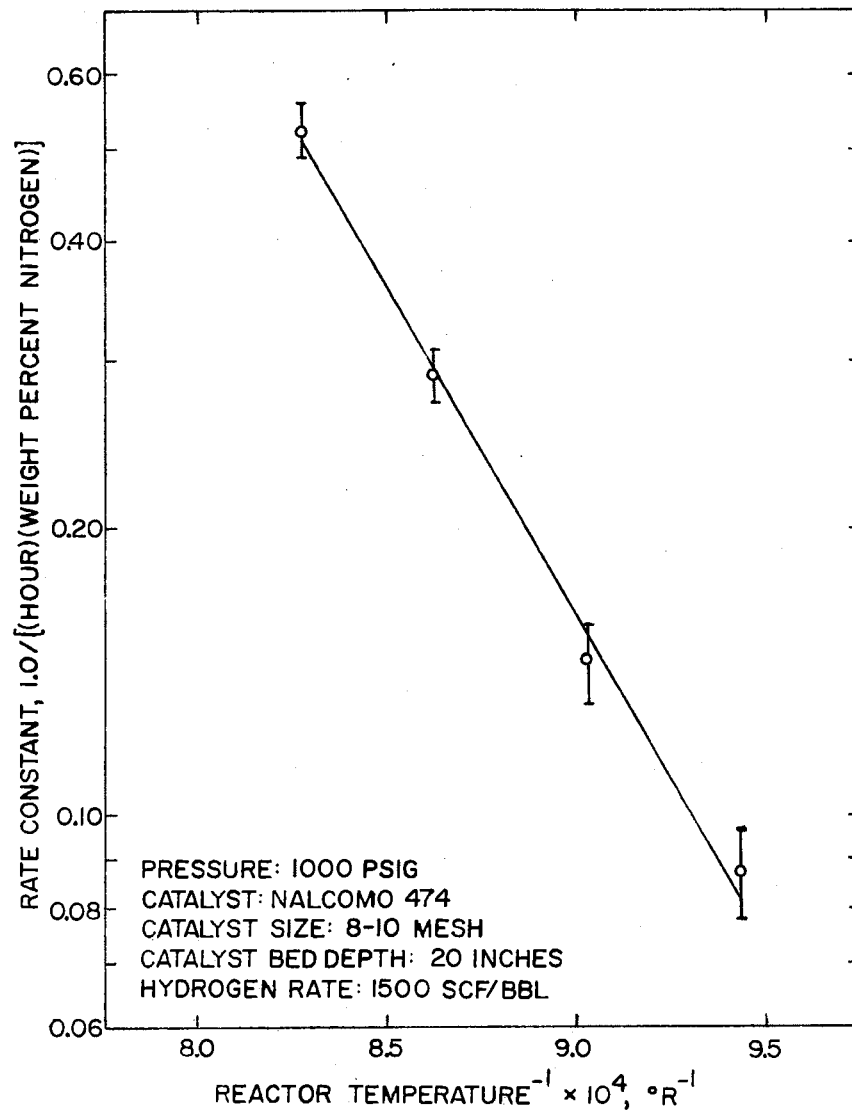
Figure 77. Arrhenius Plot for Nalcomo 474
at 1000 psig with Error Bars

Figure 78 is a plot of the logarithm of the rate constant, k_8, as a function of the logarithm of the absolute reactor pressure. Equation 6.15 predicts that such a plot should yield a straight line. Figure 78 shows that, in general, Equation 6.18 describes the effect of pressure on the rate constant within the maximum expected error. The results from the $700^{\circ}F$ and 1000 psig operation are suspect; after reloading the catalyst, the $700^{\circ}F$ and 1000 psig operation was rerun. The second run yielded a value for the rate constant, .26 hours^{-1} (weight percent nitrogen)$^{-1}$, which is within the maximum expected error of the line on Figure 78. Therefore, Equation 6.14 is a reasonable representation of the effect of pressure on the rate constant.

Considerable space and effort have been given to the development of a model to represent the data obtained in this study. The kinetic model allows a more quantitative error analysis and comparison of catalyst performance. No claims are made to the mechanistic or non-mechanistic basis of the model by Equation 6.11.

<div align="center">

Catalyst Activity as a Function

of Pore Size Distribution

</div>

The primary goal of this work is to tailor the pore size and pore size distribution to maximize the apparent activity of the catalyst. The basic approach will be to compare the performance of the three catalysts with identical metals content, but different pore size distribution, at space times of 0.375, 0.75, and 1.5 hours, reactor operating temperatures of 600, 650, 700, $750^{\circ}F$, and a reactor operating
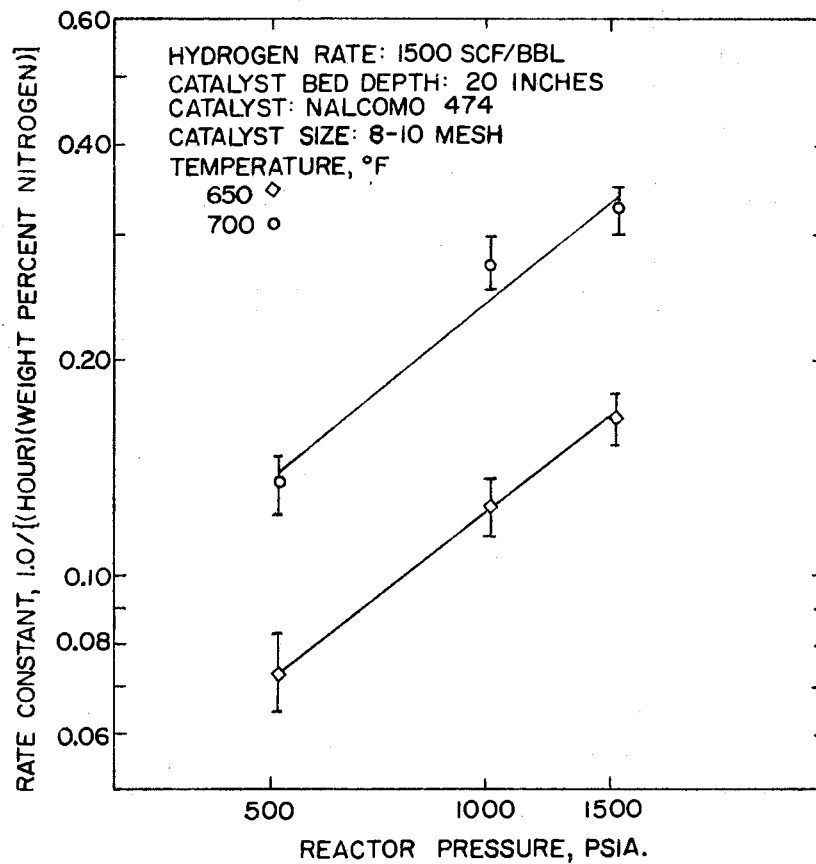
Figure 78. Effect of Reactor Pressure on the
Rate of Denitrogenation with
Error Bars

pressure of 1000 psig. Then, differences in the reactor performance will be discussed in terms of the pore size and pore size distribution.

Figure 79 is a plot of the relative frequency, $dV/d\ln r$, of the pore radius as a function of the pore radius. V is mercury intrusion, cc/gm, and r is the pore radius, angstroms. The raw data are presented in the Appendix. A standard method (20) was used to obtain the relative frequency distributions in Figure 79. This figure shows that the pore size distribution for the three catalysts are similar. However, the data show the following trends:

1. The most frequent pore radius for Nalco 72-4710A and 72-4710B, 25 angstroms, occurs at a smaller pore radius than Nalcomo 474, 33 angstroms.

2. The standard deviations of the pore size distributions for Nalcomo 474 and Nalco 72-4710B are greater than that of Nalco 72-410A.

The next step of the analysis will be to compare the performance of the three catalysts in terms of Model 2.

Figure 80 is a plot of k_8, defined by Equation 6.11 with n set at a value of 2, as a function of the reciprocal of the absolute reactor operating temperature. The bars indicate the maximum expected error in the rate constant. These results indicate that the rate constants for Nalco 72-4710A and Nalcomo 474 are within the maximum expected error for all reactor operating temperatures. The rate constant for Nalco 72-4710B is consistantly less than the corresponding value of either Nalco 72-4710A or Nalcomo 474. In addition, the difference between the rate constant for Nalco 72-4710B and Nalco 72-4710A or Nalcomo 474 is greater than the maximum expected error
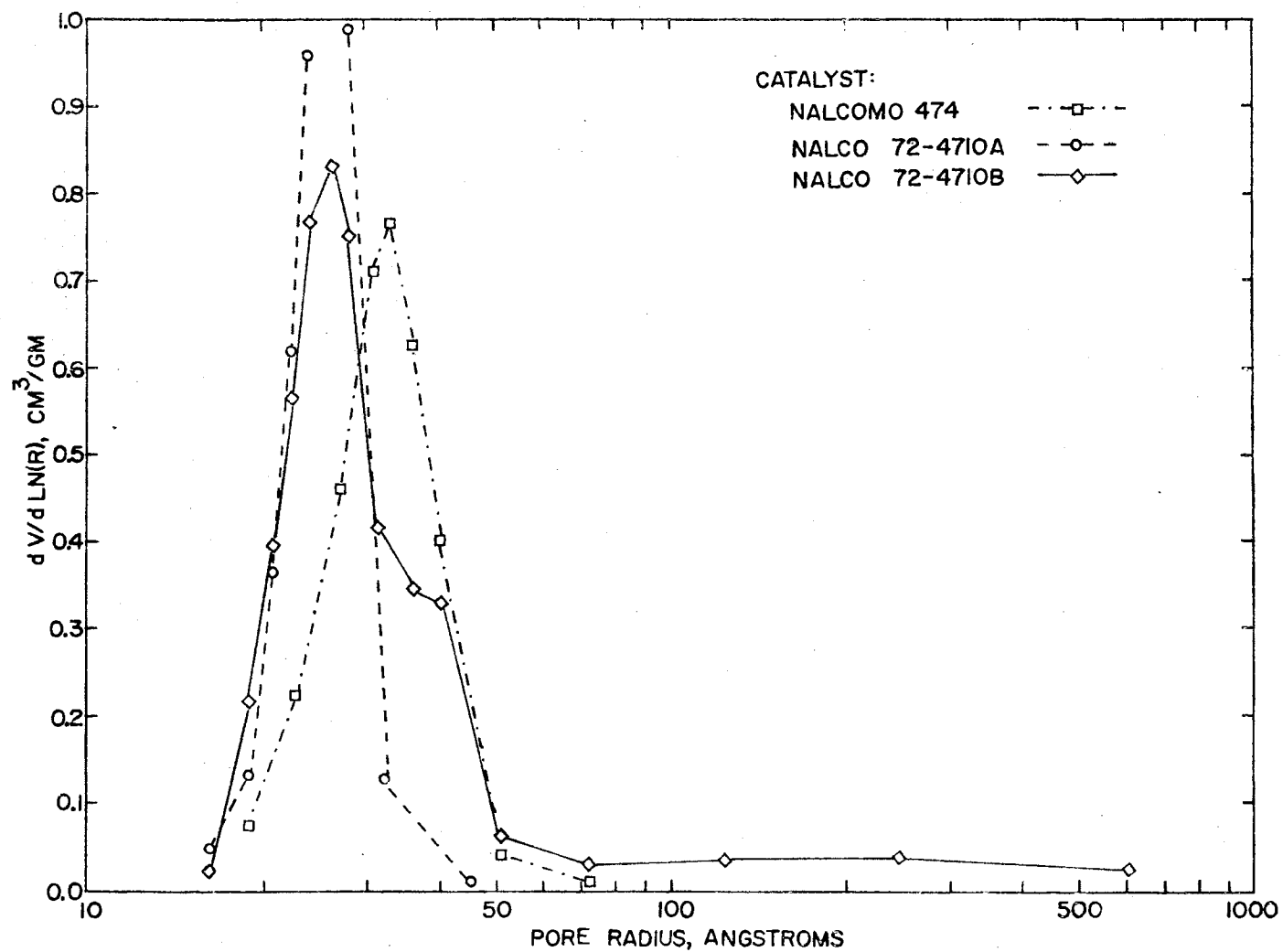
Figure 79. Relative Pore Size Distribution for Nalcomo 474 and Nalco 72-4710A and 72-4710B
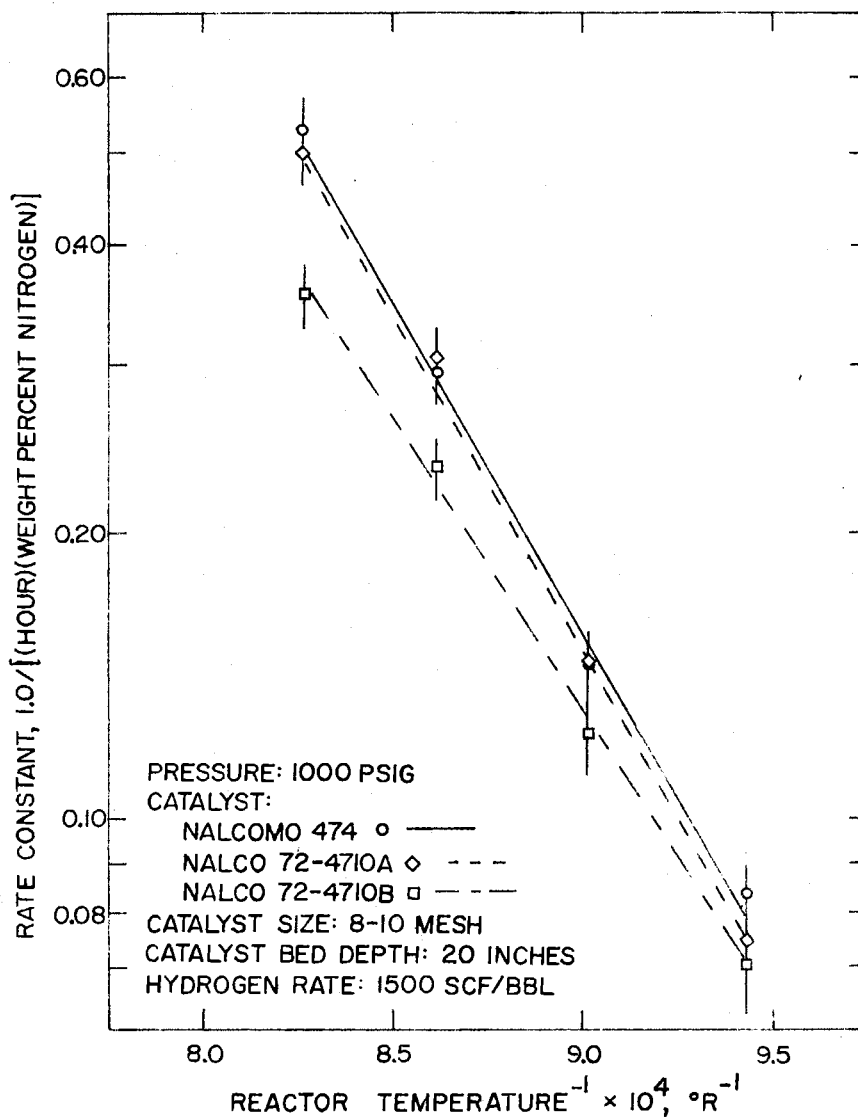
Figure 80. Arrhenius Plot for Nalcomo 474.
Nalco 72-4710A, and Nalco
72-4710B

at reactor operating temperatures of 700 and 750°F. The activation energy for Nalco 72-4710B, 28,000 BTU/lb. mole, is less than either Nalco 72-4710A, 32,700 BTU/lb. mole, or Nalcomo 474, 31,000 BTU/lb. mole. Possible rationalizations for the observed differences in the catalyst activity will be considered in the following discussion.

If the total amount of surface area of one catalyst were considerably different from the other catalysts, then a difference in the observed rate constant could result. Nalco 72-4710A, Nalco 72-4710B, and Nalcomo 474 have surface areas, measured by nitrogen adsorption (40), of 298, 303, and 240 meters^2 / gram of catalyst, respectively. These data indicate that if the surface area were a crucial variable, then Nalco 72-4710A and Nalco 72-4710B should have similar activity and Nalco 474 have a different activity, probably less. However, the observed activity of Nalco 72-4710B is less than either Nalco 72-4710A or Nalcomo 474. Therefore, differences in catalyst internal surface area is not an acceptable rationalization for the observed difference in activity.

If the catalyst bulk density of one catalyst were considerably different from the other catalyst, then a difference in the apparent activity could result from a difference in the total mass of the bed at fixed bed volume. The effect of the catalyst bulk density can be eliminated by redefining space time. The weight hourly space time, θ_w, is defined as the mass of the catalyst divided by the oil hourly mass rate. Equation 6.19 is Equation 6.11 rewritten on a weight hourly basis rather than a volume hourly basis.

$$N_p = \Sigma \frac{w_i}{k_8 \, \theta_w \, r'_i + 1.0 \, / \, N_{fi}} \tag{6.19}$$

Where, k_8' is the rate constant, grams of oil / (grams of catalyst) (hours) (weight percent nitrogen). Figure 81 is a plot of the rate constant using a mass basis, k_8', as a function of the reciprocal of the absolute reactor operating temperature, $^{\circ}R$. The bars on the graph indicate the maximum expected error in the rate constant. The values for the rate constant for Nalcomo 474 differ from the corresponding value for Nalco 72-4710A by less than the maximum expected error at all temperature levels studied. However, the values for the rate constant for Nalco 72-4710B differ from both Nalcomo 474 and Nalco 72-4710A by more than the maximum expected error at reactor operating temperatures of 700 and 750°F. Therefore, the results of the catalyst comparison on a weight basis are identical to those obtained on a volume basis. Therefore, the effect of catalyst bulk density does not account for the poor performance of Nalco 72-4710B relative to Nalcomo 474 and Nalco 72-4710A.

One might expect that the pore size distribution would affect the apparent activity of the catalyst by changing the diffusion resistance to reaction. However, the pore diffusion resistances have been shown to be negligible for Nalcomo 474 catalyst at 650 and 700°F and at a reactor operating pressure of 1000 psig. These are the reactor operating conditions under which Nalco 72-4710B's activity was observed to be less than the other two catalysts. If diffusion resistances were insignificant in the Nalcomo 474 catalyst, it seems unlikely that diffusion resistances are significant in the Nalco 72-4710B catalyst. Thus, the difference in the apparent activity probably results from a difference in the intrinsic activity of the catalyst.
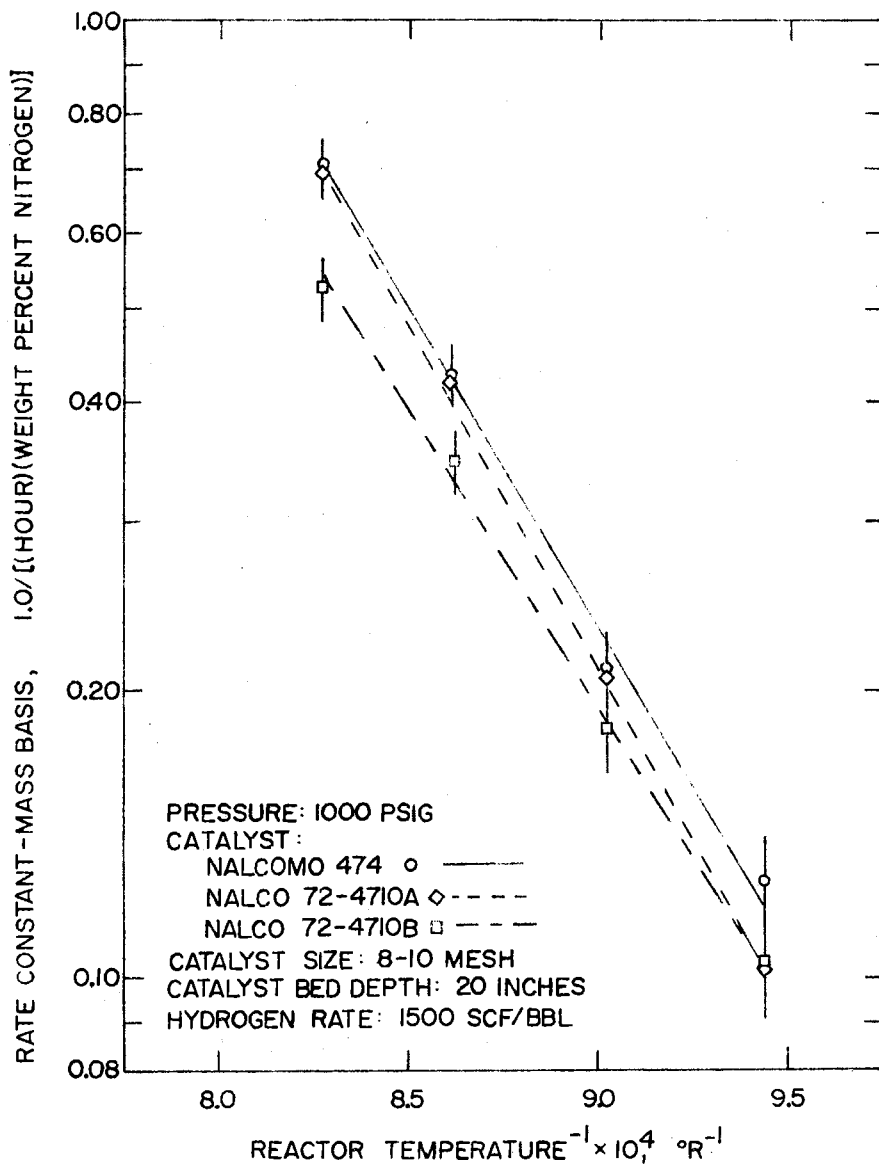
Figure 81. Arrhenius Plot for Nalcomo 474,
Nalco 72-4710A, and Nalco
72-4710B, Weight Hourly
Basis

Denitrogenation Selectivity as a Function

of Pore Size Distribution

One might expect that the weight percent nitrogen remaining in the product as a function of boiling point might be different for various pore distributions. It is difficult to draw any firm conclusions from this type of data because the denitrogenation of any given cut is the sum of denitrogenation due to hydrocracking of organonitrogen species to a lower boiling range and hydrogenolysis of organonitrogen species less the cracking of organonitrogen species from higher boiling ranges into the boiling range of interest. In order to gain a more complete understanding of denitrogenation selectivity as a function of pore size distribution, the data will be analyzed from the following viewpoints:

1. Weight percent nitrogen content as a function of product oil boiling point.

2. The total nitrogen content of the reactor product oil as a function of boiling point.

The former basis is essentially the concentration of organonitrogen species as a function of boiling point. This basis neglects the changes in the amount of material in each boiling range as a result of hydrocracking. The later basis is the summation of the product of the weight percent nitrogen in each boiling range and the mass fraction of the product oil that boils in the same range. This basis considers both changes in the nitrogen content and the oil boiling range distribution.

Figure 82 is a plot of the weight percent nitrogen in the reactor

product oil as a function of the boiling point at 50 mm Hg. This

plot indicates that no ranking of the catalysts can be made based

on the results from boiling ranges less than 450°F. However, the

following catalyst activity ranking can be made based on the

results from boiling ranges greater than 450°F.

Nalco 72-4710A > Nalcomo 474 > Nalco 72-4710B

These data indicate that the catalyst with the smallest pore size,

Nalco 72-4710A, was the most active catalyst with respect to denitro-

genation of organonitrogen species boiling above 450°F at 50 mm Hg.

Therefore, pore size distribution probably had a negligible effect on

the rate of denitrogenation.

Table XV is a tabulation of the summation of the product of the

weight percent nitrogen in each boiling range and the weight fraction

of material in the same range. These data indicate the catalyst per-

formance differ most in the higher boiling ranges. In addition, Nalco

72-4710A was more active than the other two catalyst with respect to

denitrogenation of the higher boiling fractions despite its smaller

mean size.

Comparison of the Results of this

Work with Previous Studies

The comparison of the results of this work with some selected

previous studies will be made in the following areas:

1. Liquid Maldistribution

2. The role of diffusion in denitrogenation

CATALYST BED DEPTH: 20 INCHES
CATALYST SIZE: 8-10 MESH
HYDROGEN RATE: 1500 SCF/BBL
TEMPERATURE: 700°F
PRESSURE: 1000 PSIG
SPACE TIME: 1.5 HOURS
CATALYST:
NALCO 72-4710B
NALCOMO 474
NALCO 72-4710A
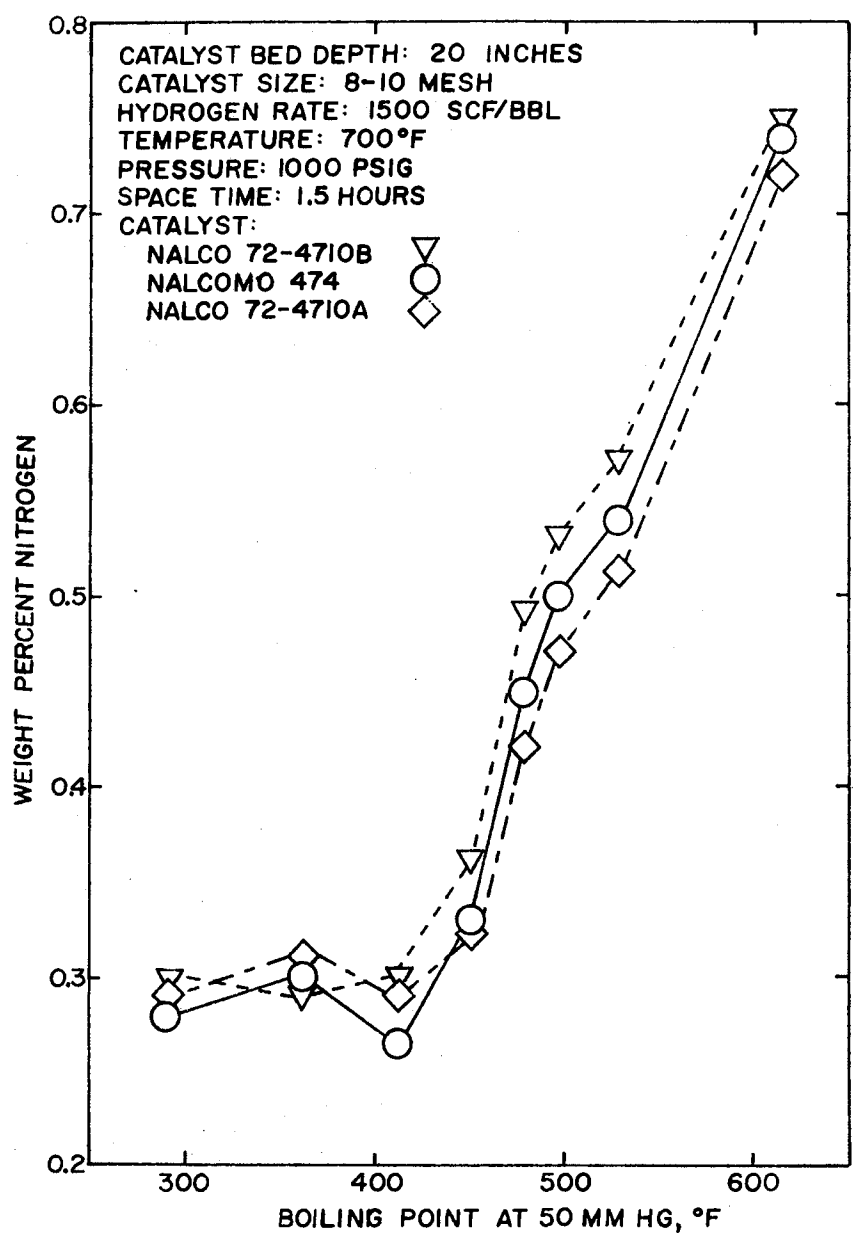
Figure 82. Denitrogenation as a Function
of Boiling Point

3. The effect of temperature on the rate of reaction

4. The effect of pressure on the rate of reaction

4. The effect of hydrogen rate on the rate of denitrogenation

6. The effect of pore radius on the rate of reaction

A full literature review was given in Chapter II and only certain published works, directly comparable with this study, are presented here.

TABLE XV

TOTAL NITROGEN DISTRIBUTION

Cut Temperature	$\Sigma\ w_i\ N_{pi}$		
	Nalcomo 474	Nalco 72-4710A	Nalco 72-4710B
328	.0468	.0510	.0458
394	.0996	.101	.0931
429	.139	.149	.139
472	.184	.190	.187
485	.242	.258	.252
507	.273	.277	.285
548	.319	.314	.334
–	.400	.386	.418

Liquid Maldistribution

The general approach to the study of maldistribution of the liquid oil in a trickle flow reactor in this study was to monitor the reactor performance as a function of the liquid flux at constant space time. The inferior reactor performance associated with a decrease in liquid flux at constant space time is usually attributed to poor liquid distribution.

The effect of liquid flux on hydrotreating a COED oil, a coal derived liquid, was studied (23) over the range of 3.8 to 15.3 gallons per hour per square foot at a reactor temperature of 720^OF and pressure of 3000 psig. The effect of liquid flux on the reactor performance was found to be small.

This study considered the effect of reactant mass flux over the range of 4.84 to 9.69 gallons per square foot per hour on the rate of denitrogenation. Doubling the oil mass flux resulted in an eight percent increase in the observed denitrogenation rate constant.

Experience with petroleum hydrotreating (13) indicates that the liquid flux should be in the range of 150-500 gallons per hour per square foot. Since the range of liquid fluxes used in the above tests were much less than those encountered in a commercial reactor, it is risky to assume that the difference in the oil flux between a commercial reactor and these bench scale reactors will have a negligible effect on the rate of denitrogenation.

Role of Diffusion in Denitrogenation

The results of this work indicate that at a reactor operating temperature of 650^OF and 1000 psig, the effectiveness factor is

essentially one. At a reactor operating temperature of $700^{\circ}F$ and 1000 psig, the effectiveness factor is approximately 0.95. Since film diffusion resistances encountered in the transport of reactants and products between the catalyst outer surface and the bulk gas phase are typically much less than pore diffusion resistances to reaction (18), these results indicate that the rate of denitrogenation of the oil used in this study was controlled by the rate of surface reaction.

The kinetics of hydrodenitrogenation of COED coal derived liquids were studied (23) as a function of the particle size at $770^{\circ}F$ and 3000 psig over Nalco MN-502 hydrotreating catalyst. A three fold reduction in the catalyst particle diameter resulted in almost a four fold reduction in the percent nitrogen remaining in the product. Thus, the rate of reaction was roughly proportional to the catalyst outer surface area, which implies that film diffusion controlled the rate of denitrogenation of the coal derived liquid and the effectiveness factor was near zero.

Van Zoonan and Douwes (22) hydrotreated a straight run gas oil, a petroleum fraction with approximately the same boiling range as the oil used in this study, at about 500 psig and $707^{\circ}F$ over two sizes of cobalt-molybdenum-alumina catalyst with dimensions of 3 x 3 millimeters and 25-30 mesh. This greater than four fold reduction in particle size did not result in an increase in nitrogen removal. This indicates that the effectiveness factor was near one for this work and that the rate of denitrogenation was controlled by the rate of surface reaction.

Temperature Effect

White et al. (29) studied hydrotreating of COED oil derived from Utah coal using HDS-3A catalyst, a nickel-molybdate catalyst manufactured by the American Cyanamid Company. A first order rate expression was used to calculate an activation energy. At temperatures below 750°F, an activation energy of 48,500 BTU/lb. mole was observed. At temperatures above 750°F, an activation energy of 16,400 was observed. No explanation for the break in the activation energy was offered.

In a batch autoclave study, Quader and Hill (34) studied hydrotreating of low temperature coal tar at 1500 psig over the temperature range of 752 to 932°F over a cobalt-molybdate catalyst. An activation energy of 15,900 BTU/lb. mole was observed.

This study found that the activation energy of 28,000, 31,000, and 32,700 BTU/lb. mole for Nalco 72-4710B, Nalcomo 474, and Nalco 72-4710A catalyst, respectively, on the temperature range of 600 to 750°F. An activation energy of 12,300 BTU/lb. mole was observed on the temperature range of 750 to 800°F using Nalco 474 catalyst.

The work of White (29), Quader and Hill (34), and this work indicate that there is an abrupt decrease in the apparent activation energy at about 750°F. The activation energies calculated in this work are lower than the other studies at temperature both above and below 750°F. The fact that different feeds and catalysts were used in each study could account for the difference in the activation energies. In addition, the fact that all the other studies cited above

used a first order rate expression while this work used a second order rate expression could account for some of the difference in the activation energy.

Pressure Effect

The effect of reactor operating pressure on the kinetics of hydrodenitrogenation of COED oil from Utah coal was studied (23) over the pressure range of 2000 to 3100 psig at $723^{O}F$. These data indicate that the assumed first order rate constant is proportional to the absolute reactor pressure to the 1.1 power.

This work studied the effect of reactor operating pressure over the pressure range of 500 to 1500 psig at 650 and $700^{O}F$ using Nalcomo 474 catalyst. The results of this work indicate that the rate constant is proportional to the absolute pressure to the .76 and .84 at 650 and $700^{O}F$, respectively.

Hydrogen Rate Effect

Wan (28) found that increasing the hydrogen rate from 3980 to 39,800 SCF/bbl resulted in an increase of the percent nitrogen conversion from 61.2 to 69.2. The reactor was operated at $800^{O}F$, 1000 psig, and a space time of .901 horus using Nalcomo 474 catalyst.

This work tested the effect of hydrogen flow rate over the range of 1500 to 20,000 SCF/bbl using the same feedstock and catalyst as Wan (28). The reactor was operated at $700^{O}F$, 1000 psig, and a space time of 1.5 hours. The conversion obtained was found to be essentially independent of the hydrogen rate.

Effect of Pore Size

Van Zoonen and Douwes (22) studied the effect of the volume average pore diameter in the range of 66 to 464 angstorms with a cobalt-molybdenum of alumina catalyst on the rate of denitrogenation of a Middle East gas oil at $707^{\circ}F$ and about 500 psig. The study found that the volume average diameter had a negligible effect on the rate of denitrogenation over the entire range studied.

This study found that Nalco 72-4710B's performance was slightly inferior to Nalco 72-4710A and Nalcomo 474. However, there is little justification for attributing the difference in activity to the difference in pore diameter distribution.

In this chapter, all the data of this work were analyzed in detail. In the next chapter, the conclusions from this analysis are summarized.

CHAPTER VII

CONCLUSIONS AND RECOMMENDATIONS

Conclusions

1. The activity of Nalco 72-4710B was less than either Nalcomo
   474 or Nalco 72-4710A. The difference in the apparent
   activity probably results from a difference in the intrinsic
   activity of the catalysts.

2. The effectiveness factor for denitrogenation over Nalcomo
   474 catalyst was found to be nearly one with reactor operating
   temperatures of 650 and 700°F and 1000 psig.

3. The data were satisfactorily correlated using a second order
   rate constant and allowing the rate constant to be a linear
   function of boiling point.

4. The activation energies were found to be 28,000, 31,000 and
   33,000 BTU/lb. mole (±3,000 BTU/lb. mole) for Nalco 72-4710B,
   Nalcomo 474, and Nalco 72-4710A catalysts over the temperature
   range from 600 to 750°F.

5. The activation energy for denitrogenation over Nalcomo 474
   catalyst between 750 and 800°F was 12,000 (±9300) BTU/lb.
   mole.

6. The rate of denitrogenation was found to be proportional
   to the total reactor pressure to .76 (±.16) power at 650°F

and .84 ($\pm$.15) at 700°F over the pressure range of 500 to 1500 psig.

7. Catalyst activity stablized after about 35 hours of continuous operation.

8. Halving the reactor bed height at constant reactor operating conditions yielded a small reduction in the rate of nitro-genation, about eight percent.

9. The high pressure separator gas rates over the range of 1500 to 20,000 SCF/bbl had little effect on the rate of denitro-genation.

Recommendations

1. Test pore size and pore size distribution over a much broader range.

2. Test real coal process derived liquids where ash content could be a problem.

3. Detailed activity tests of long duration should be made.

BIBLIOGRAPHY

1. "Development of a Process for Producing an Ashless Low Sulfur Fuel
     from Coal." Office of Coal Research R&D Report No. 53, 1970.

2. Mills, G. A., E. R. Boedeker and A. G. Oblad. "Poisoning of
     Cracking Catalyst by Nitrogen Compounds and Potassium Ion."
     J. Am. Chem. Soc., Vol. 72 (1950), 1554.

3. King, R. W. and W. B. M. Faulconer. "Determination of Total
     Nitrogen in Reformer Charge Stock." Analytical Chemistry,
     Vol. 28 (1956), 255.

4. Hettinger, W. P., Jr., C. D. Keith, J. L. Gring and J. W. Teter.
     "Hydroforming Reactions: Effect of Certain Catalyst
     Properties and Poisons." Ind. Eng. Chem., Vol. 47 (1955), 719.

5. Haensel, V. and L. O. Stine. "To Convert or Desulfurize Residuals."
     Hydrocarbon Processing, Vol. 46, No. 6 (1967), 155.

6. Beuther, H. and B. K. Schmid. "Upgrade Heavy Oil - Increase
     Profits." Chem. Eng. Prog., Vol. 61, No. 3 (1965), 59.

7. Thono, R. W. and J. Limido. Brit Patent 905,809.

8. Hoog, H., H. G. Klinkert and A. Schaafsma. "New Shell Hydro-
     desulfurization Process." Petroleum Refiner, Vol. 32, No. 5
     (1953), 137.

9. Jones, J. F. and L. D. Friedman. "Char Oil Energy Development
     Final Report." Office of Coal Research Report No. 56, 1972.

10. Chervenak, M. C., C. A. Johnson and S. C. Schuman. "H-Oil Process
     Treats Wide Range of Oils." Petroleum Refiner, Vol. 39,
     No. 10 (1960), 151.

11. Schwartz, J. G. and G. W. Roberts. "Analysis of Trickle-Bed
     Reactors: Liquid Backmixing and Liquid-Solid Contacting."
     74th National Meeting of A.I.Ch.E., New Orleans (1973).

12. Schuman, C. and H. Shalit. "Hydrodesulfurization." Catalyst
     Reviews, Vol. 4, No. 2 (1970), 283.

13. Docksey, P. and R. J. H. Gilbert. Seventh World Petroleum Congress,
     Mexico City (1967).

14. Scott, A. H. "Liquid Distribution in Packed Towers." _Trans. Inst. Chem. Engr._, Vol. 13 (1935), 211.

15. Mears, D. E. "The Role of Axial Dispersion in Trickle-Flow Laboratory Reactors." _Chem. Engr. Sci._, Vol. 26 (1971), 1361.

16. Ross, L. D. "Performance of Trickle Bed Reactor." _Chem. Eng. Prog._, Vol. 61, No. 10 (1965), 77.

17. Schuman, C. and H. Shilit. "Hydrodesulfurization." _Catalyst Reviews_, Vol. 4, No. 2 (1970), 284.

18. Satterfield, C. N., A. A. Pelossof and T. K. Sherwood. "Mass Transfer Limitations in a Trickle-Bed Reactor." _A.I.Ch.E.J._, Vol. 15 (1969), 226.

19. Schuman, C. and H. Shilit. "Hydrodesulfurization." _Catalyst Reviews_, Vol. 4, No. 2 (1970), 283.

20. Smith, J. M. _Chemical Engineering Kinetics_, New York: McGraw Hill, 1970.

21. Satterfield, C. N. _Mass Transfer in Heterogeneous Catalyst_, Cambridge: M.I.T. Press, 1970.

22. Van Zoonen, D. and C. T. Douwes. "Effect of Pellet Pore Structure on Catalyst Performance in the Hydrodesulfurization of Straight Run Gas Oil." _Journal of the Petroleum_, Vol. 49 (1963), 383.

23. Jones, J. F. and L. D. Friedman. "Char Oil Energy Development Final REport." _Office of Coal Research Report No. 56_, 1970, 25.

24. McIlvried, H. G. "Kinetics of the Hydrodenitrification of Pyridine." _Ind. Eng. Chem. Process Des. Develop._, Vol. 10, No. 1 (1971), 125.

25. Doelman, J., and J. C. Vlugter. _Proc. for Sixth World Petrol. Cong._, Section III, Paper 12-PD7, 1963.

26. Cox, K. E. (Unpub. Ph.D. thesis, Montana State College, 1961).

27. Flinn, R. A., O. A. Larson and H. Beuther. "How Easy is Hydrodenitrogenation?" _Hydrocarbon Processing_, Vol. 42, No. 9 (1963), 129.

28. Wan, K. T. "Establishment of Equipment and Its Operation for Hydrotreating of a Coal Derived Liquid." (Unpub. M.S. thesis, Oklahoma State Unviersity, 1972).

29. White, P. J., J. F. Jone and R. T. Eddinger. "To Treat and Crack Oil from Coal." _Hydrocarbon Processing_, Vol. 47, No. 12 (1968), 97.

30. Alder, H. L. and E. B. Roessler. *Introduction* to *Probability and Statistics*, San Francisco: W. H. Freeman and Co., 1968.

31. Van Meter, R. A., G. R. Lake, P. McCutchan and J. C. Neel. "Effects of Digestion Temperature on Kjeldahl Analysis." *Analytical Chemistry*, Vol. 23, No. 11 (1958), 1634.

32. *1971 Annual Book of ASTM Standards*, Part 18, Standard Designation D1160.

33. Sooter, M. C. "Effect of Pore Size on Hydrodesulfurization of a Coal Derived Liquid." (Unpub. Ph.D. thesis, Oklahoma State University, 1974).

APPENDIX

DATA

The following tables contain all the data of this work that were
analyzed in previous chapters. The data will be presented in the same
order as it was introduced in the body of this work.

Tablies XVI and XVII are tabulations of the data used as a basis
for the discussion, in Chapter IV, of the relative ease of analysis of
the model organonitrogen species and boiling point ranges of the
anthracene oil feedstock. This data was obtained using the procedure
presented in Chapter IV with the following exceptions:

1. The applied voltage on the heating mantle was 100 volts

    throughout the digestion step.

2. Several digestion times were run on each sample.

Table XVIII is a summary of the catalyst type, pellet size, bed
depth, catalyst bed volume and mass, and the range of run numbers for
each catalyst loading. Table XIX is a summary of the nominal reactor
temperature, measured pressure, volume hourly space time, weight per-
cent nitrogen in the reactor product, and the number of continuous hours
of oil.

TABLE XVI

EASE OF NITROGEN ANALYSIS OF MODEL ORGANONITROGEN SPECIES

Compound	Digestion Time, Hours	Weight Percent Nitrogen Analyzed	Percent Nitrogen in Sample that Remained Unanalyzed	Solvent
Pyridine	24	.574	39.6	Cyclohexane
	48	.761	20.0	
	72	.851	10.5	
Quinoline	24	.722	23.8	
	36	.846	10.7	
Indole	24	.837	19.0	
	37	.945	8.52	
Aniline	2	.980	7.20	
Pyridine	24	.619	37.5	Toluene
	48	.831	16.1	
	72	.919	7.17	

TABLE XVII

EAST OF NITROGEN ANALYSIS OF THE FEEDSTOCK AS
A FUNCTION OF BOILING RANGE

Cut Number	Digestion Time, Hours	Weight % Nitrogen	% Nitrogen Remaining
1	5	.39	35.0
1	7	.43	28.3
1	11	.46	23.4
1	14	.50	16.6
1	30	.57	5.0
2	5	.67	37.4
2	10	.79	26.2
2	17	.93	13.2
2	25	1.00	6.5
3	4	.56	39.9
3	8	.78	26.8
3	24	.86	7.5
4	8	.58	28.4
4	12	.74	8.6
4	16	.77	4.9
5	4	.65	27.5
5	8	.73	18.3
5	24	.88	2.2
6	4	.70	29.0
6	8	.75	20.0
7	4	.84	18.4
8	2	.94	22.2
8	4	1.05	13.5
Feedstock	48	.984	–
↓	↓	.990	–
		.985	–
		.980	–
		.985	–
		.980	

TABLE XVIII

SUMMARY OF CATALYST LOADINGS

Catalyst Loading Number	Nalco Catalyst	Pellet Size, Mesh	Bed Depth, Inches	Bed Volume, cm.	Bed Mass, grams.	Run Numbers
1	Inerts	8-10	20	37	-	1-26
2	474	8-10	20	37	-	27-70
3	474	8-10	20	37	-	71-134
4	474	40-48	20	37	31.0	135-174
5	474	8-10	10	18.5	14.8	175-211
6	72-4710B	8-10	20	37	29.2	212-239
7	72-4710A	8-10	20	37	31.2	240-275
8	Inerts	8-10	20	37	-	276-287
9	474	8-10	20	37	29.9	288-328

TABLE XIX

RESULTS OF HYDROTREATING RUNS

Run Number	Catalyst Loading Number	Temper- ature, °F	Pres- sure, psig	Space Time, Hours	Hydrogen to Oil Ratio SCF/bbl	Wt% Nitrogen in Product	Hours on Oil
1	1	700	1000	1.5	1500	.89	—
2						.90	—
3						.91	—
4						.90	—
5						.91	—
6					20,000	.91	—
7					20,000	.90	—
8		750			1500	.86	—
9						.85	—
10		800				.80	—
11						.79	—
12				.75		.88	—
13						.87	—
14						.91	—
15				.375		.91	—
16				1.5	20,000	.83	—
17					1500	.91	—
18						.92	—
19				.75		.91	—
20				.375		.91	—
21						.91	—
22		750		1.5		.85	—
23			1015	.75		.90	—
24						.89	—
25				.375		.91	—
26						.90	—
27	2	700	1010	1.5	1500	.36	31
28						.39	33
29						.39	35
30						.40	37
31						.39	39
32						.39	41
33				.75		.56	49
34			1008	.75		.55	50
35			1012	.375		.67	57
36				.375		.68	58
37		750		1.5		.32	70
38				1.5		.31	72
39			1020	.75		.42	79
40			1020	.75		.44	81
41			1010	.375		.57	89

TABLE XIX (Continued)

Run Number	Catalyst Loading Number	Temperature, °F	Pressure, psig	Space Time Hours	Hydrogen to Oil Ratio SCF/bbl	Wt% Nitrogen in Product	Hours on Oil
42	2	750	1010	.375	1500	.57	90
43			1020	1.5		.32	95
44		800		1.5		.28	103
45				1.5		.29	105
46			1025	.75		.39	115
47			1030	.75		.39	119
48				.375		.53	122
49				.375		.51	123
50			990	1.5		.33	138
51		700	995			.53	146
52			995			.53	150
53			995	1.5	20,000	.54	155
54			995		20,000	.53	157
55		650	1004		1500	.65	170
56			1004			.65	172
57			1005	.75		.72	178
58			1000	.75		.72	179
59				.375		.80	182
60				.375		.80	183
61				1.5		.64	187
62						.65	189
63					20,000	.68	192
64					20,000	.68	194
65		600			1500	.81	198
66			1005			.81	200
67				.75		.84	205
68				.75		.84	206
69				.375		.89	209
70				375		.90	210
71	3	700	1010	1.5		.45	12
72			1010			.43	16
73			1010			.44	20
74			1015			.42	24
75			1015			.40	28
76			1014			.40	32
77			1012			.41	36
78			1015			.39	40
79			1015			.39	44
80			1015			.40	48
81			1021	.75		.55	55
82			1020	.75		.54	58
83				.375		.65	61
84				.375		.67	62

TABLE XIX (Continued)

Run Number	Catalyst Loading Number	Temperature, °F	Pressure, psig	Space Time Hours	Hydrogen to Oil Ratio SCF/bbl	Wt% Nitrogen in Product	Hours on Oil
85	3	700	1020	1.5	1500	.41	66
86			1020	1.5		.39	68
87			1015	.375		.68	74
88			1005	.375		.68	75
89			1480	1.5		.37	83
90				1.5		.36	85
91				.75		.51	91
92				.75		.51	92
93				.375		.62	98
94				.375		.63	100
95				1.5		.36	105
96						.35	107
97			505			.60	115
98			508			.59	116
99			507	.75		.66	120
100			507	.75		.67	121
101			507	.375		.73	125
102			507	.375		.74	126
103		650	995	1.5		.58	135
104			995	1.5		.59	138
105			997	.75		.68	142
106			997	.75		.68	143
107			996	.375		.77	146
108			996	.375		.77	147
109			995	1.5		.59	151
110			995	1.5		.57	153
111			1505	1.5		.53	161
112			1505	1.5		.54	162
113			1510	.75		.62	167
114			1510	.75		.63	168
115			1510	.375		.72	173
116			1510	.375		.72	174
117			1510	1.5		.55	178
118			1510	1.5		.54	180
119			479	1.5		.71	192
120			526	1.5		.71	194
121			520	.75		.75	196
122			520	.75		.77	197
123			520	.375		.81	200
124			520	.375		.82	201
125			520	1.5		.70	213
126			520	1.5		.71	215
127		600	1005	1.5		.71	222

TABLE XIX (Continued)

Run Number	Catalyst Loading Number	Temperature, °F	Pressure, psig	Space Time Hours	Hydrogen to Oil Ratio SCF/bbl	Wt% Nitrogen in Product	Hours on Oil
128	3	600	1000	1.5	1500	.72	224
129			1010	.75		.77	228
130			1010	.75		.78	229
131			1000	.375		.85	236
132			1000	.375		.83	238
133			1000	1.5		.71	243
134			1000	1.5		.71	245
135	4	700	1015			.43	24
136			1010			.44	32
137			1010			.43	36
138			1010			.42	40
139			1010			.43	44
140			1010			.42	48
141			1010	.75		.54	54
142			1010	.75		.55	55
143			1010	.375		.67	61
144			1010	.375		.66	63
145			1016	1.5		.42	71
146			1016			.42	73
147		750	1010			.26	88
148			1010			.25	89
149			1017	.75		.43	96
150			1017	.75		.39	97
151			1015	.375		.50	103
152			1015	.375		.50	106
153			1010	1.5		.28	111
154			1010			.29	113
155		650	1014			.55	122
156			1010			.57	124
157			1010	.75		.67	129
158				.375		.67	130
159				.375		.76	135
160				1.5		.77	136
161				1.5		.55	139
162				1.5		.56	141
163		600		1.5		.66	150
164				1.5		.67	152
165				.75		.72	158
166				.75		.74	159
167			1012	.375		.81	163
168			1012	.375		.80	164
169			1012	1.5		.67	169
170			1010	1.5		.66	172

TABLE XIX (Continued)

Run Number	Catalyst Loading Number	Temperature, °F	Pressure, psig	Space Time Hours	Hydrogen to Oil Ratio SCF/bbl	Wt% Nitrogen in Product	Hours on Oil
171	4	700	1010	1.5	1500	.42	176
172				1.5		.40	179
173				.375		.67	186
174				.375		.68	187
175	5	650	990	.75		.69	15
176			995			.69	19
177			993			.71	25
178			995			.71	33
179			995			.70	38
180			995			.70	42
181			996			.69	46
182			995	1.5		.59	55
183			995	1.5		.59	58
184			995	.75		.68	63
185			995	.75		.69	65
186			995	.375		.76	69
187			995	.375		.77	70
188			995	1.5		.58	79
189			995			.57	81
190		700	995			.41	91
191			999			.43	95
192			998	.75		.55	100
193			998	.75		.57	102
194			998	.375		.70	106
195			995	.375		.69	107
196			995	1.5		.43	111
197			997	1.5		.43	119
198		650	997	.75		.70	121
199		650	995	.75		.72	123
200	6	600	1000	1.5		.73	11
201						.71	15
202						.73	20
203						.71	24
204						.71	28
205						.73	32
206						.73	36
207						.73	40
208						.70	44
209			1005			.70	48
210			1005	.75		.76	50
211			1010	.75		.77	52
212			1010	.375		.84	55
213			1010	.375		.85	57

TABLE XIX (Continued)

Run Number	Catalyst Loading Number	Temperature, °F	Pressure, psig	Space Time Hours	Hydrogen to Oil Ratio SCF/bbl	Wt% Nitrogen in Product	Hours on Oil
214	6	600	1005	1.5	1500	.72	59
215			1005	1.5		.69	61
216		650	1008	1.5		.58	74
217			1008	1.5		.57	76
218			1020	.75		.68	80
219			1020	.75		.67	81
220			998	.375		.81	85
221			998	.375		.80	86
222			995	1.5		.61	90
223			995	1.5		.59	92
224		700	1002	1.5		.45	101
225			1002	1.5		.43	103
226			1002	.75		.55	106
227			1004	.75		.56	107
228			1005	.375		.69	112
229			1000	.375		.68	113
230			1000	1.5		.43	117
231			1000			.44	120
232		750	1000			.29	130
233			1000			.28	132
234			1000	.75		.46	138
235			1000	.75		.47	139
236			1006	.375		.67	143
237			1006	.375		.68	145
238			1005	1.5		.29	150
239			1005			.29	151
240	7	600	1000			.71	4
241			1000			.72	8
242			1000			.71	12
243			995			.71	16
244			995			.71	20
245			995			.70	27
246			997			.71	30
247			997			.70	34
248			997			.70	38
249			995			.71	42
250			996			.71	46
251			1007	.75		.76	50
252			1007	.75		.76	51
253			1010	.375		.82	56
254				.375		.80	57
255				1.5		.67	61
256						.67	63

TABLE XIX (Continued)

Run Number	Catalyst Loading Number	Temperature, °F	Pressure, psig	Space Time Hours	Hydrogen to Oil Ratio SCF/bbl	Wt% Nitrogen in Product	Hours on Oil
257	7	650	1010	1.5	1500	.57	69
258						.55	71
259				.75		.61	74
260				.75		.67	75
261				.375		.75	79
262				.375		.77	80
263				1.5		.56	84
264				1.5		.55	86
265		700		1.5		.37	92
266			1015	1.5		.39	99
267				.75		.51	102
268				.75		.50	103
269				.375		.64	107
270				.375		.64	108
271			1015	1.5		.37	117
272			1019	1.5		.38	119
273		750	1019	1.5		.26	124
274			1015	1.5		.25	126
275			1010	.75		.43	130
276	8	600	1005	1.5		.93	4
277				1.5		.94	8
278				.75		.96	11
297				.75		.96	12
280				.375		.97	15
281				.375		.96	16
282		650		1.5		.92	22
283				1.5		.93	24
284				.75		.96	26
285				.75		.96	27
286				.375		.97	30
287				.375		.96	31
288	9	600	1002	1.5		.67	7
289			1001			.67	12
290			1000			.67	16
291			1003			.68	20
292			1003			.68	24
293			1002			.66	28
294			1002			.68	32
295			1002			.67	36
296			1000			.66	40
297			1006			.66	44
298			1005			.66	48
299			1005	.75		.76	50

TABLE XIX (Continued)

Run Number	Catalyst Loading Number	Temperature, °F	Pressure, psig	Space Time Hours	Hydrogen to Oil Ratio SCF/bbl	Wt% Nitrogen in Product	Hours on Oil
300	9	600	1005	.75	1500	.75	52
301			1007	.375		.80	56
302			1007	.375		.82	57
303			1005	1.5		.67	60
304		↓	1006	1.5		.65	62
305		650	1014	1.5		.54	68
306			1012	1.5		.55	70
307			1010	.75		.69	76
308				.75		.63	77
309				.375		.76	80
310				.375		.76	81
311				1.5		.55	85
312		↓		1.5		.56	87
313		700		1.5		.39	92
314				1.5		.38	96
315				.75		.52	100
316				.75		.54	101
317				.375		.63	104
318			↓	.375		.65	105
319		↓	1005	1.5		.40	109
320			1005	1.5		.40	111
321		750	1006	1.5		.25	118
322			1006	1.5		.26	120
323			1005	.75		.42	125
324				.75		.41	128
325				.375		.52	128
326				.375		.52	129
327				1.5		.29	134
328	↓	↓	↓	1.5	↓	.30	136

Table XX is a tabulation of the mercury penetration data used to calculate the pore radius distribution presented on Figure 79. Both the data acquisition and reduction methods were standard (20).

Table XXI presents the nitrogen content of the reactor product oil as a function of the boiling point. Recall, that w_i is the mass fraction of the oil in cut i and N_{pi} is the weight percent nitrogen in cut i.

TABLE XX

PORE SIZE DISTRIBUTION BY MERCURY PENETRATION

Nalcomo 474		Nalco 72-4710A		Nalco 72-4710B	
Absolute Pressure, psia	Intru-sion, cc/gm	Absolute Pressure, psia	Intru-sion, cc/gm	Absolute Pressure, psia	Intru-sion cc/gm
1.8	0.000	1.8	0.000	1.8	0.000
9.9	0.000	9.9	0.005	9.9	0.013
49.9	0.004	49.9	0.009	40.0	0.020
250	0.011	159.9	0.019	100.0	0.026
500	0.019	500	0.028	300	0.030
1,200	0.022	2,500	0.033	1,000	0.033
2,500	0.030	5,000	0.038	2,500	0.049
5,000	0.049	10,000	0.038	5,000	0.072
10,000	0.060	15,000	0.047	10,000	0.092
15,000	0.078	25,000	0.052	15,000	0.105
20,000	0.105	30,000	0.075	20,000	0.122
23,000	0.161	32,000	0.141	23,000	0.168
25,000	0.213	34,000	0.216	26,000	0.210
27,000	0.272	36,000	0.291	30,000	0.270
30,000	0.347	38,000	0.343	33,000	0.342
35,000	0.418	40,000	0.375	35,000	0.391
40,000	0.448	45,000	0.418	38,000	0.454
50,000	0.463	50,000	0.432	40,000	0.483
60,000	0.463	60,000	0.441	50,000	0.552
				60,000	0.566

TABLE XXI

NITROGEN LEVEL AS A FUNCTION OF BOILING POINT

Boiling Range Endpoint, °F at 50 mm		Feed	Run 3	Run 31	Run 265	Run 225
328	w_1	.105	.104	.167	.176	.158
	N_{p1}	.60	.61	.28	.29	.29
394	w_2	.106	.132	.176	.162	.163
	N_{p2}	1.07	.91	.30	.31	.29
429	w_3	.110	.121	.136	.168	.153
	N_{p3}	.93	.77	.29	.29	.30
472	w_4	.112	.094	.135	.120	.132
	N_{p4}	.81	.73	.33	.33	.36
485	w_5	.120	.158	.129	.140	.133
	N_{p5}	.96	.84	.45	.42	.49
507	w_6	.110	.095	.063	.061	.063
	N_{p6}	.99	.98	.50	.47	.53
548	w_7	.127	.130	.085	.072	.086
	N_{p7}	1.03	.99	.54	.51	.57
—	w_8	.210	.166	.109	.101	.112
	N_{p8}	1.21	1.22	.74	.72	.75

VITA 2

Don P. Satchell

Candidate for the Degree of

Doctor of Philosophy

Thesis: HYDRODENITROGENATION OF A COAL DERIVED LIQUID

Major Field: Chemical Engineering

Biographical:

  Personal Data: Born in Lansing, Michigan, April 18, 1947, to
      Donald and Clara Satchell.

  Education: Attended elementary school at State College, Pennsyl-
      vania; attended Westfield High School, Westfield, New Jersey;
      received the Degree of Bachelor of Science in Chemical
      Engineering at Michigan State University, East Lansing,
      Michigan on June 22, 1969. Completed the requirements for
      Master of Science in Chemical Engineering at Oklahoma State
      University in August, 1972. Completed the requirements for
      Doctor of Philosophy in Chemical Engineering at Oklahoma
      State University in May, 1974.